REPORT NO. DOT-TSC-UMTA-72-2

PRELIMINARY VIBRATION MEASUREMENTS ON MARK I VEHICLE

U.S. International Transportation Exposition
Dulles International Airport
Washington, D.C.
May 27-June 4, 1972

J.E.NICKLES
H.WEINSTOCK
TRANSPORTATION SYSTEMS CENTER
55 BROADWAY
CAMBRIDGE,MA. 02142

OCTOBER 1971
TECHNICAL MEMORANDUM

Prepared for

DEPARTMENT OF TRANSPORTATION
URBAN MASS TRANSPORTATION ADMINISTRATION
WASHINGTON, D.C. 20590

1. Report No. DOT-TSC-UMTA-72-2	2. Government Accession No.	3. Recipient's Catalog No.
4. Title and Subtitle PRELIMINARY VIBRATION MEASUREMENTS ON MARK I VEHICLE		5. Report Date October, 1971 6. Performing Organization Code
7. Author(s) Herbert Weinstock and John E. Nickles		8. Performing Organization Report No.
9. Performing Organization Name and Address Department of Transportation Transportation Systems Center 55 Broadway, Cambridge, MA 02142		10. Work Unit No. R2728 11. Contract or Grant No. UM 204 13. Type of Report and Period Covered Technical Memorandum
12. Sponsoring Agency Name and Address Department of Transportation Urban Mass Transportation Administration Washington, D.C. 20590		14. Sponsoring Agency Code
15. Supplementary Notes		

16. Abstract Preliminary measurements have been made on the acceleration and vibration environment of the Mark I vehicle while operating on the New York City Transit System. Measurements at the journal box indicated short period high acceleration pulses as large as 120g with durations of about one milli-second occurring at infrequent intervals. The rms accelerations, however, were of the order of 2g and correlated closely with speed. A close correlation of vibration level and sound level was also observed. Changes in track roughness were observable from the accelerometer traces.

The ride vibration translational accelerometers indicated vertical accelerations of the order of 0.1 to 0.3g rms and lateral accelerations of 0.05 to 0.08g rms. The in-car vibration appears to be dominated by vehicle pitch and lateral body and roll body modes of vibration. The frequencies of vibration below 10 Hz appear to be independent of speed indicating that the response of the vehicle is governed by the natural modes of vibration excited by either a succession of transients or by random roadbed irregularities which do not have a regular speed. The levels of vibration and frequency distribution fall within ride comfort standards proposed by the International Standards Organization.

17. Key Words	18. Distribution Statement
• Rail Vehicles • Rail Transit • Ride Quality • Urban Mass Transit • Vibration	Approval for UMTA only. Transmittal of this document outside the UMTA and TSC of DOT must have prior approval of the UMTA

19. Security Classif. (of this report)	20. Security Classif. (of this page)	21. No. of Pages	22. Price
Unclassified	Unclassified	180	

TABLE OF CONTENTS

	Page
INTRODUCTION	1
DISCUSSION OF RESULTS	4
Journal Box Accelerations	4
Ride Vibration	16
Lateral Vibration	23
Comparison of Results with Previous Vibration Measurements	36
Comparison of Results with Ride Vibration Standards	37
TEST INSTRUMENTATION	41
Journal Box Acceleration Measurement	41
Car - Body Floor Acceleration Measurement	45
DESCRIPTION OF TESTS	49
Test Route	49
Sequence of Events	49
Run No. 1	49
Run No. 2	50
Run No. 3	50
TEST DATA PROCESSING	51
Summary	51
Test Data Processing, Description	51
REFERENCES	58
APPENDIX A	A-1
APPENDIX B	B-1
APPENDIX C	C-1
APPENDIX D	D-1
APPENDIX E	E-1

LIST OF ILLUSTRATIONS

Figure		Page
1.	R-42 Truck as Instrumented for Tests at DOT Ground Test Center 8/18/71.....	5
2.	Run #1 Journal Box Acceleration RMS Values, Stone Ballast Road Bed.....	6
3.	Run #1 Journal Box Acceleration RMS Values, on Manhattan Bridge.....	7
4.	Run #1 Journal Box Acceleration RMS Values, Concrete Road Bed.....	8
5.	Run #1 Journal Box Acceleration RMS Values.....	9/10
6.	Run #1 Sound Level Values.....	11/12
7.	Run #1 Vertical Acceleration Power Spectral Density, Stone Ballast Road Bed.....	13
8.	Run #1 Linear Acceleration Power Spectral Density, Stone Ballast Road Bed.....	14
9.	Run #1 Linear Acceleration Power Spectral Density, Concrete Road Bed.....	15
10.	Run #2 Vertical Acceleration Power Spectral Density, Stone Ballast Road Bed.....	17
11.	Run #2 Vertical Acceleration Power Spectral Density, Concrete Road Bed.....	18
12.	Run #2 Vertical Acceleration Power Spectral Density, on Manhattan Bridge.....	19
13.	Run #2 Pitch Angular Acceleration Power Spectral Density, Stone Ballast Road Bed.....	20
14.	Run #2 Pitch Angular Acceleration Power Spectral Density, Concrete Road Bed.....	21
15.	Run #2 Pitch Angular Acceleration Power Spectral Density, on Manhattan Bridge.....	22
16.	Run #3 Longitudinal Acceleration Power Spectral Density, Stone Ballast Road Bed.....	24
17.	Run #3 Longitudinal Acceleration Power Spectral Density, Concrete Road Bed.....	25
18.	Run #3 Longitudinal Acceleration Power Spectral Density, on Manhattan Bridge.....	26

LIST OF ILLUSTRATIONS (CONTINUED)

Figure		Page
19.	Run #2 Lateral Acceleration Power Spectral Density, Stone Ballast Road Bed	27
20.	Run #2 Lateral Acceleration Power Spectral Density, Concrete Road Bed	28
21.	Run #2 Lateral Acceleration Power Spectral Density, on Manhattan Bridge	29
22.	Run #2 Roll Angular Acceleration Power Spectral Density, Stone Ballast Road Bed	30
23.	Run #2 Roll Angular Acceleration Power Spectral Density, Concrete Road Bed	31
24.	Run #2 Roll Angular Acceleration Power Spectral Density, on Manhattan Bridge	32
25.	Run #2 Yaw Angular Acceleration Power Spectral Density, Stone Ballast Road Bed	33
26.	Run #2 Yaw Angular Acceleration Power Spectral Density, Concrete Road Bed	34
27.	Run #2 Yaw Angular Acceleration Power Spectral Density, on Manhattan Bridge	35
28.	Vertical Vibration Acceleration Levels in Octave Band Format	38
29.	Lateral Vibration Acceleration Levels in Octave Band Format	40
30.	Journal Box Accelerometer Location	42
31.	Instrumentation Block Diagram for Journal Box Acceleration Measurement	43
32.	Car-Body Acceleration Sensor Assembly	46
33.	Instrumentation Block Diagram for Car-Body Acceleration Measurement	47
34.	Spectrum Analyzer Frequency Calibration	53
A-1.	Model for Derivation of Pitch and Bounce Motions	A-4
A-2.	Pitch and Bounce Mode Descriptions	A-6
A-3.	Roll Model	A-8
A-4.	Swing Link Suspension Kinematic Model	A-10
A-5.	Yaw Model	A-10

LIST OF ILLUSTRATIONS (CONTINUED)

Figure		Page
A-6.	Truck Lateral Motion	A-11
A-7.	Kinematic Hunting	A-14
A-8.	Beam Bending Models	A-15
A-9.	Damped Vertical Dynamic Model	A-17
A-10.	Simplified Models for Vertical Dynamics	A-19
E-1.	Run #1 Journal Box Acceleration RMS Values, Stone Ballast Road Bed	E-2
E-2.	Run #1 Vertical Acceleration PSD, Stone Ballast Road Bed	E-3
E-3.	Run #1 Linear Acceleration PSD, Stone Ballast Road Bed, Left Wheels	E-4
E-4.	Run #1 Linear Acceleration PSD, Stone Ballast Road Bed, Right Wheels	E-5
E-5.	Run #1 Journal Box Acceleration RMS Values, Concrete Road Bed	E-6
E-6.	Run #1 Vertical Acceleration PSD, Concrete Road Bed	E-7
E-7.	Run #1 Linear Acceleration PSD, Concrete Road Bed	E-8
E-8.	Run #1 Journal Box Acceleration RMS Values on Manhattan Bridge	E-9
E-9.	Run #1 Vertical Acceleration PSD, on Manhattan Bridge	E-10
E-10.	Run #1 Linear Acceleration PSD, on Manhattan Bridge	E-11
E-11.	Run #1 Instrumentation Noise RMS Values	E-12
E-12.	Run #2 Acceleration RMS Values, Stone Ballast Road Bed	E-13
E-13.	Run #2 Acceleration Data Through 5Hz Low Pass Filter, Stone Ballast Road Bed, 10 sec/cm	E-14
E-14.	Run #2 Acceleration Data Through 5Hz Low Pass Filter, Stone Ballast Road Bed, 1 sec/cm	E-15
E-15.	Run #2 Vertical Acceleration PSD, Stone Ballast Road Bed	E-16

LIST OF ILLUSTRATIONS (CONTINUED)

Figure		Page
E-16.	Run #2 Lateral Acceleration PSD, Stone Ballast Road Bed	E-17
E-17.	Run #2 Longitudinal Acceleration PSD, Stone Ballast Road Bed	E-18
E-18.	Run #2 Roll Angular Acceleration PSD, Stone Ballast Road Bed	E-19
E-19.	Run #2 Pitch Angular Acceleration PSD, Stone Ballast Road Bed	E-20
E-20.	Run #2 Yaw Angular Acceleration PSD, Stone Ballast Road Bed	E-21
E-21.	Run #2 Acceleration RMS Values, Concrete Road Bed	E-22
E-22.	Run #2 Acceleration Data Through 5Hz Low Pass Filter, Concrete Road Bed, 10 sec/cm	E-23
E-23.	Run #2 Acceleration Data Through 5Hz Low Pass Filter, Concrete Road Bed, 1 sec/cm	E-24
E-24.	Run #2 Vertical Acceleration PSD, Concrete Road Bed	E-25
E-25.	Run #2 Lateral Acceleration PSD, Concrete Road Bed	E-26
E-26.	Run #2 Longitudinal Acceleration PSD, Concrete Road Bed	E-27
E-27.	Run #2 Roll Angular Acceleration PSD, Concrete Road Bed	E-28
E-28.	Run #2 Pitch Angular Acceleration PSD, Concrete Road Bed	E-29
E-29.	Run #2 Yaw Angular Acceleration PSD, Concrete Road Bed	E-30
E-30.	Run #2 Acceleration RMS Values, on Manhattan Bridge	E-31
E-31.	Run #2 Acceleration Data Through 5Hz Low Pass Filter, on Manhattan Bridge, 10 sec/cm	E-32
E-32.	Run #2 Acceleration Data Through 5Hz Low Pass Filter, on Manhattan Bridge, 1 sec/cm	E-33
E-33.	Run #2 Vertical Acceleration PSD, on Manhattan Bridge	E-34

LIST OF ILLUSTRATIONS (CONTINUED)

Figure		Page
E-34.	Run #2 Lateral Acceleration PSD, on Manhattan Bridge	E-35
E-35.	Run #2 Longitudinal Acceleration PSD, on Manhattan Bridge	E-36
E-36.	Run #2 Roll Angular Acceleration PSD, on Manhattan Bridge	E-37
E-37.	Run #2 Pitch Angular Acceleration PSD, on Manhattan Bridge	E-38
E-38.	Run #2 Yaw Angular Acceleration PSD, on Manhattan Bridge	E-39
E-39.	Run #2 RMS Instrumentation Noise	E-40
E-40.	Run #2 Instrumentation Through 5Hz Low Pass Filter	E-41
E-41.	Run #3 Acceleration Levels, Stone Ballast Road Bed	E-42
E-42.	Run #3 Acceleration Data Through 5Hz Low Pass Filter, Stone Ballast Road Bed, 10 sec/cm	E-43
E-43.	Run #3 Acceleration Data Through 5Hz Low Pass Filter, Stone Ballast Road Bed	E-44
E-44.	Run #3 Vertical Acceleration PSD, Stone Ballast Road Bed	E-45
E-45.	Run #3 Lateral Acceleration PSD, Stone Ballast Road Bed	E-46
E-46.	Run #3 Longitudinal Acceleration PSD, Stone Ballast Road Bed	E-47
E-47.	Run #3 Roll Angular Acceleration PSD, Stone Ballast Road Bed	E-48
E-48.	Run #3 Pitch Angular Acceleration PSD, Stone Ballast Road Bed	E-49
E-49.	Run #3 Yaw Angular Acceleration PSD, Stone Ballast Road Bed	E-50
E-50.	Run #3 RMS Acceleration Levels, Concrete Road Bed	E-51
E-51.	Run #3 Acceleration Data Through 5Hz Low Pass Filter, Concrete Road Bed, 10 sec/cm	E-52

LIST OF ILLUSTRATIONS (CONTINUED)

Figure		Page
E-52.	Run #3 Acceleration Data Through 5Hz Low Pass Filter, Concrete Road Bed, 1 sec/cm.....	E-53
E-53.	Run #3 Vertical Acceleration PSD, Concrete Road Bed.....	E-54
E-54.	Run #3 Lateral Acceleration PSD, Concrete Road Bed.....	E-55
E-55.	Run #3 Longitudinal Acceleration PSD, Concrete Road Bed.....	E-56
E-56.	Run #3 Roll Angular Acceleration PSD, Concrete Road Bed.....	E-57
E-57.	Run #3 Pitch Angular Acceleration PSD, Concrete Road Bed.....	E-58
E-58.	Run #3 Yaw Angular Acceleration, Concrete Road Bed.....	E-59
E-59.	Run #3 RMS Acceleration Levels, on Manhattan Bridge.....	E-60
E-60.	Run #3 Acceleration Data Through 5Hz Low Pass Filter, on Manhattan Bridge, 10 sec/cm.....	E-61
E-61.	Run #3 Acceleration Data Through 5Hz Low Pass Filter, on Manhattan Bridge, 10 sec.....	E-62
E-62.	Run #3 Vertical Acceleration PSD, on Manhattan Bridge.....	E-63
E-63.	Run #3 Lateral Acceleration PSD, on Manhattan Bridge.....	E-64
E-64.	Run #3 Longitudinal Acceleration PSD, on Manhattan Bridge.....	E-65
E-65.	Run #3 Roll Angular Acceleration PSD, on Manhattan Bridge.....	E-66
E-66.	Run #3 Pitch Angular Acceleration PSD, on Manhattan Bridge.....	E-67
E-67.	Run #3 Yaw Angular Acceleration PSD, on Manhattan Bridge.....	E-68
E-68.	Run #3 Instrumentation Noise RMS Values.....	E-69
E-69.	Run #3 Instrumentation Noise Through 5Hz Low Pass Filter.....	E-70

LIST OF TABLES

Table		Page
1.	Typical Indicated RMS Accelerations (g) Measured in Test Runs.....	3
2.	Octave Band Frequencies.....	36
3.	Low Pass Filter Frequency Response and Data Recorded on Each Track of Tape (By Run).....	55
A-1.	Estimated Natural Frequencies of R-42 Cars.....	A-2

ACKNOWLEDGEMENTS

This report describes part of the Urban Rail Supporting Technology Program which is sponsored by the Rail Projects Branch of the Urban Mass Transit Administration.

Thomas Hayes and Phillip Silvia assembled, installed, and operated the instrumentation used for these measurements. Kevin Cawley performed the reduction of the data into the many spectrum analyses presented herein. Professor A. B. Perlman of the Tufts University Department of Mechanical Engineering performed the natural frequency analyses presented in Appendix A. The authors are grateful to the New York City Transit Authority for their helpful cooperation and for the use of their vehicles and track.

SUMMARY

Preliminary measurements have been made on the acceleration and vibration environment of the Mark I vehicle while operating on the New York City Transit System. Measurements at the journal box indicated short period high acceleration pulses as large as 120g with durations of about one milli-second occuring at infrequent intervals. The rms accelerations, however, were of the order of 2g. Accelerometers in future experiments should be rescaled from the 100g full scale to 10g full scale to improve the signal-to-noise ratio and permit analysis of the frequency spectrum of the journal box accelerations. The rms vibration levels correlated closely with speed. A close correlation of vibration level and sound level was also observed. Changes in track roughness were observable from the accelerameter traces. The environment at the journal box appears compatible with the use of servo accelerometers for track geometry measurements.

The ride vibration translational accelerometers indicated vertical accelerations of the order of 0.1 to 0.3g rms and lateral accelerations of 0.05 to 0.08g rms. The in-car vibration appears to be dominated by vehicle pitch and lateral body and roll body modes of vibration. The frequencies of vibration below 10 Hz appear to be independent of speed indicating that the response of the vehicle is governed by the natural modes of vibration excited by either a succession of transients or by random roadbed irregularities which do not have a regular spacing. The levels of vibration and frequency distribution fall within ride comfort standards proposed by the International Standards Organization. The angular accelerometers should be rescaled from 30 rad/sec^2 full scale to 3 rad/sec^2 full scale to improve the signal-to-noise ratio.

Significant differences in ride vibration were observed on different types of track structures along the test route. The lowest vibration levels were observed on a new section of concrete road bed. The highest level was on conventional stone ballast. The Manhattan Bridge had a larger number of higher frequency of high impact shocks but a lower rms acceleration level than the stone ballast roadway.

The measurements reported here are primarily intended to provide a set of baseline data for the design of further experimental investigations of the dynamics of rail transit systems and to provide environmental data for equipment design.

INTRODUCTION

The Urban Mass Transit Administration Rail System Supporting Technology Program, (Transportation Systems Center) is developing instrumentation to measure the characteristics of rail transit systems using a diagnostic vehicle. This vehicle will provide a mobile laboratory for use in UMTA experiments on new and existing equipment and will also carry instrumentation for track geometry measurements, track adhesion measurements, acoustic noise measurements and measurements of vehicle dynamics.

Two R-42 cars have been borrowed from the New York City Transit Authority to provide a vehicle for breadboard tests on the instrumentation being developed, provide preliminary data on the dynamics of transit vehicles and to obtain operational experience with the instrumentation to be used in the Mark II Diagnostic Vehicle. The two R-42 vehicles have been designated as the UMTA Mark I diagnostic vehicle.

Initial tests on the Mark I vehicle consisted of vibration and sound measurements while the cars were operating on the "N" line of the New York system. The tests were conducted on May 6, 1971. The objectives of these tests were:

a. Obtain a set of baseline data on the vibration environment in which on-board track geometry and other instrumentation will be required to function in operation of the diagnostic vehicle.

b. Obtain typical sound and vibration data in the passenger compartment of the transit vehicle under typical operating conditions.

c. Gain operational experience with the vibration and sound measurement instrumentation to be used in future experiments.

The tests were conducted on the "Sea Beach" (N) line from 86th Street in Brooklyn to 57th Street in Manhattan. The two R-42 cars which have been selected as the Mark I vehicle were the lead cars of a special (no passenger) 8 car train. The train operator was instructed to operate the car at the speeds he would normally use if the car was in typical service except that no station stops were to be included in order to reduce test time.

From 86th Street Brooklyn to 59th Street Brooklyn, the track consists of conventional wood ties on stone ballast in an open cut and fill roadway. At 59th Street Brooklyn the track

enters the subway tunnel and continues with wood tie , stone ballast construction until 36th Street Brooklyn. From 36th Street Brooklyn to Pacific Street there is a new section of track which consists of split-wood ties fastened directly to the concrete floor of the tunnel. After Pacific Street, the track continues with the conventional wood tie, stone ballast construction in the tunnel. The track leaves the tunnel to cross the Manhattan Bridge where the track is an open wood tie on steel girder type of construction typical of elevated lines. After crossing the Manhattan Bridge, the track re-enters tunnel with wood tie, stone ballast construction until the end of the line at 57th Street in Manhattan. Thus, the use of this line permitted obtaining data on three different types of typical construction in a single set of test runs.

The vibration measurements were made by six piezo-electric crystal accelerometers mounted on the journal boxes of the forward truck, three high sensitivity force-rebalance translational accelerometers and three torque rebalance angular accelerometers mounted on a plate located on the floor of the passenger compartment. The plate carrying the ride vibration transducers was mounted at two locations. During one run, the plate was directly above the forward truck and during the other, it was located at the centerline of car near the second door (about 1/3 the car length from the forward truck). Sound measurements were made by three calibrated microphones located inside the transit car and one microphone between cars.

Since large impacts were expected at rail joints and switches the journal box accelerometers were scaled for a 100g range. Although infrequent (100 seconds or longer) short duration (less than 1 millisecond) pulses of 60 to 80g and some up to 120g were observed at sharp irregularities and switches, typical rms accelerations were of the order of 2g or less. It is therefore recommended that a range of 10g full scale be used in future measurements to provide a better signal to noise ratio and finer resolution of the data.

Table 1 summarizes the rms accelerations obtained during the test runs. In all cases the new concrete construction produced the lowest vibration levels. The Manhattan Bridge data showed a larger number and higher frequency of very high acceleration peaks, however, had a lower rms vibration level than the stone ballast construction. For the most part, the ride vibration appeared to be dominated by transient vibrations occuring at natural frequencies of the vehicle structures. Although the amount of energy in each mode changed with speed and track structure the dominant frequencies of vibration remain relatively constant. The most noticeable vibrations occur at the lateral body natural frequency of about 0.8 Hz and the body-pitch natural frequency at 2.5 - 3 Hz.

TABLE 1. TYPICAL INDICATED RMS ACCELERATIONS (g) MEASURED IN TEST RUNS

	Instrumentation Noise Levels	Stone Ballast		New Concrete Construction		Bridge-open tie	
Vertical Journal Box	1.1	1.8		1.6		1.8	
Lateral Journal Box	1.1	1.2		1.2		1.2	
Longitudinal Journal Box	1.1	1.2		1.2		1.4	
Vertical Passenger Compartment	0.005	0.24	0.08	0.12	0.05	0.18	0.07
Lateral Passenger Compartment	0.005	0.06	0.04	0.03	0.02	0.05	0.03
Longitudinal Passenger Compartment	0.005	0.03	0.03	0.02	0.01	0.03	0.03
		Above Truck	Mid Car	Above Truck	Mid Car	Above Truck	Mid Car

This document presents a discussion of the results of these vibration measurements and a description of the instrumentation, test procedures and data analysis techniques used to obtain and reduce the vibration data. The sound measurements and data analysis are described in detail in Reference 1.

DISCUSSION OF RESULTS

JOURNAL BOX ACCELERATIONS

The journal box accelerometers were mounted in the locations shown in figure 1. High amplitude (60-80g with some as high as 120g) acceleration impacts were observed at irregular periods of the order of 100 to 200 seconds in the vertical direction. For the most part, the rms accelerations were of the order of 2g. The 100g range required for measuring the high acceleration impacts resulted in an instrumentation noise of 1.1g rms limiting the resolution of the measurement. Typical rms vibration acceleration data obtained on the stone ballast, concrete and bridge type track structures are shown in figures 2, 3, and 4.

The observed lateral and longitudinal accelerations are, for the most part, within the instrumentation noise. As indicated in figure 5, there is a close correlation between the vehicle speed and the levels of observed vibration. There is an even closer correlation between the observed vibration levels with the observed sound levels as shown in figure 6 (from Reference 1) indicating common sources for both the acoustic noise and vibration disturbances.

As indicated in figures 7, 8, and 9 the instrumentation noise is in the same frequency bands as the journal box vibration accelerations and spectral analysis does not provide any significantly new information. The difference in spectra between the vertical accelerometer mounted on the triaxial mounting block on the rear left journal box and the other vertical accelerometers is a result of resonant frequencies in the journal box structure. The accelerometers mounted on the triaxial mounting block appear to provide faithful reproduction of the axle response to track irregularities.

Instrumentation to be mounted on the journal boxes should be designed to withstand shocks of about 100g of 1 millisecond duration. The rms vibration levels to be expected are less than 3g for the normal transit operation. Future vibration measurements should include accelerometers scaled to provide a better signal to noise ratio. This can be accomplished by a reduced full scale range (e.g.,: a 10g full scale range) of the accelerometers, since most of the noise is produced by the tape recorder.

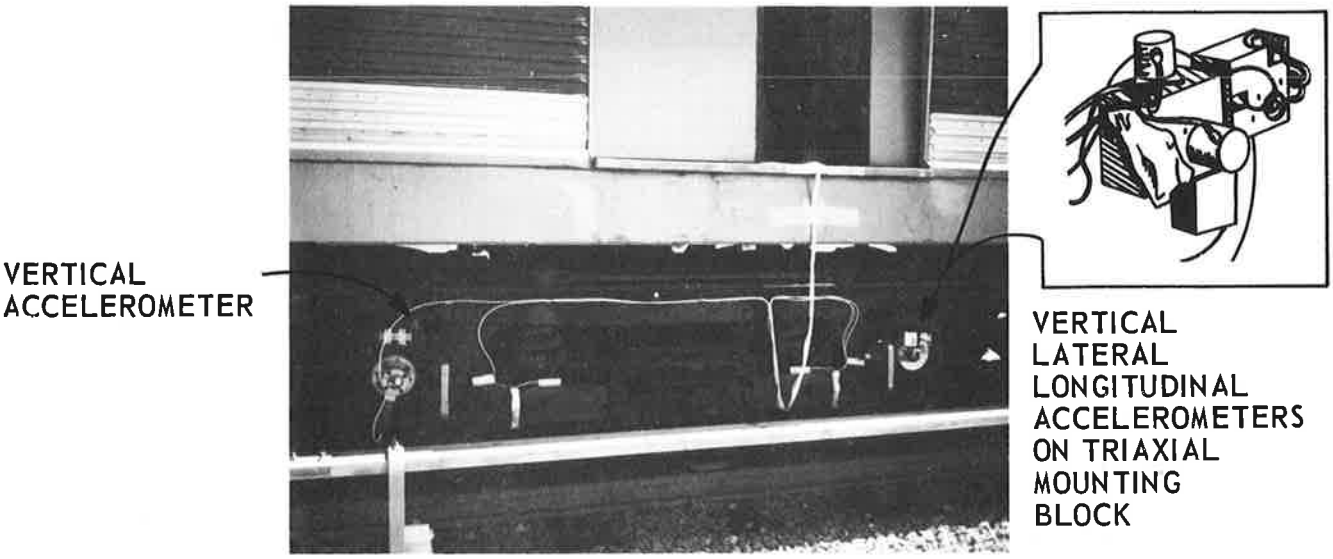

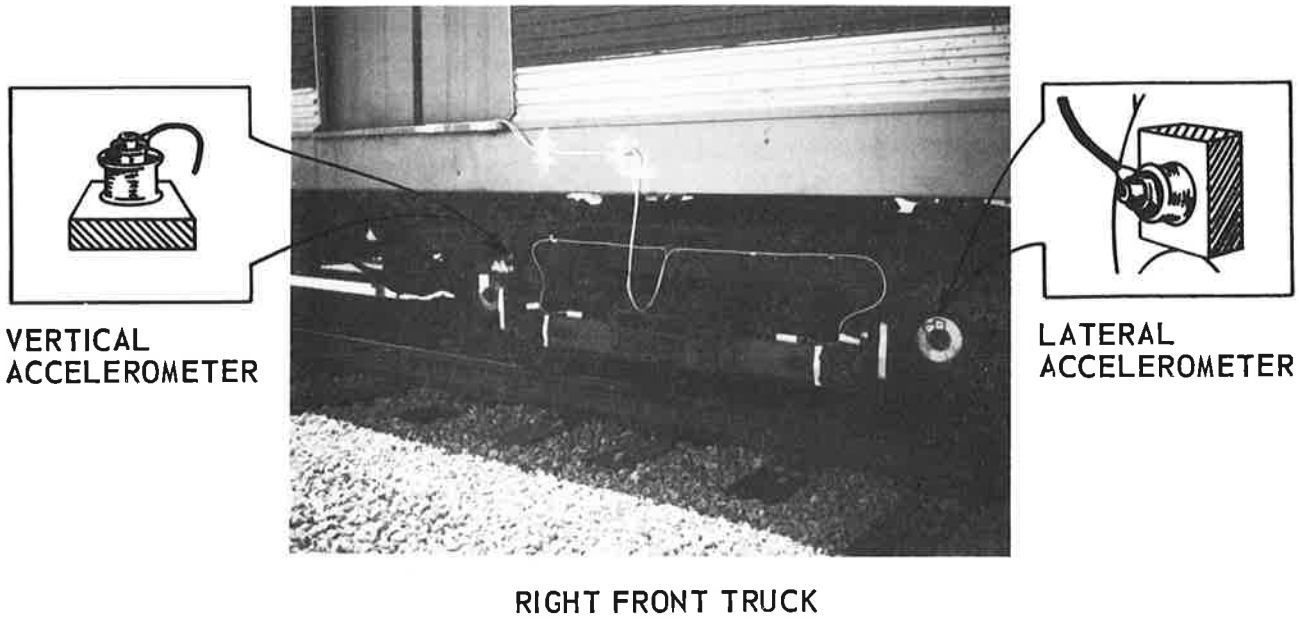

Figure 1. R-42 Truck as Instrumented for Tests at DOT Ground Test Center 8/18/71

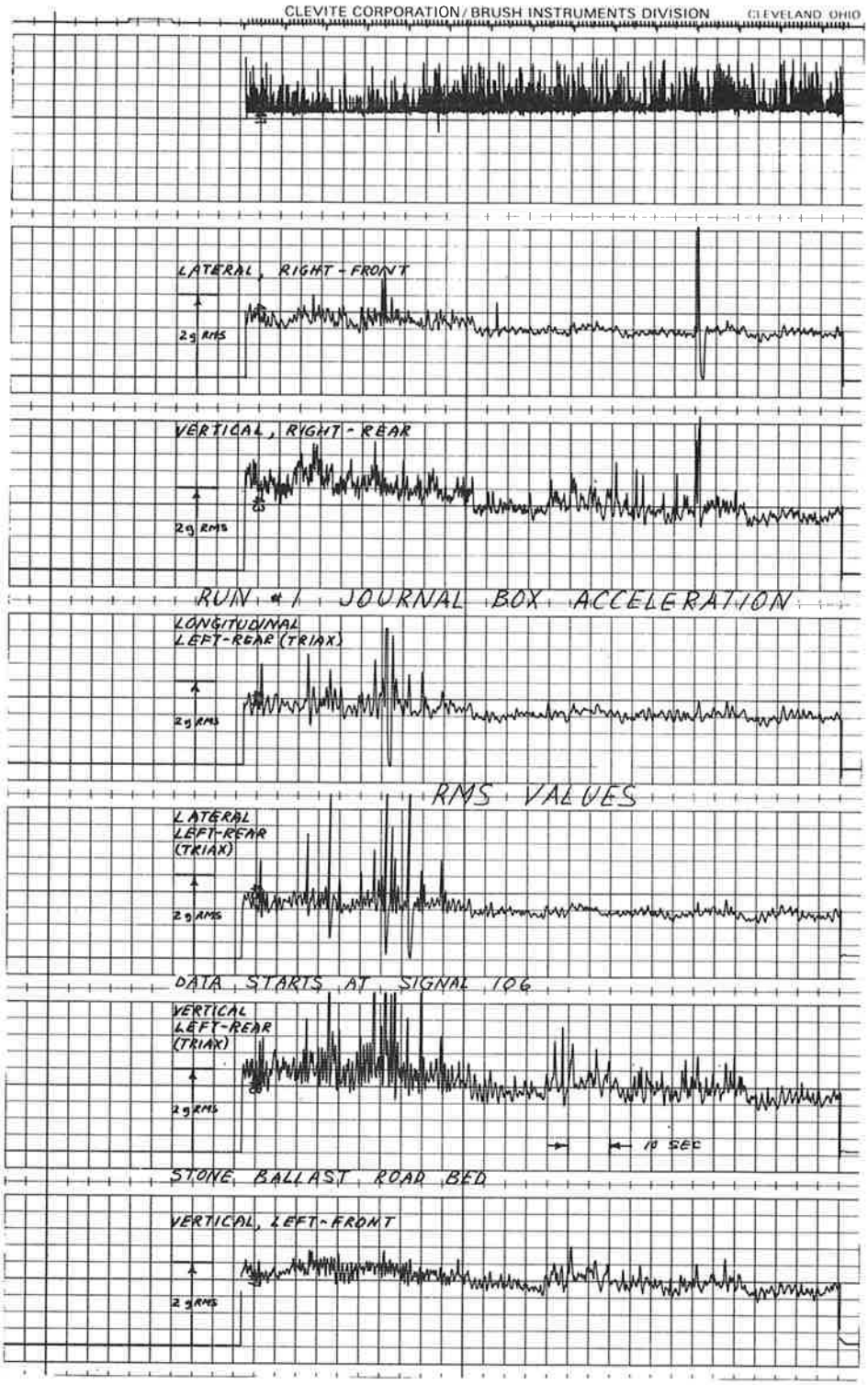

Figure 2. Run #1 Journal Box Acceleration RMS Values, Stone Ballast Road Bed

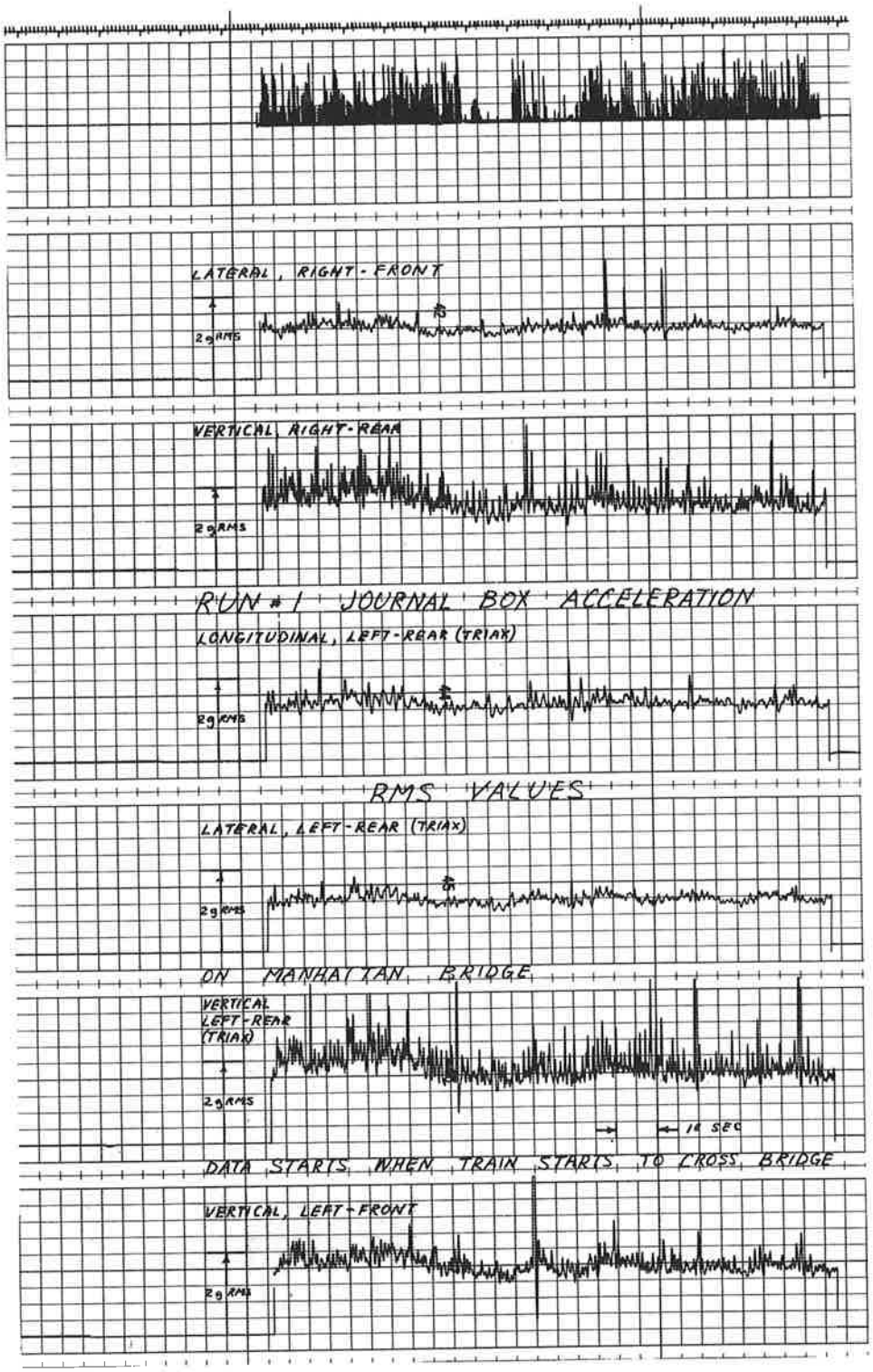

Figure 3. Run #1 Journal Box Acceleration RMS Values, on Manhattan Bridge

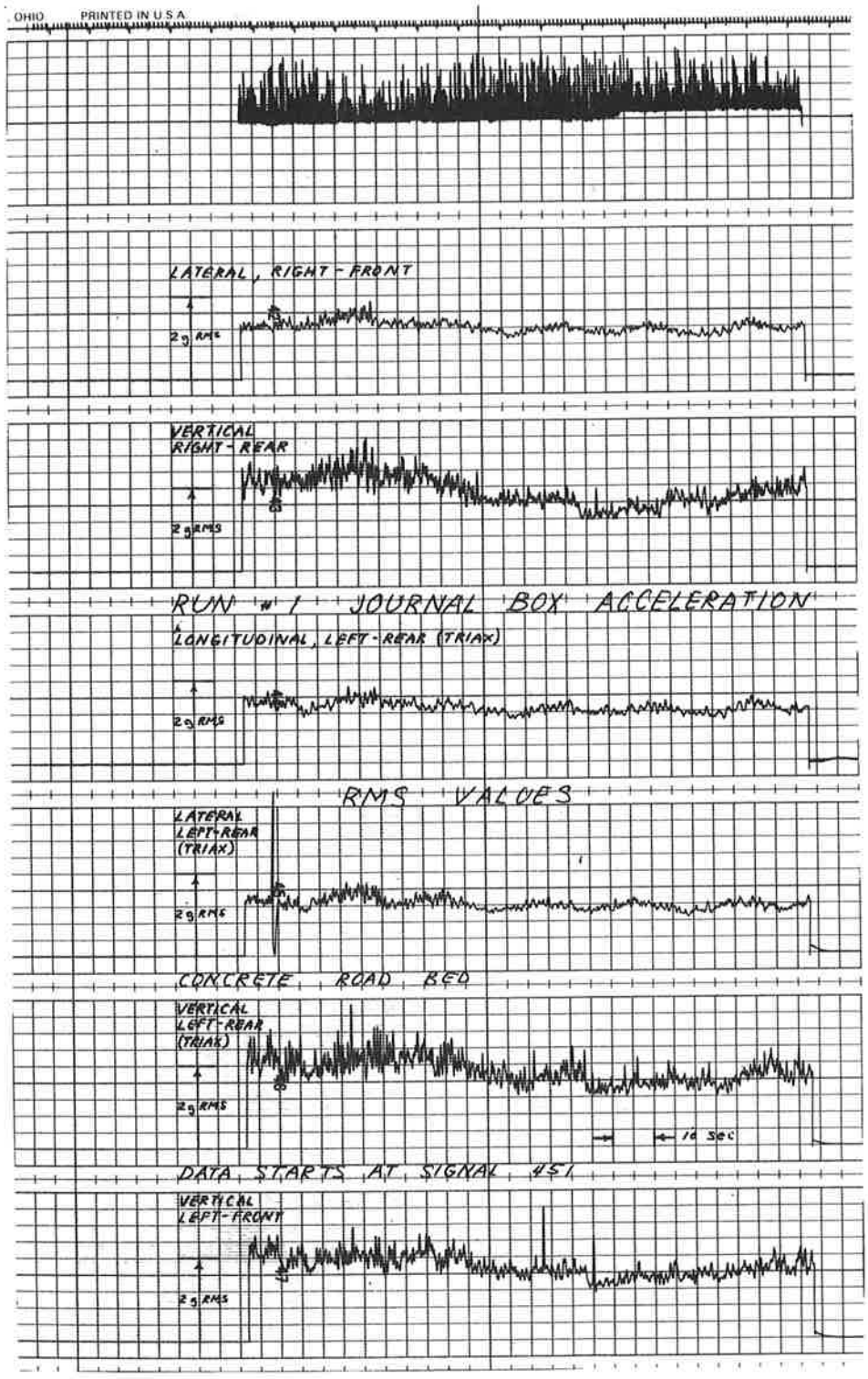

Figure 4. Run #1 Journal Box Acceleration RMS Values, Concrete Road Bed

Figure 5. Run #1 Journal Box Acceleration RMS Values

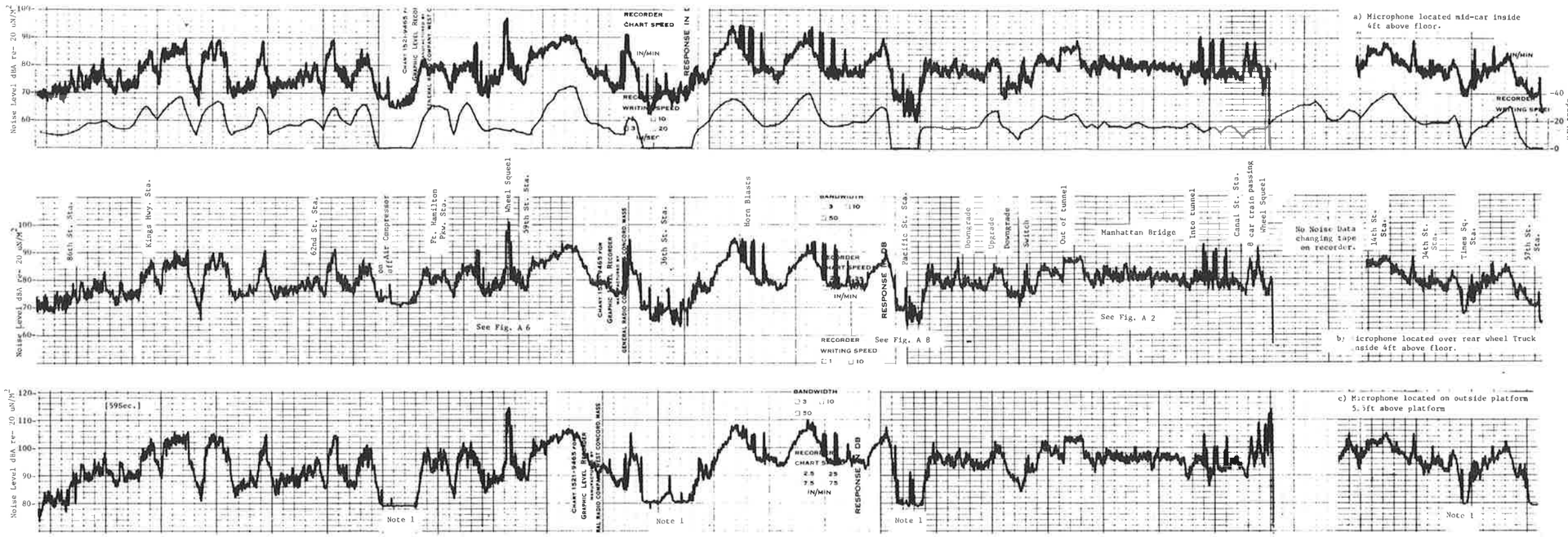

Figure 6. Run #1 Sound Level Values

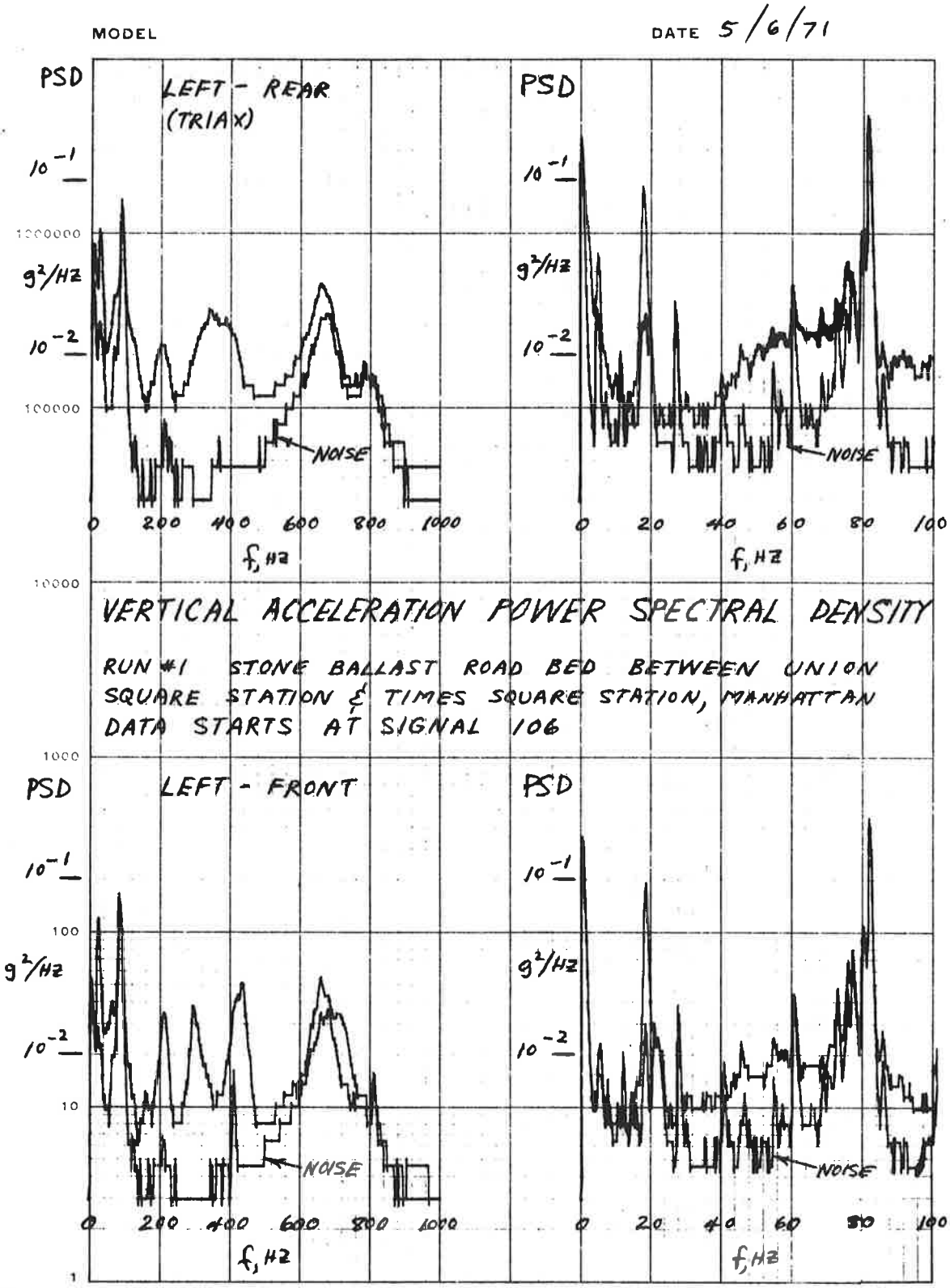

Figure 7. Run #1 Vertical Acceleration Power Spectral Density, Stone Ballast Road Bed

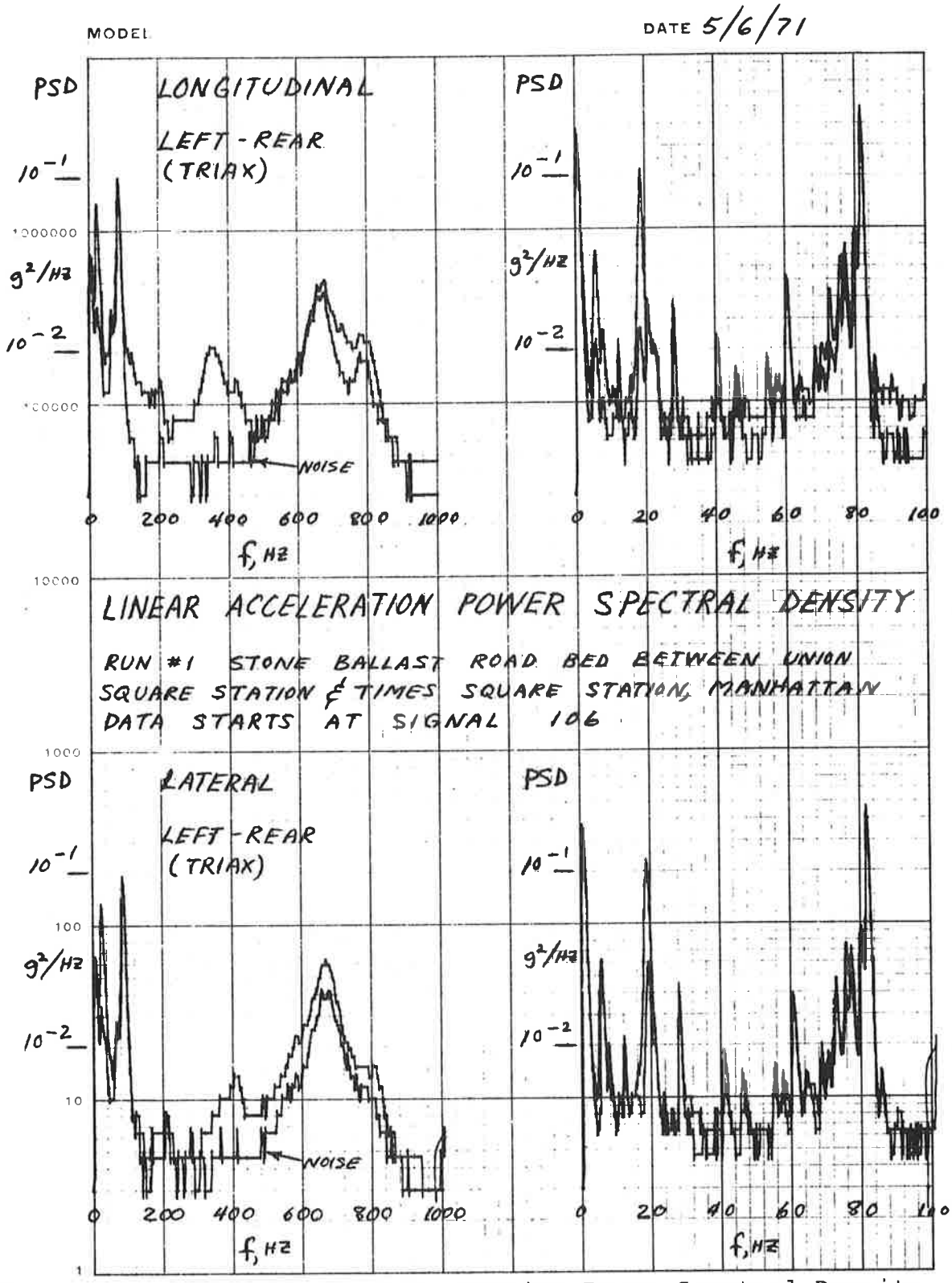

Figure 8. Run #1 Linear Acceleration Power Spectral Density, Stone Ballast Road Bed

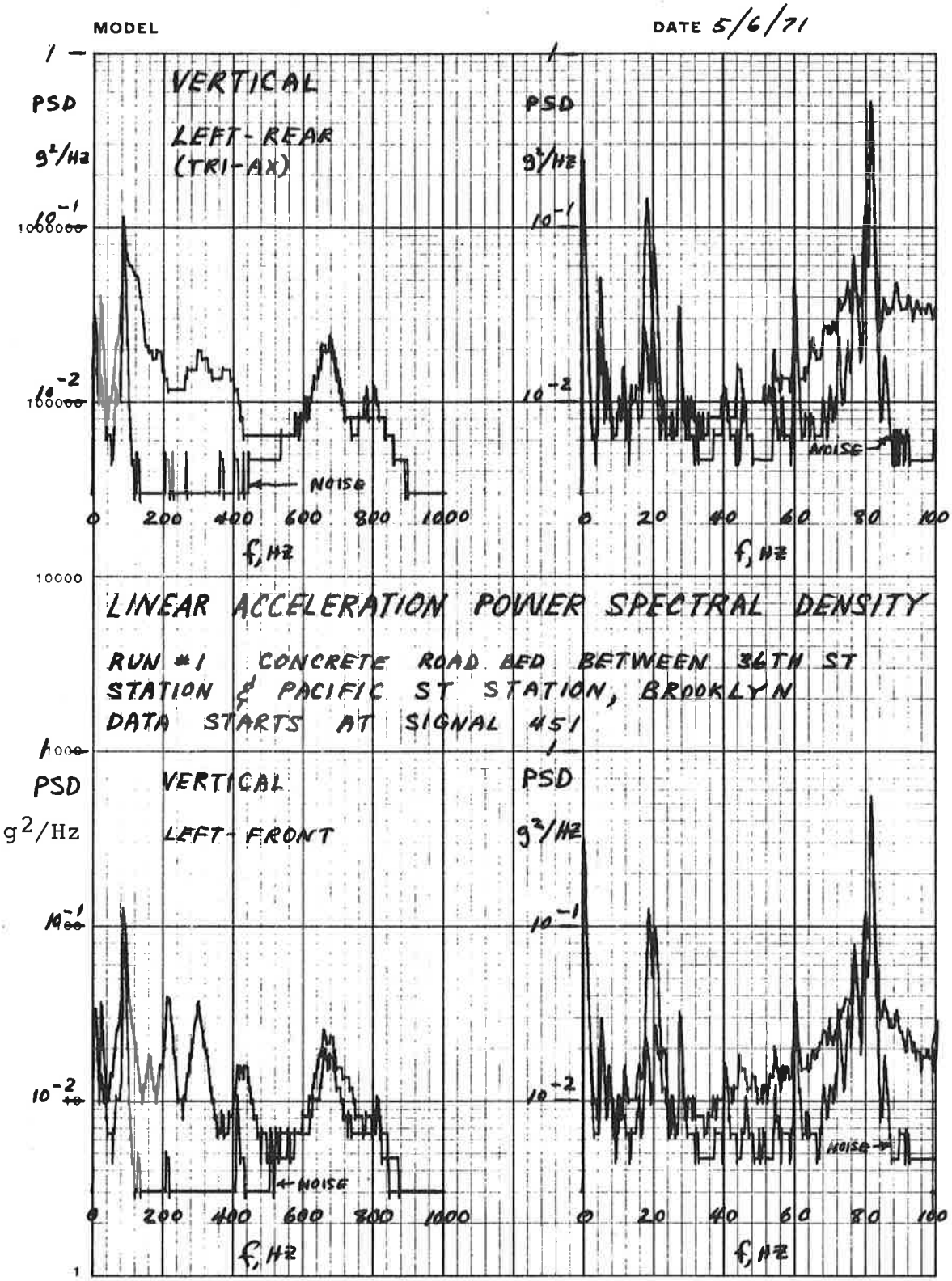

Figure 9. Run #1 Linear Acceleration Power Spectral Density, Concrete Road Bed

RIDE VIBRATION

Vertical Vibration

Estimates of the natural frequencies and modes of vibration expected for the R-42 cars are obtained in Appendix A. For vertical motions the following modes of vibration are expected to be significant:

Mode	Natural Frequency
First Body Bounce	1.6 Hz
Second Body Bounce	5.5 Hz
First Body Pitch	2.1 Hz
Second Body Pitch	5.6 Hz
Truck Pitch	5.2 Hz
Body Bending	19-27 Hz

Additional bending modes of elements of the structure are also possible at frequencies below 20 Hz as well as at higher frequencies, however these modes would be expected to produce localized effects in the car and would require a complete survey of many locations within the car to identify.

As indicated in Table 1 the vertical vibration levels measured above the truck (0.1 to 0.25 g rms) are two to two and a half times greater than those observed at a distance of about 1/3 the car length back from the truck location (0.05 to 0.08 g rms). This indicates the presence of a strong pitching mode of vibration.

Figures 10, 11 and 12 show the spectral analyses of the vertical vibration at the third car length location for the three types of track construction traversed during this test run. The dominant frequency that is observed is between 2.1 and 2.8 Hz. The dominant frequency of vibration does not appear to be strongly sensitive to speed indicating that the vibration is the result of repeated transient responses to occasional irregularities or a response to continuously varying random irregularities.

The dominant frequency of 2.1 to 2.2 Hz appears to correspond to the first body pitch mode of oscillation. Some vibration energy is present at 1.2 Hz, which may correspond to the first body bounce natural frequency of 1.6 Hz.

The presence of a strong pitch mode of angular vibration is confirmed by the pitch angular vibration spectra shown in figures 13, 14 and 15. If the vertical vibration was produced primarily by vertical track irregularities, it would be

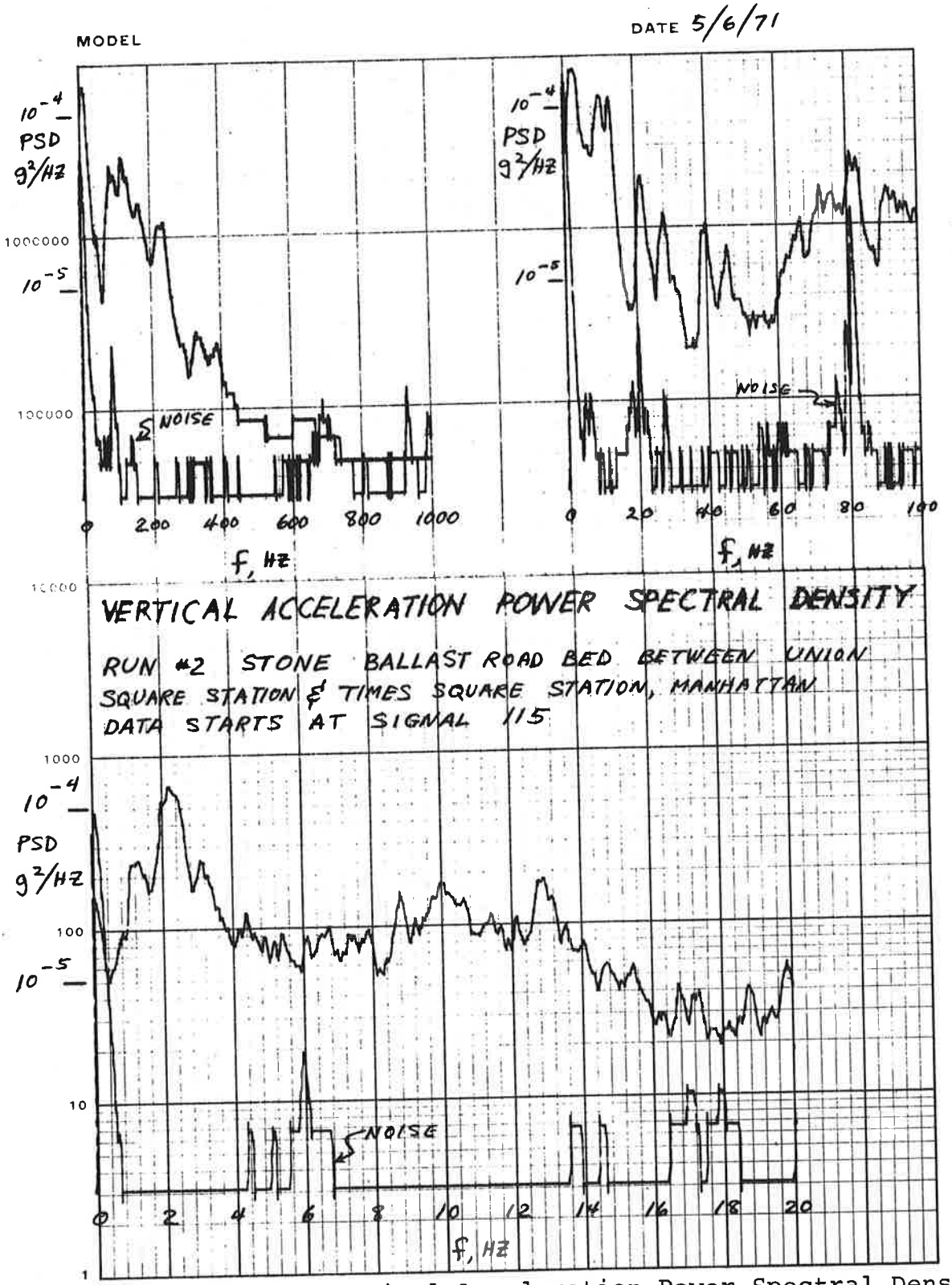

Figure 10. Run #2 Vertical Acceleration Power Spectral Density, Stone Ballast Road Bed

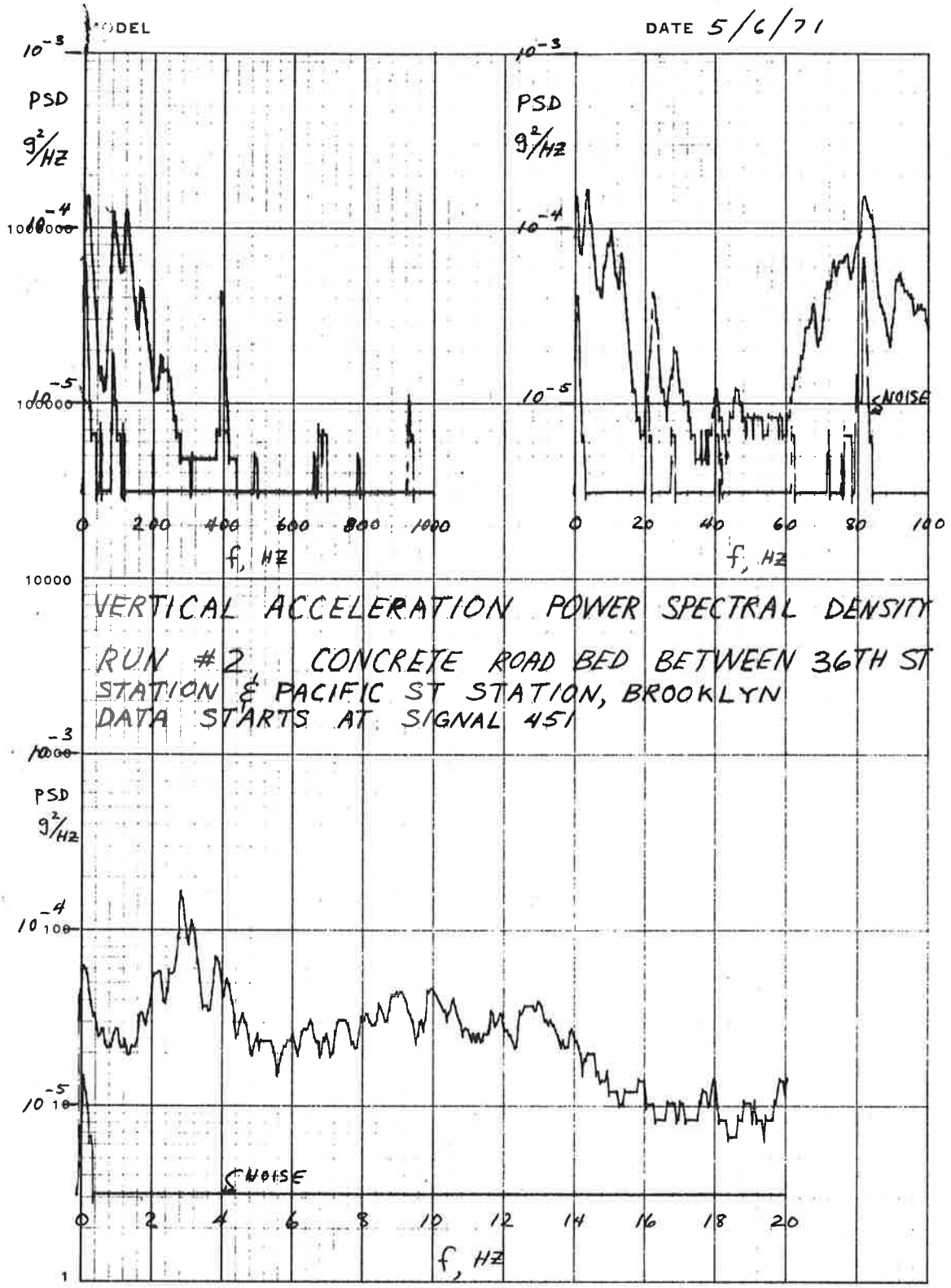

Figure 11. Run #2 Vertical Acceleration Power Spectral Density, Concrete Road Bed

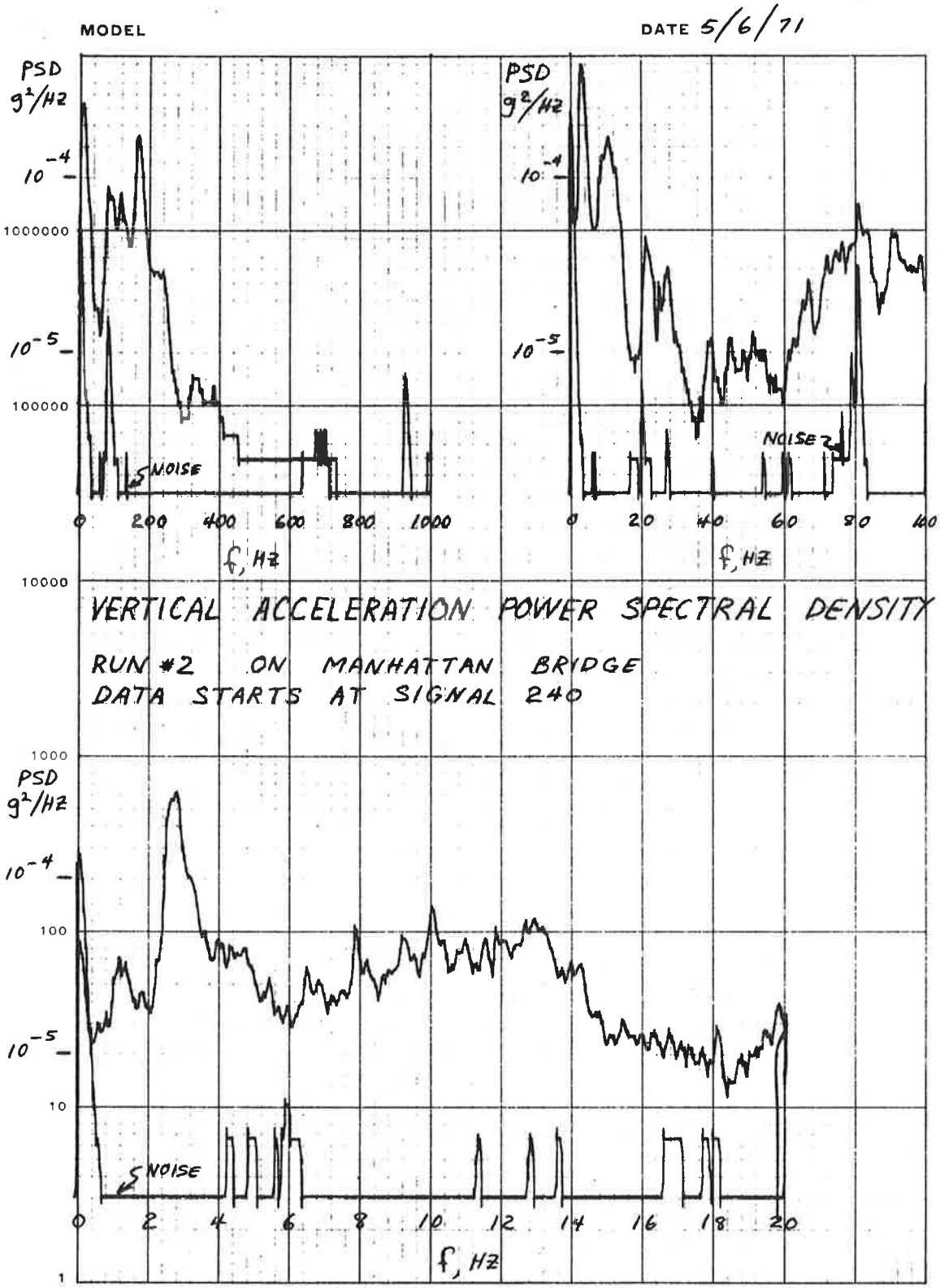

Figure 12. Run #2 Vertical Acceleration Power Spectral Density, on Manhattan Bridge

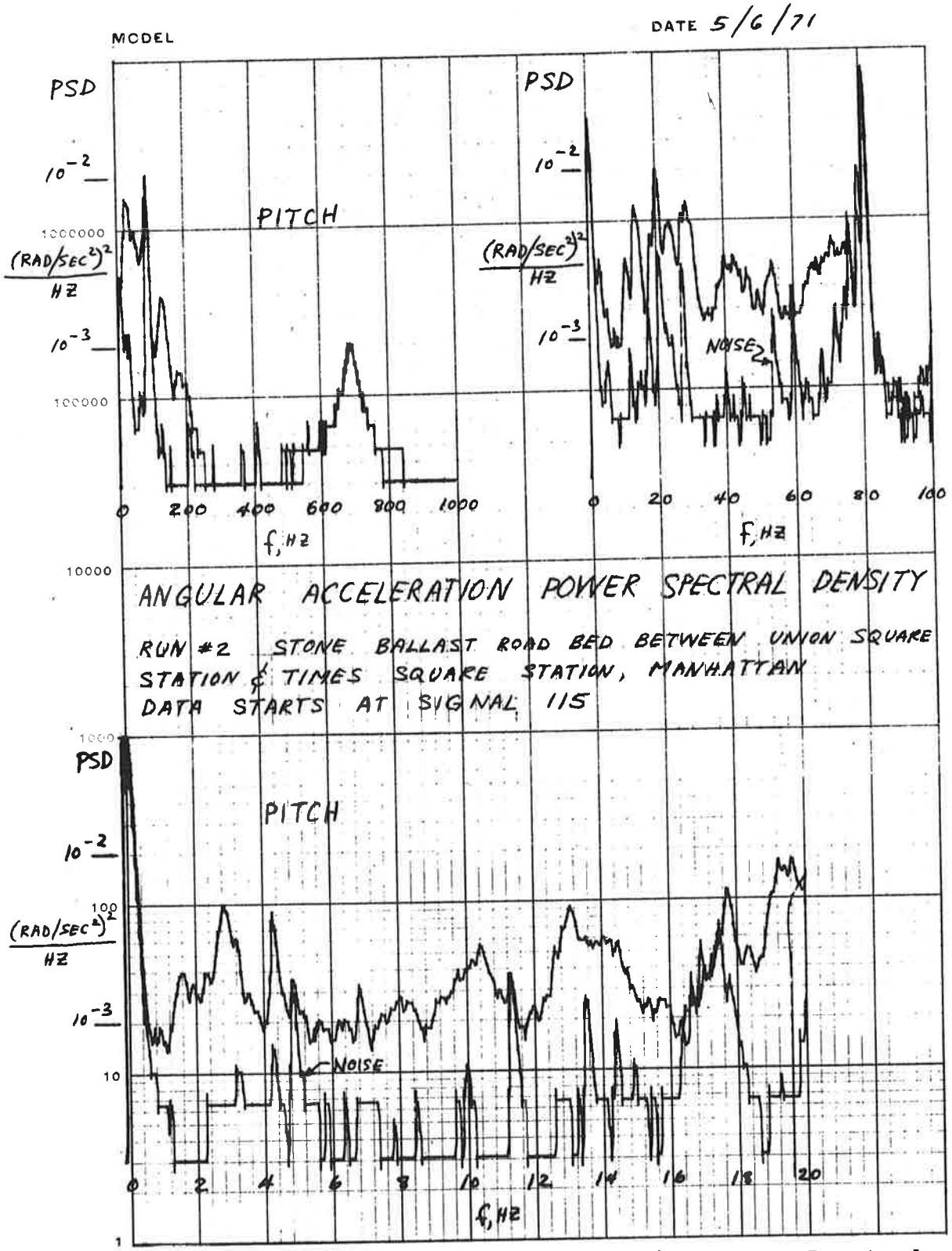

Figure 13. Run #2 Pitch Angular Acceleration Power Spectral Density, Stone Ballast Road Bed

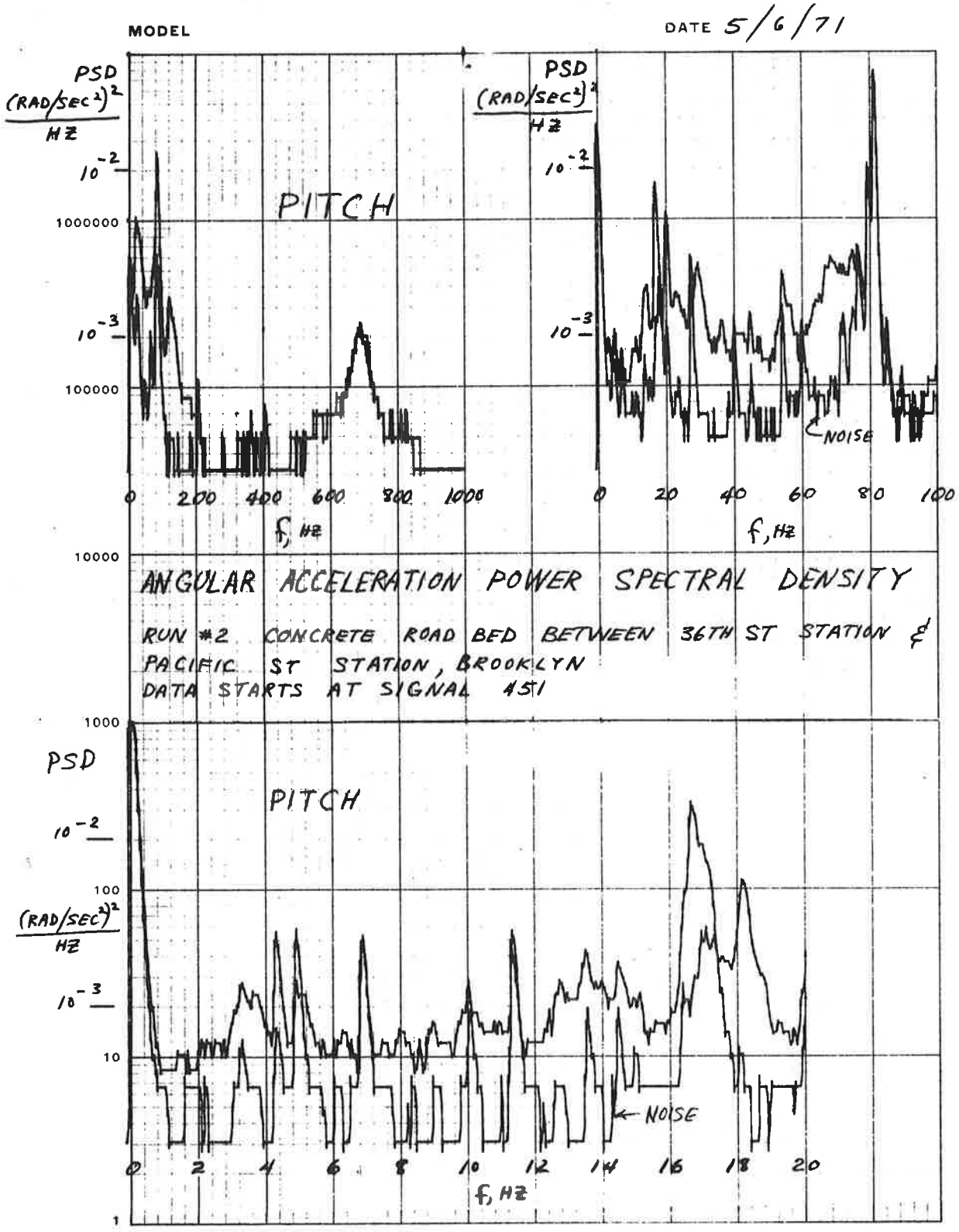

Figure 14. Run #2 Pitch Angular Acceleration Power Spectral Density, Concrete Road Bed

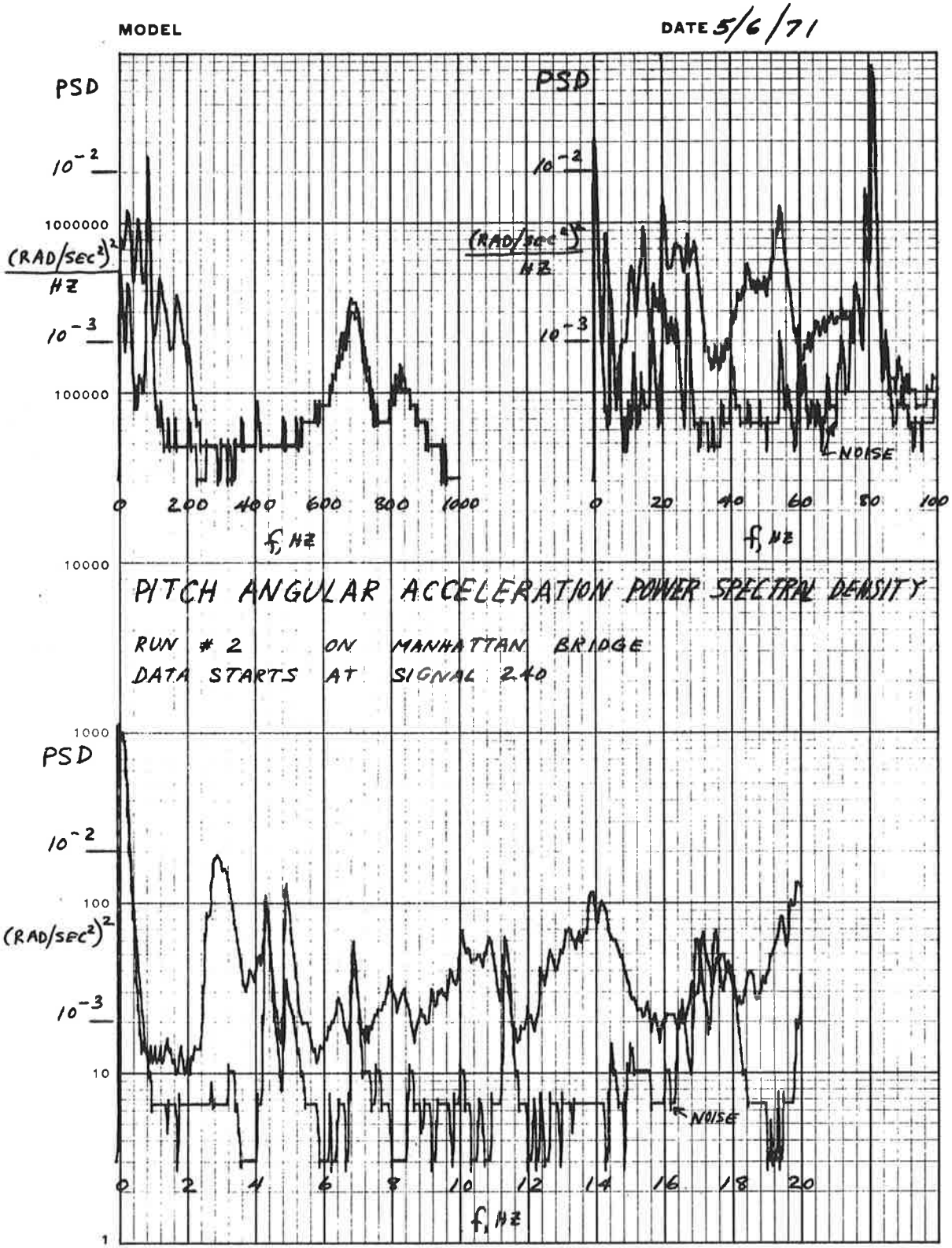

Figure 15. Run #2 Pitch Angular Acceleration Power Spectral Density, on Manhattan Bridge

expected that the dominant modes of vibration would be the first body bounce and first body pitch modes. It is somewhat surprising that the first body bounce mode is not strongly evident.

This may be the result of strong coupling between the longitudinal vibrations of the vehicle and the pitch motions and is somewhat confirmed by the presence of significant energy levels in the longitudinal vibration spectra in the 2-4 Hz as shown in figures 16, 17 and 18.

To confirm this hypothesis more detailed data would be required on the track irregularities and on the vehicle vibrations than is currently available. A more detailed definition of the dynamics of the vehicle and the track irregularities will be the objective of future tests.

Lateral Vibration

The analyses of Appendix A indicate that the following modes of vibration are expected to be significant for lateral motions:

Mode	Natural Frequency
Lateral Body	0.74 Hz
First Body Roll	1.2 Hz
Body Yaw	2.0 Hz
Second Body Roll	7.1 Hz

The rms lateral vibrations measured during the test runs were between 0.02 and 0.06 g rms. The dominant frequencies of about 0.8 Hz to 1.2 Hz and 8.7 Hz shown in the power spectral Densities of figures 19, 20 and 21 appear to be the lateral body, first body roll and second body roll natural frequencies. The coupling between the lateral vibrations and body roll motions is evidenced by the roll motion power spectral densities shown in figures 22, 23 and 24.

The changes in the dominant frequency between 0.8 and 1.2 Hz may be the result of a beat between the two modes and an energy transfer that is averaged by the data analysis equipment.

The yaw spectra shown in figures 25, 26 and 27 do not indicate any significant dominant frequencies. The peaks between 4 and 8 Hz may be due to changes in instrumentation noise rather than vibration sensed by the accelerometer. A higher sensitivity will be required for future yaw motion measurements.

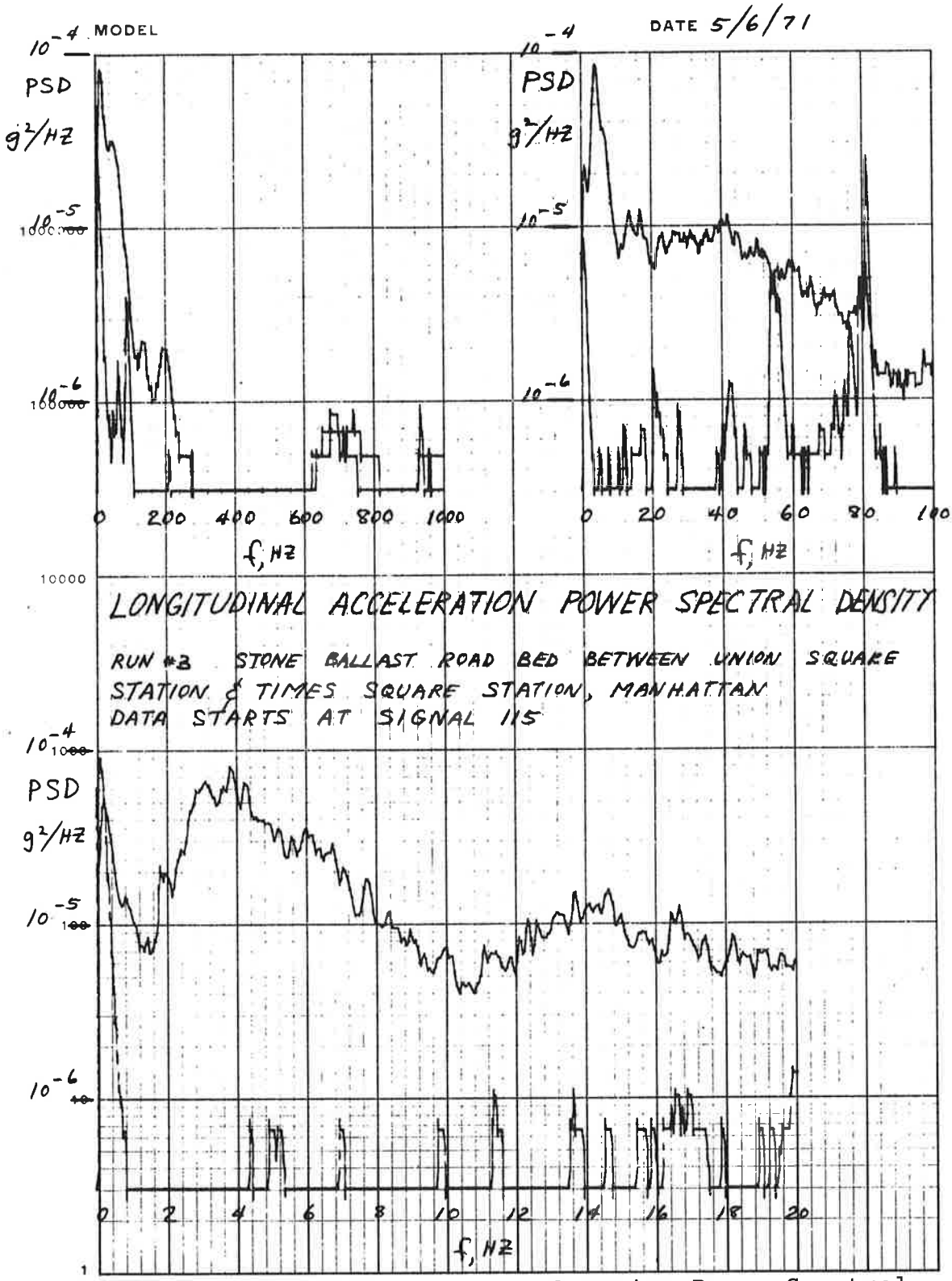

Figure 16. Run #3 Longitudinal Acceleration Power Spectral Density, Stone Ballast Road Bed

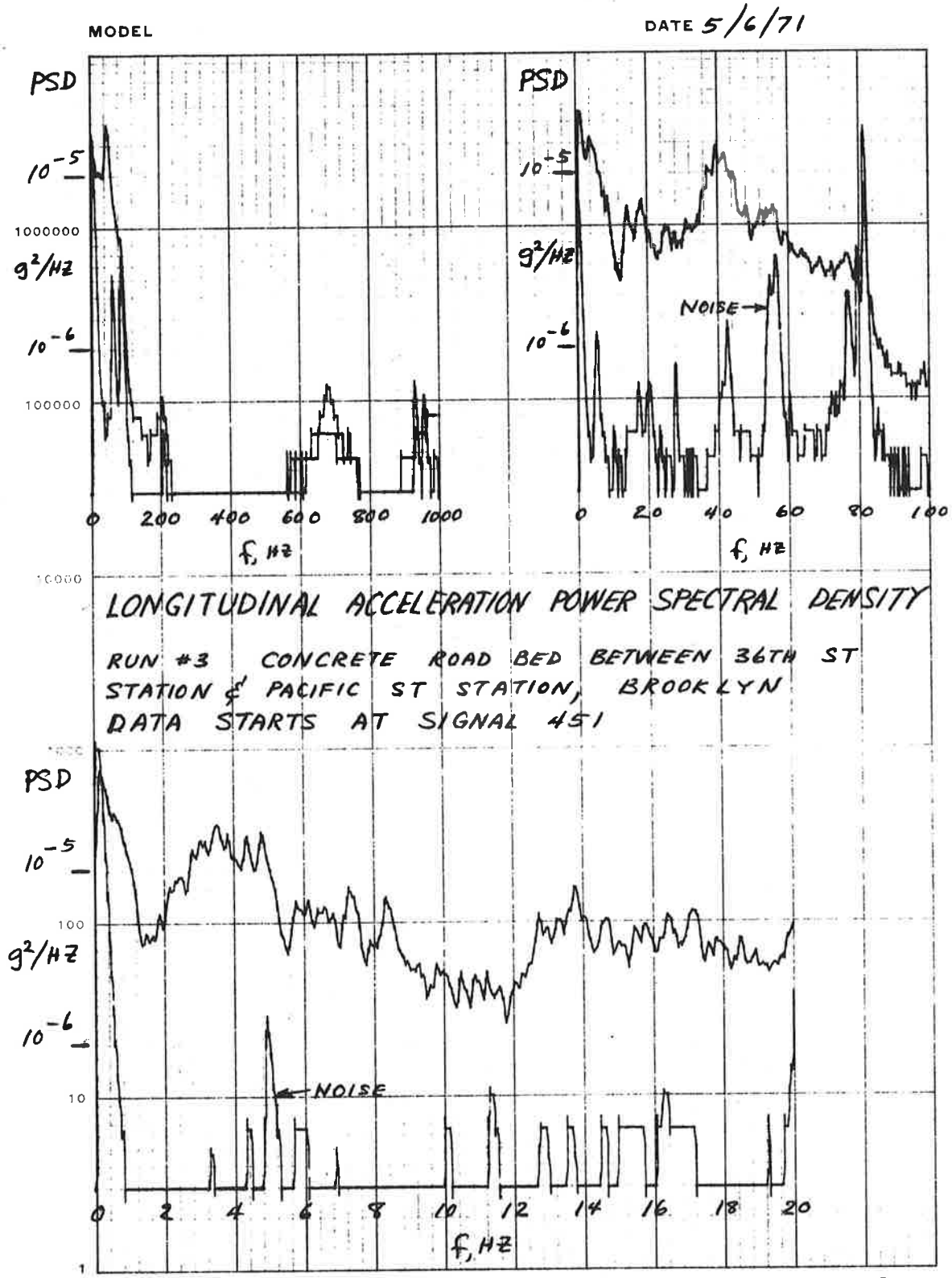

Figure 17. Run #3 Longitudinal Acceleration Power Spectral Density, Concrete Road Bed

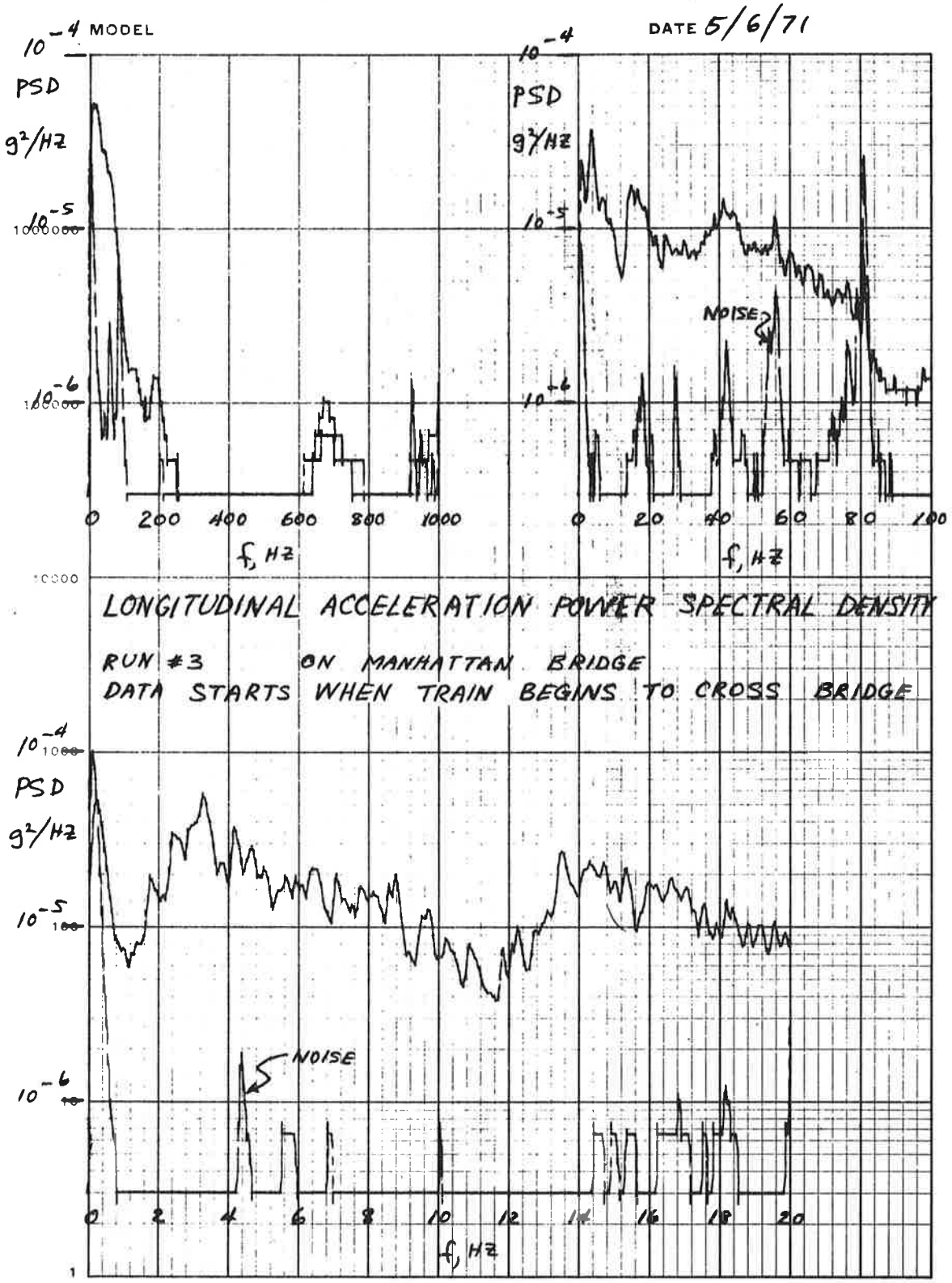

Figure 18. Run #3 Longitudinal Acceleration Power Spectral Density, on Manhattan Bridge

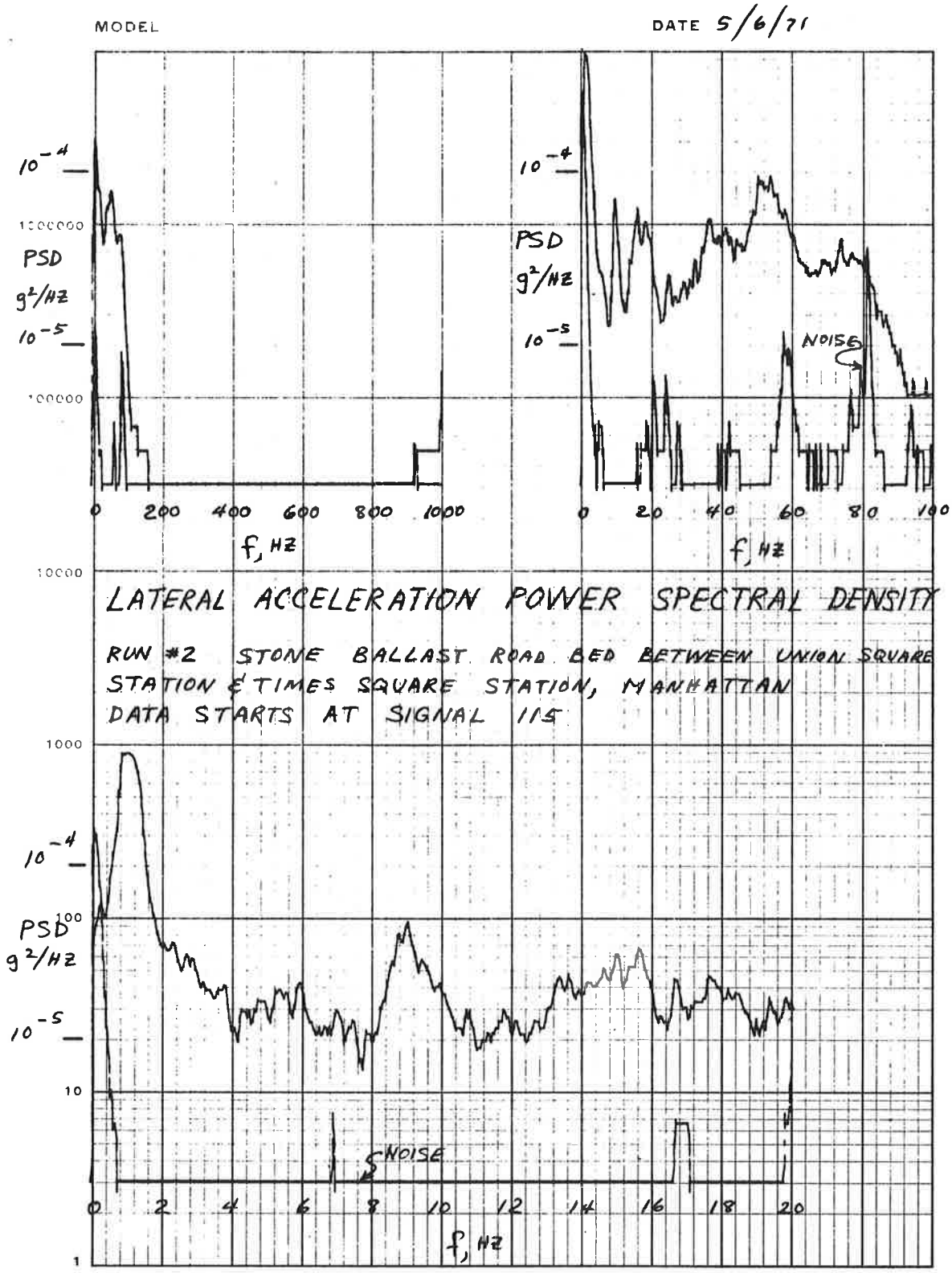

Figure 19. Run #2 Lateral Acceleration Power Spectral Density, Stone Ballast Road Bed

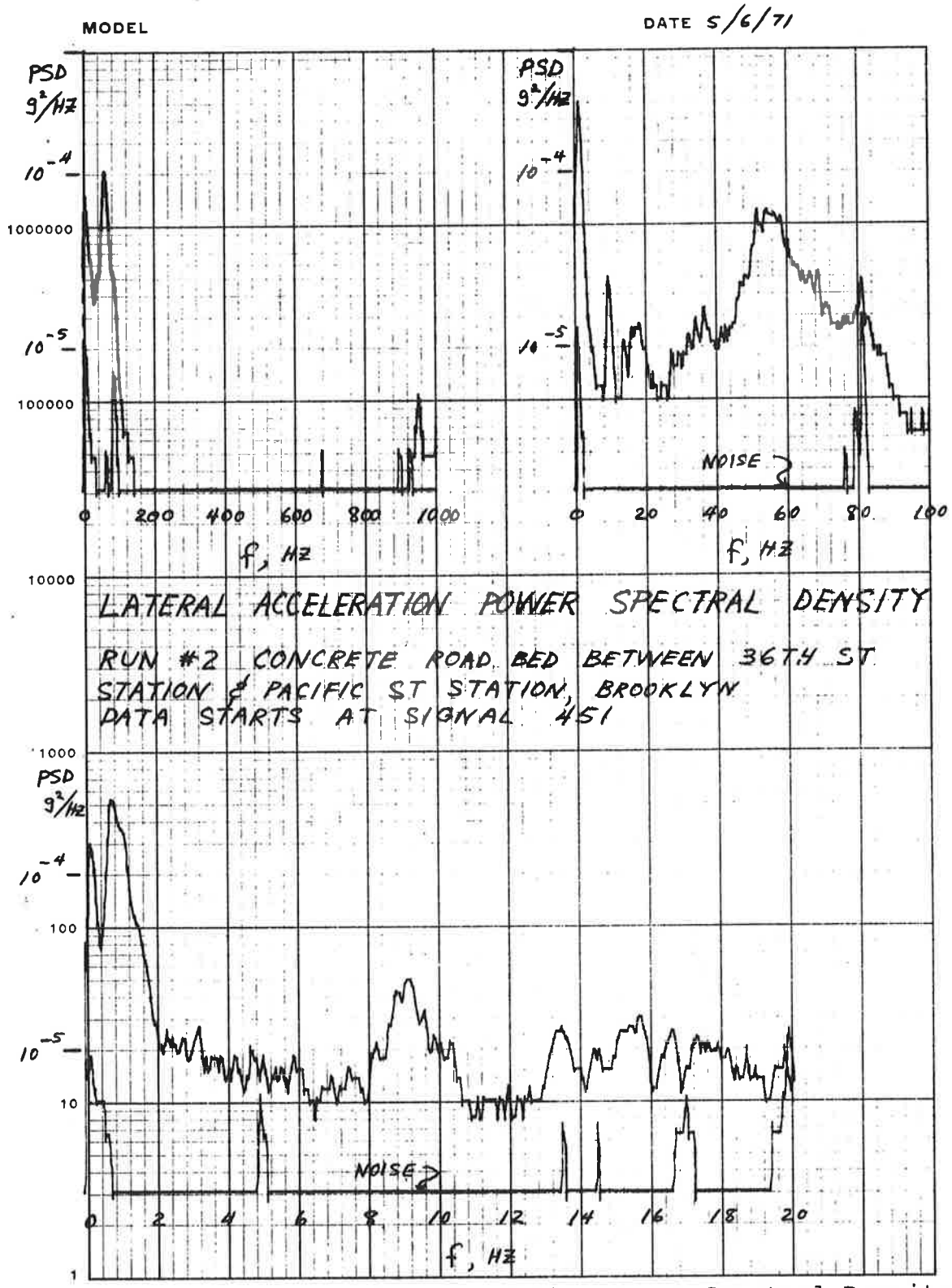

Figure 20. Run #2 Lateral Acceleration Power Spectral Density, Concrete Road Bed

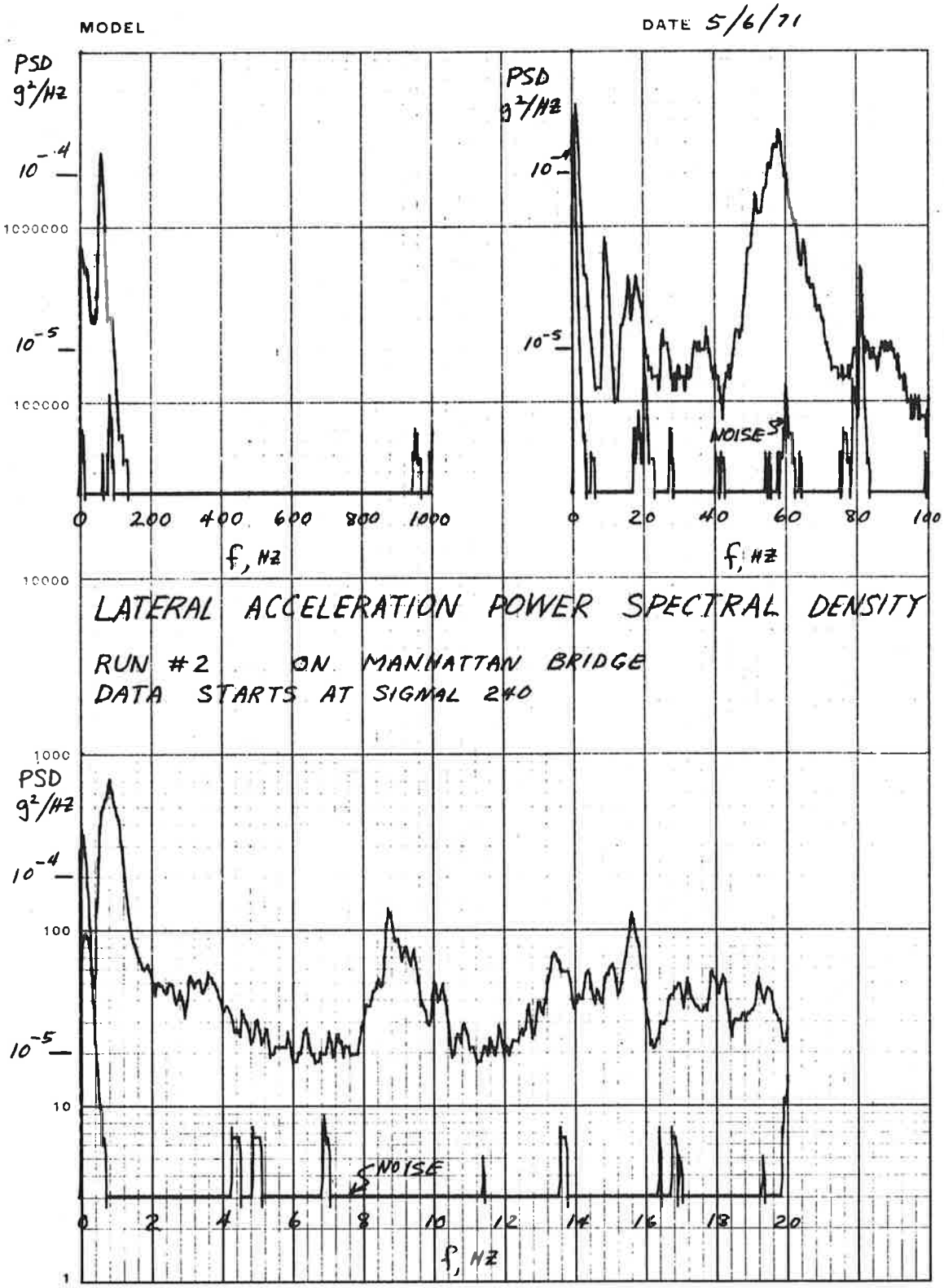

Figure 21. Run #2 Lateral Acceleration Power Spectral Density, on Manhattan Bridge

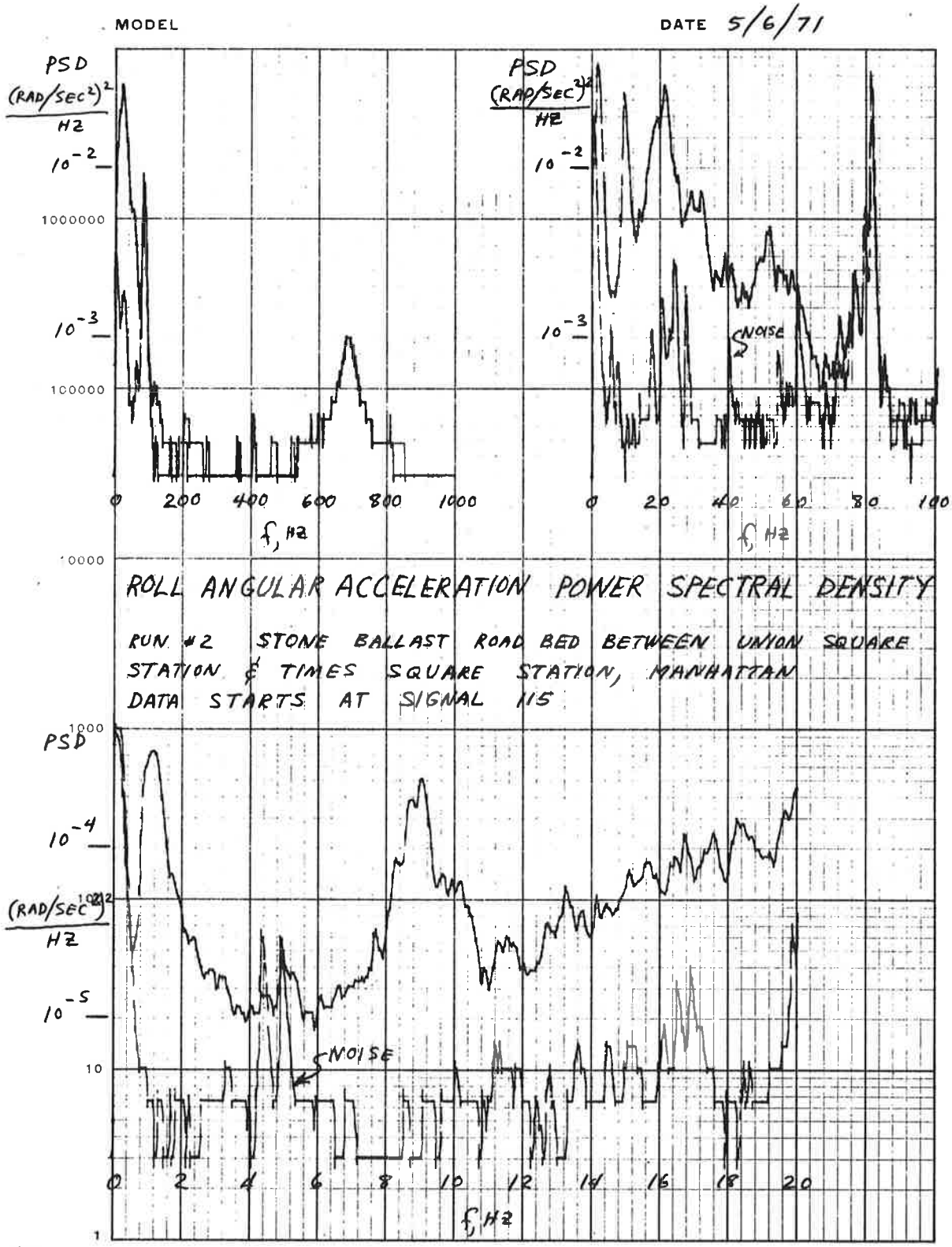

Figure 22. Run #2 Roll Angular Acceleration Power Spectral Density, Stone Ballast Road Bed

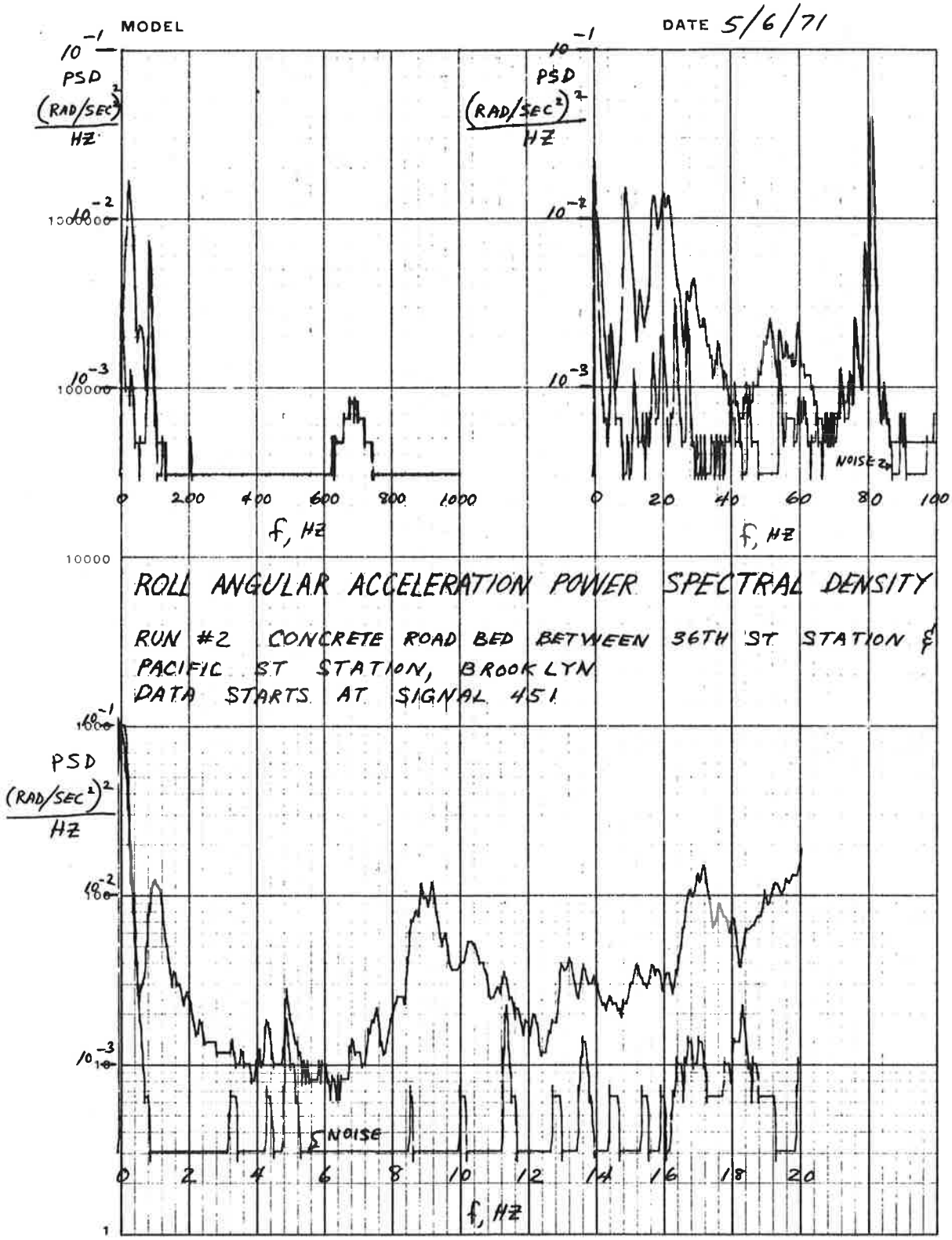

Figure 23. Run #2 Roll Angular Acceleration Power Spectral Density, Concrete Road Bed

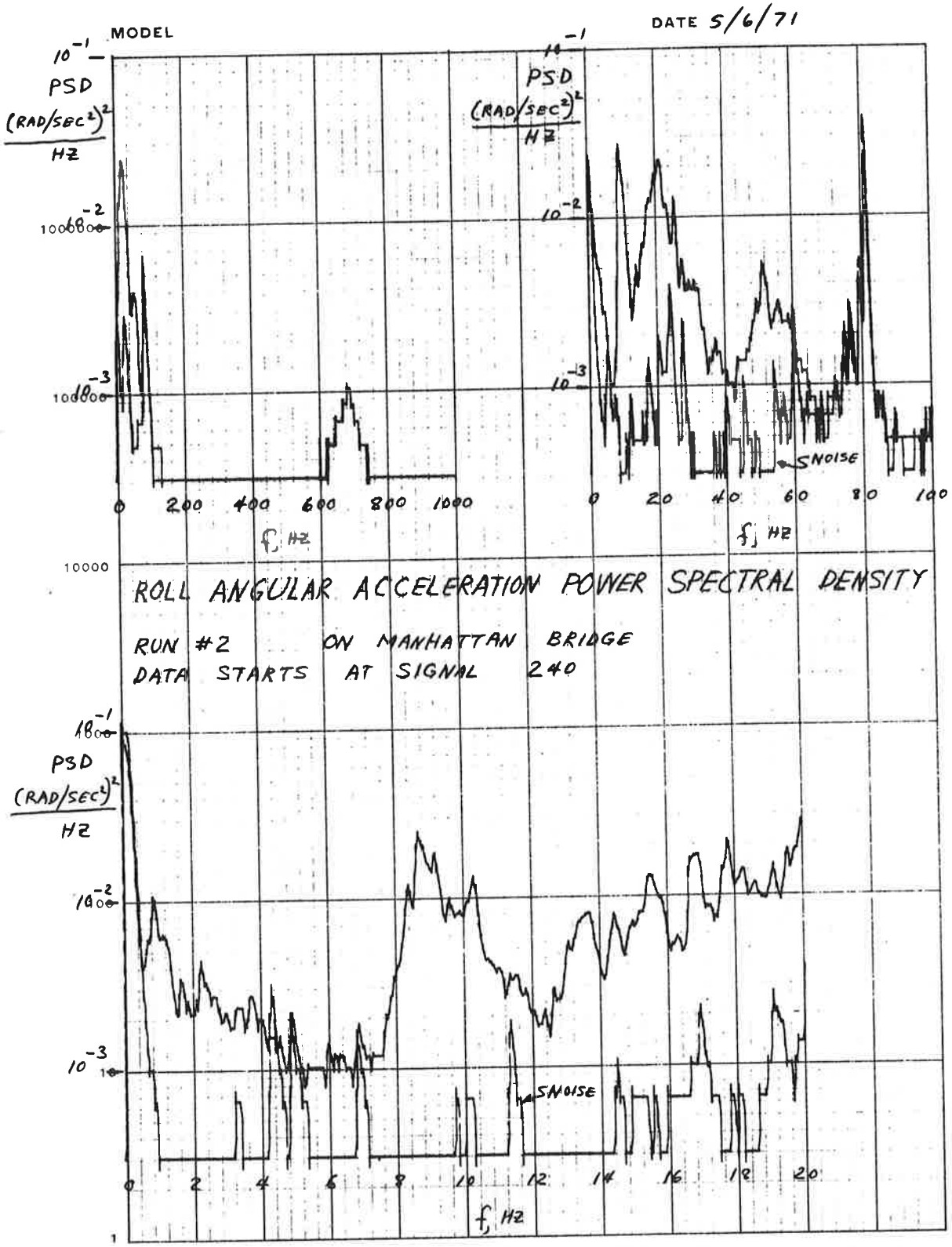

Figure 24. Run #2 Roll Angular Acceleration Power Spectral Density, on Manhattan Bridge

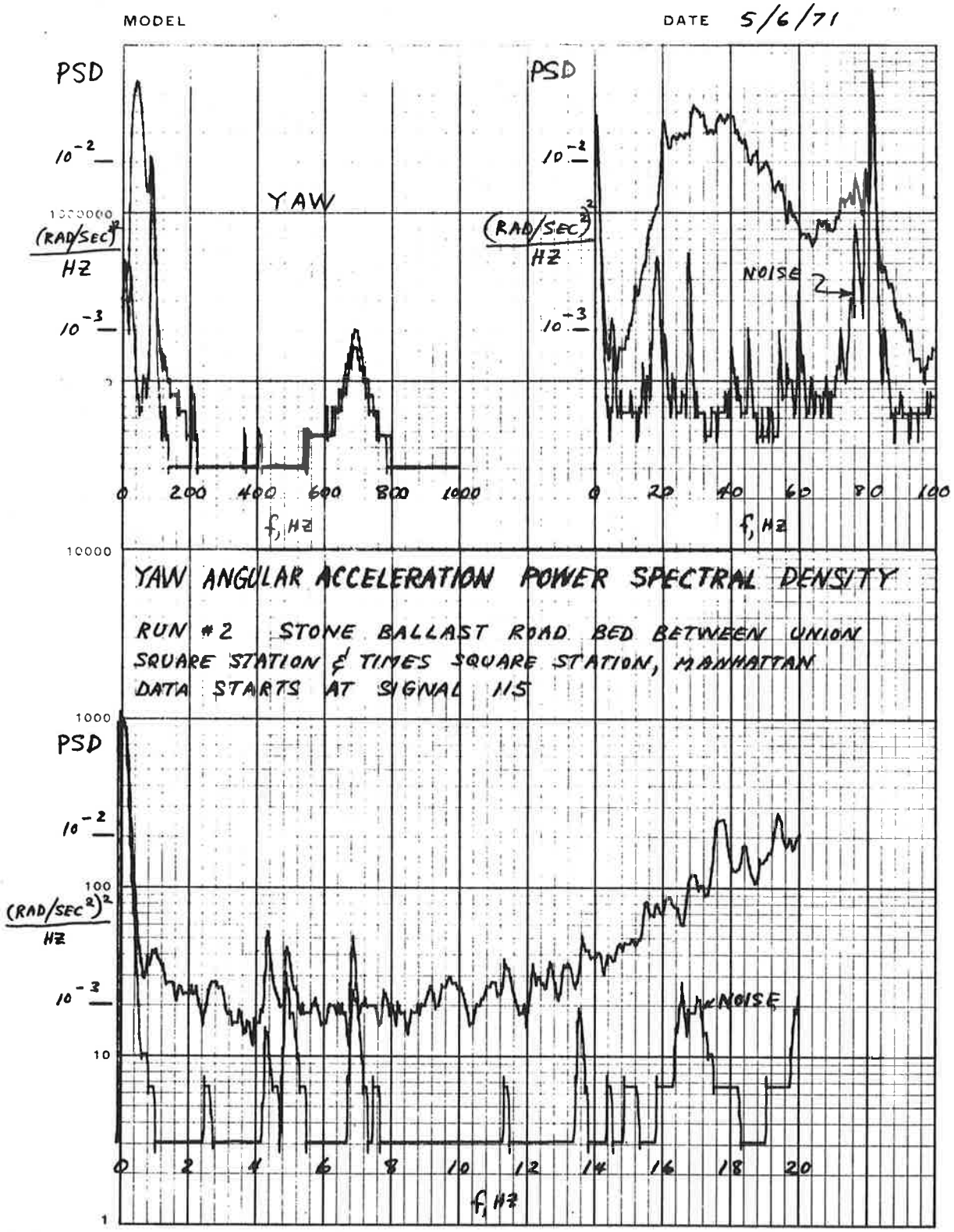

Figure 25. Run #2 Yaw Angular Acceleration Power Spectral Density, Stone Ballast Road Bed

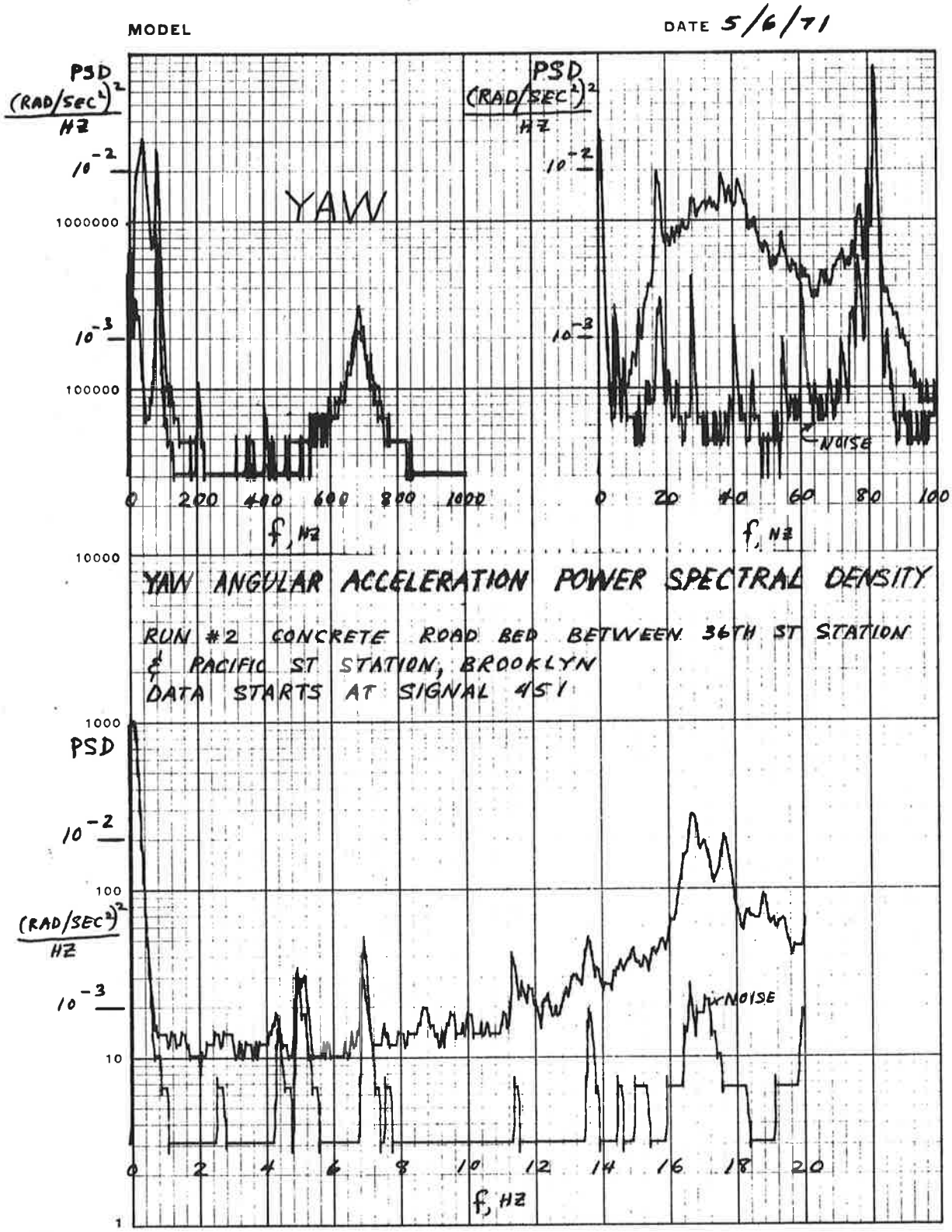

Figure 26. Run #2 Yaw Angular Acceleration Power Spectral Density, Concrete Road Bed

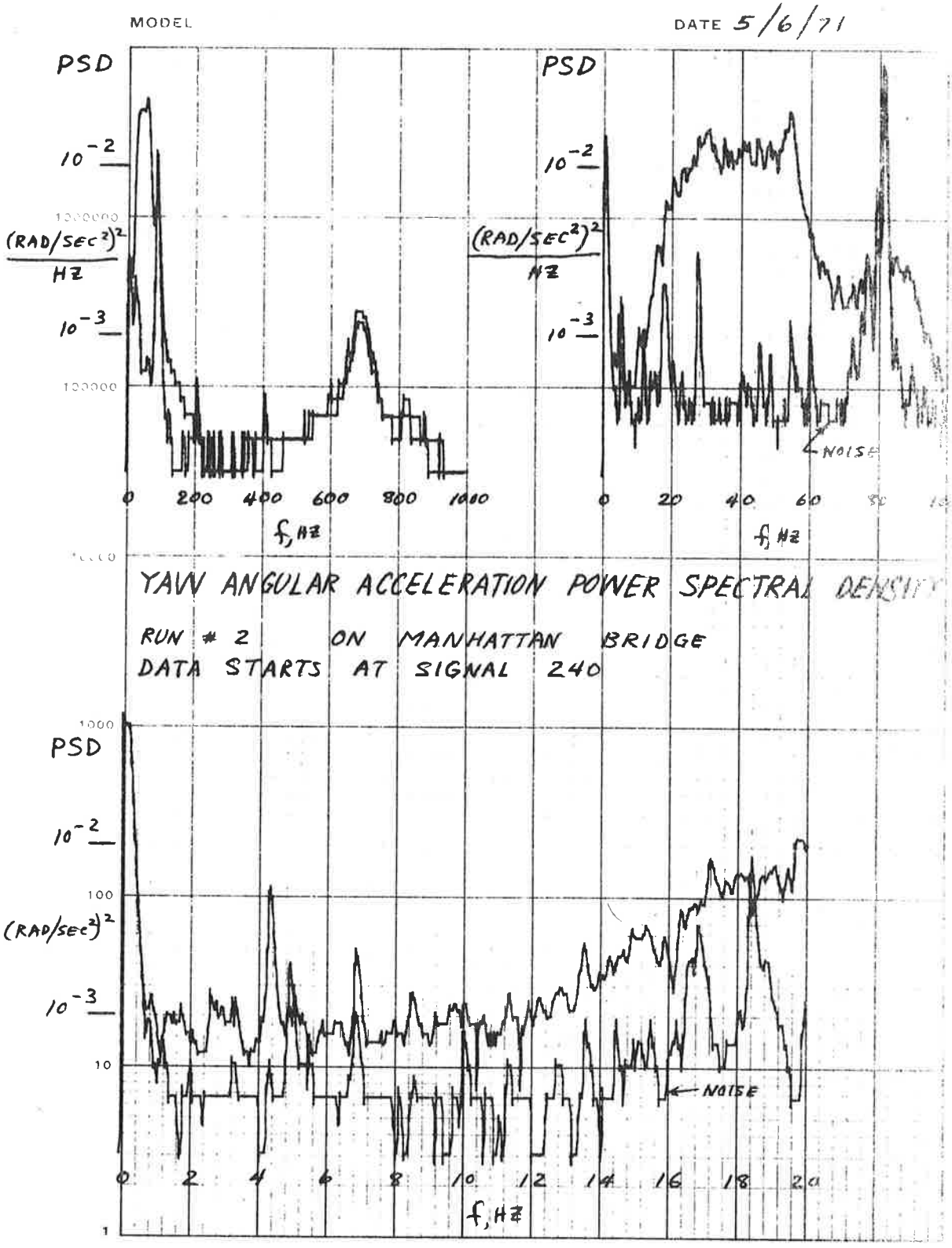

Figure 27. Run #2 Yaw Angular Acceleration Power Spectral Density, on Manhattan Bridge

Comparison of Results with Previous Vibration Measurements

In 1963, Operations Research Incorporated carried out a noise and vibration measurement program for the National Capital Transportation Agency on major rapid transit systems throughout the world[2]. Their tests in New York City were carried out on sections of the express track of the BMT line between 14th Street and 57th Street in mid-Manhattan. The test run was on wooden cross ties set in concrete, with an empty invert between the rails. Their vibration pickups were located on the floor over the front truck of the third car of a four-car train of empty cars. Their test runs were constant speed runs at 15 and 30 mph of 60 seconds duration on straight level track in the subway tunnel.

ORI processed their data by performing an octave-band frequency-spectrum analysis between 4.5 and 1200Hz yielding the magnitude of vibration acceleration in each octave band in g rms. They also computed an amplitude histogram for vibrations in the frequency range 2.2 to 10 Hz. The data reduced in this report can be compared with the ORI spectrum analysis by reducing the appropriate PSD to an octave band presentation. The octave bands used by ORI are shown in Table 2.

TABLE 2. OCTAVE BAND FREQUENCIES

Operations Research Inc.

Center Frequency Hz	Lower Band Edge Hz	Upper Band Edge Hz
6.25	4.5	9
12.5	9	18
25	18	37
50	37	75
100	75	150
200	150	300
400	300	600
800	600	1200

International Organization for Standardization

Center Frequency Hz	Lower Band Edge Hz	Upper Band Edge Hz
1.4	1	2
2.8	2	4
5.6	4	8
11.2	8	16
22.5	16	31.5

TABLE 2. OCTAVE BAND FREQUENCIES (CONTINUED)

Center Frequency Hz	Lower Band Edge Hz	Upper Band Edge Hz
45	31.5	63
75	63	90

The TSC run, reported on here, that most clearly compares with the ORI data, is run 3 on the concrete roadbed. The octave band presentation of the TSC data is an approximation because the logarithmic PSD plots were used to calculate areas under the best straight line approximation to the plotted curves in each octave band. Thus the octave band approximation of the TSC data would tend to be higher than the actual value, perhaps on the order of 10% or more. Since, the average speed during Run 3 was if anything higher than during Run 1, the appropriate ORI data to compare with the TSC run 3 on concrete is their 30 mph data. This is done in figure 28 for vertical vibration with the dashed - line curves. Observe that from 9 to 75 Hz the two data sets are in very close agreement. The divergence of these curves above and below this frequency range could be for many diverse reasons. Some of which would be differences in train speed, differences in instrumentation, different trains, different sections of concrete road bed, differences in data processing, etc. In the light of these differences, it is perhaps surprising that such close agreement has been achieved over the 9 to 75 Hz range.

Comparison of Results with Ride Vibration Standards

In 1968, the International Organization for Standardization published a Guide for the Evaluation of Human Exposure to Whole-Body Vibration.[3] The recommended vibration limits were presented in terms of three main human criteria: the preservation of working efficiency; the preservation of health or safety; and the preservation of comfort. Four physical factors considered of primary importance in determining the human response to vibration were the intensity, frequency, the direction, and the duration (exposure time) of the vibration.

The first of the human criteria, the preservation of working efficiency is delineated by the "Fatigue Decreased Proficiency Boundary".

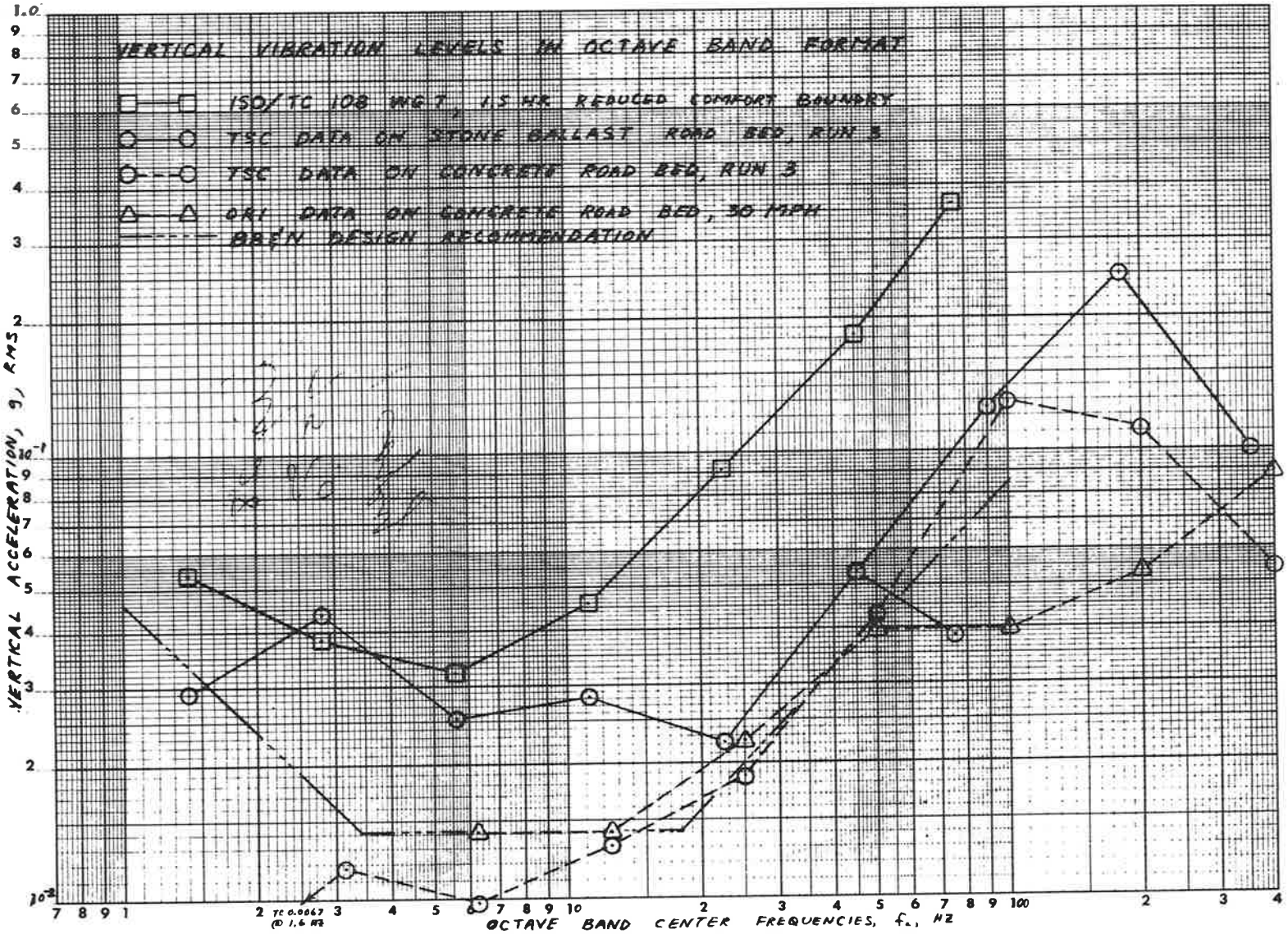

Figure 28. Vertical Vibration Acceleration Levels in Octave Band Format

The preservation of health or safety is proscribed by the "Exposure Limit". The Exposure Limit is of the same general form as the Fatigue Decrease Proficiency Boundary but the corresponding levels are increased by a factor of 2. The preservation of comfort is achieved when vibration levels are below the "Reduced Comfort Boundary". In the ISO standard, the Reduced Comfort Boundary is approximately one third the corresponding intensity of the Fatigue Decreased Proficiency Boundary. It is the ISO, 8 hour exposure Fatigue Decreased Proficiency Boundary for vertical (head-to-foot) vibrations that is presented in Figure 28 for comparison with the data recorded by TSC.

This same curve is also the 1.5 hour exposure Reduced Comfort Boundary. The TSC data that is reduced for comparison with the 1.5 hour Reduced Comfort Boundary is from the roughest ride observed during the testing, the section of track on stone ballast from 14th Street to 42nd Street. The TSC data (solid lines) lies under the 1.5 hour Reduced Comfort Boundary except for one frequency point and the measured vibration level at that point does not exceed the boundary point by more than the approximation error in calculating the octave band values from the PSD curves. Considering that subway passengers would rarely ride for more than 1.5 hours and that the rest of the ride was smoother than the portion represented by the data presented here, one can conclude that the R-42 cars operated on the New York Transit Authority meet the ISO standards of ride comfort with respect to vertical vibrations. Incidentally, the octave bands used in the ISO standards differ from the octave bands used by ORI. The octave band frequency specifications for the ISO standards are also included in Table 2.

A similar comparison for lateral vibrations is shown in figure 29. In this instance the level of lateral vibrations recorded by TSC on the concrete roadbed are lower than those of ORI for low frequencies (12.5 Hz and less) and greater than those of ORI for higher frequencies (25 Hz and above). This pattern more or less repeats the comparitive results of the vertical data except that there is no significant frequency range over which the two curves run close together.

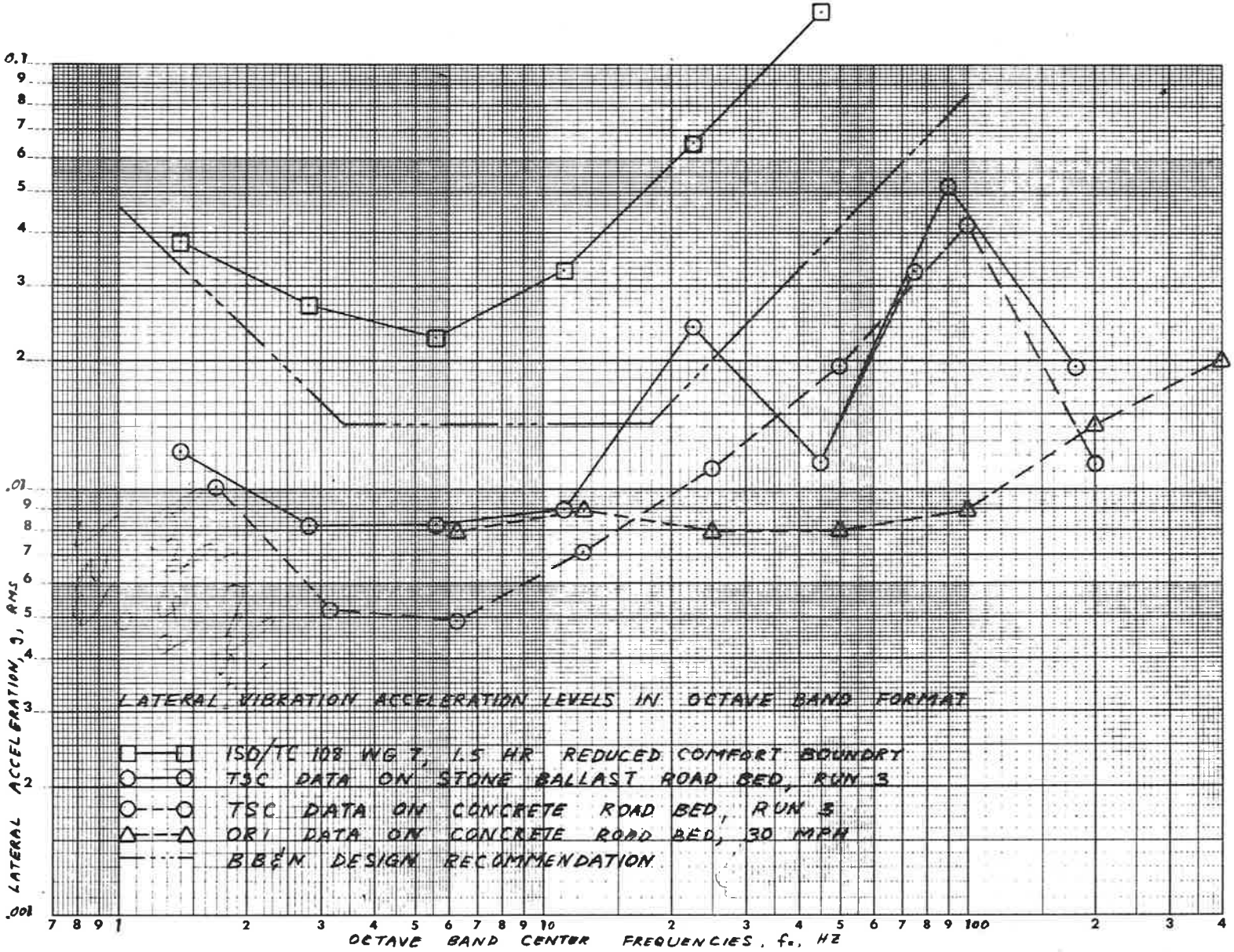

Figure 29. Lateral Vibration Acceleration Levels in Octave Band Format

TEST INSTRUMENTATION

JOURNAL BOX ACCELERATION MEASUREMENT

To measure journal box accelerations, piezoelectric accelerometers are mounted on each of the four journal boxes of one truck of the R-42 car. Figure 30 schematically indicates the location of the accelerometers and the direction of their sensitive axes. The tri-axial accelerometer package was mounted on the left rear journal box. The truck instrumented was the front truck of the lead car.

The output of each piezoelectric accelerometer is processed by a charge amplifier prior to recording on magnetic tape. The particular charge amplifiers used were designed for standard telemetry output. That is, +2.5 volts dc corresponded to zero signal. To make these units compatible with the rest of the system (0 vdc corresponding to zero signal and +2.5 volts to full scale), a 2.2 uf blocking capacitor was inserted in tandem with the charge amplifier output and a 10K load resistor was placed in shunt across the charge amplifier output. The load resistor was required to prevent charge building on the blocking capacitor. If this charge buildup was not drained off, saturation of the signal output channel occurred in a matter of seconds. The 2.2 uf blocking capacitor forms a derivative network with the 100K input impedance of the FM record amplifier. Its break frequency is less than 1 Hz so that it should not influence the data output of the charge amplifier, whose low frequency roll-off break is at 5 Hz. Each accelerometer/charge amplifier pair was calibrated with the load resistor, blocking capacitor, and simulated 100K input resistor in the system

There is wide divergence of opinion on what constitutes a comfortable ride. In 1966, Bolt, Bernek, and Newman did a study for the Massachusetts Bay Transit Authority. In this study, BB&N recommended a design peak vibration level for rapid transit cars. This design boundary, converted to rms g level, is shown in Figure 28. Note that the ride quality obtained on concrete road bed very closely approximates this recommendation.

Figure 29 shows the ISO 1.5 hour exposure Reduced Comfort Boundary for lateral vibration and the BB&N design vibration limit. In the case of lateral vibrations, all of the data lies well below the ISO curve and all except one point lies below the BB&N curve. From this, it is seen that the ride observed is very smooth with respect to lateral vibrations.

A block diagram of the instrumentation setup for this measurement is shown in Figure 31. As shown, the "raw data"

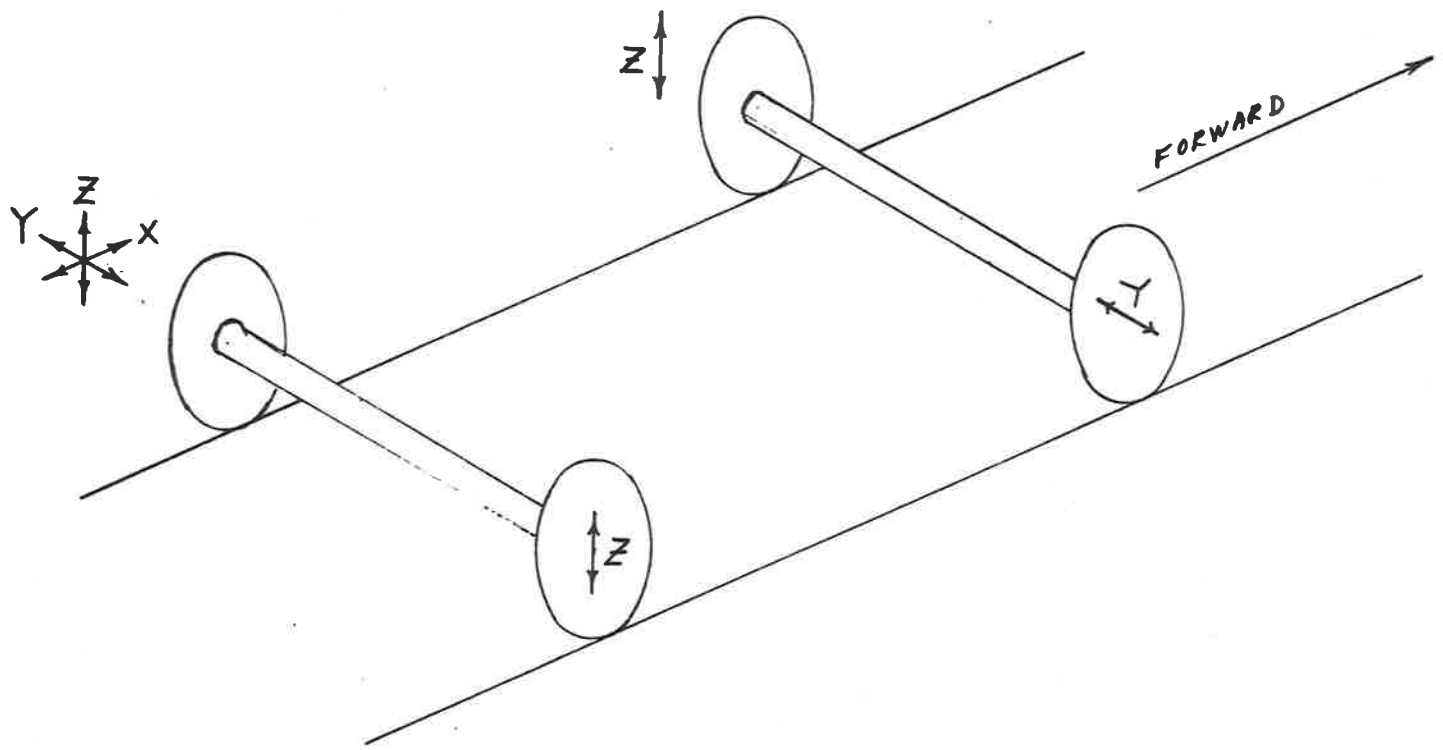

Figure 30. Journal Box Accelerometer Location

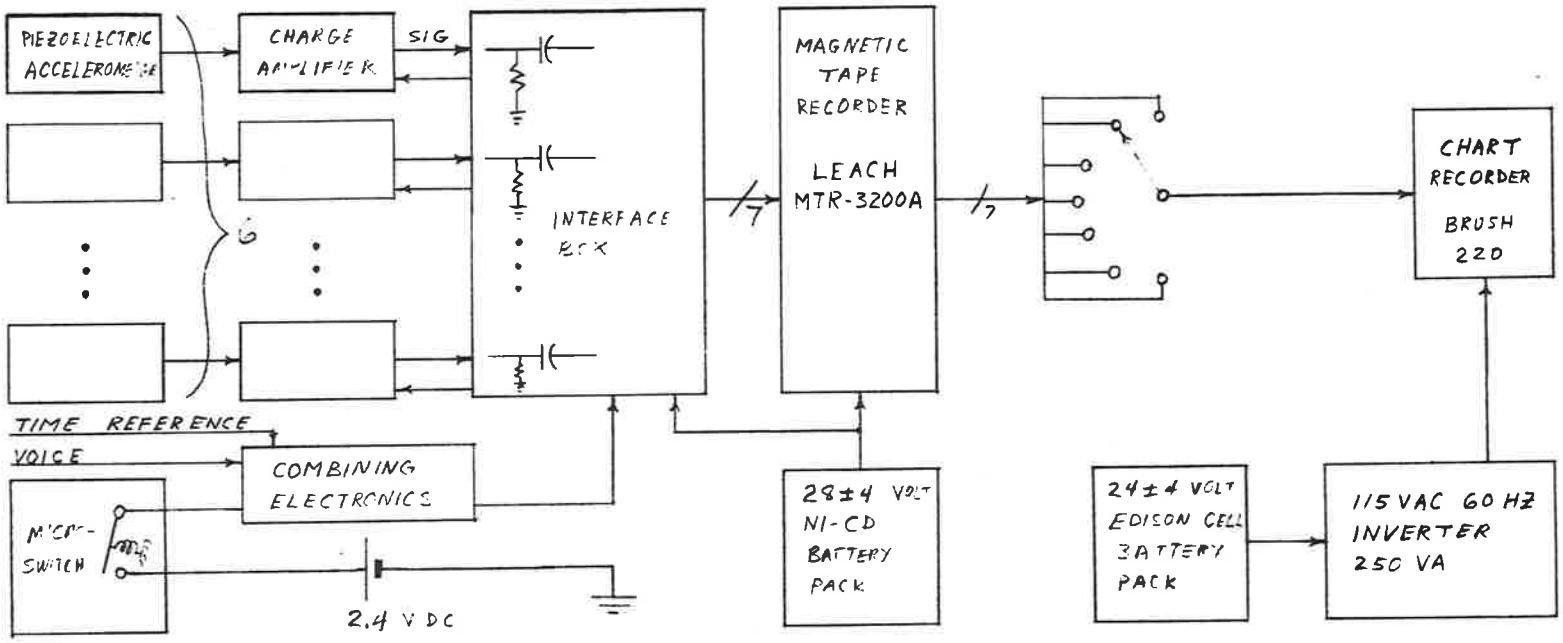

Figure 31. Instrumentation Block Diagram for Journal Box Acceleration Measurement

from the accelerometers are FM recorded on six tracks of the half inch magnetic tape. On the seventh track, a pulse train was direct recorded. The pulse train was generated by the closing of a micro-switch which applied a low battery voltage across the direct record input amplifier. The micro-switch was mounted under the car near the axle. A bolt screwed into a tapped hole in the axle was used to cam the micro-switch. Thus one pulse per revolution was generated. A voice annotation was used to modulate a time reference signal (10 kHz - 15 kHz) that was generated by the accoustic measurement system. This amplitude modulated signal was also combined with the pulse train prior to direct recording.

During the test, the tape recorder reproduce electronics were activated to provide capability to monitor and chart record the signals being recorded on tape. The second channel of the two-channel chart recorder was used to display a pulse train from a second micro-switch mounted near the axle and cammed by the same bolt.

In Figure 31, the arrowheads indicate the direction of the signal flow or power flow as appropriate. The entire instrumentation package was powered by a 28 volt Ni-Cd battery pack and a 24 volt railcar Edison cell battery driving a 115 volt ac 60 Hz inverter.

Copies of the specifications of the equipment used in this test are given in Appendix B. A list of equipment make and model number follows:

Piezoelectric accelerometer, Columbia Model No. 704
Charge amplifier, Endevco Model 2642M26
Magnetic tape recorder, Leach MTR-3200A
Chart recorder, Brush Mark 220
Inverter, Topaz 250 GW-12-24-60

Prior to going to New York City for the tests the piezoelectric accelerometer and charge amplifier pairs were calibrated by bolting the accelerometer to the head of an M-B shaker, connecting accelerometer to charge amplifier, connecting charge amplifier to load resistor, blocking capacitor, and dummy input resistor (100K). The voltage developed across the 100K-resistor was read on an oscilliscope. The charge amplifier was supplied with 28 vdc power. The double amplitude of the motion of the shaker head was measured using a tool maker's microscope to measure the length of the blur specularly reflected from an illuminated piece of emory paper attached to the shaker head. For a given desired peak acceleration, $\ddot{x}_{pk}$, in g's, a frequency and double amplitude were selected that would satisfy the performance limitations of the M-B shaker and the following equation

$$\ddot{x}_{pk} = 0.051\ f^2 (DA)$$

where f = frequency, Hz

$\ddot{x}_{pk}$ = peak acceleration, g's

DA = double amplitude, inches

The gain of the charge amplifier was adjusted to yield a full scale output ($\pm$ 2.5 volts) corresponding to $\pm$ 100g acceleration or a scale factor of 25 mv/g.

CAR - BODY FLOOR ACCELERATION MEASUREMENT

To measure "whole-body" vibrations of the rail car, a sensor block was placed on the floor of the car. This sensor block contained three linear and three angular accelerometers mounted so as to measure accelerations along and about three orthogonal axes. All six accelerometers were of the force-balanced type. The sensor block with accelerometer locations is diagrammed in Figure 32. This sensor block rests on three conical, pointed feet so arranged that they form the apexes of an equilateral triangle. Normally, it is expected that during a test these feet, which are threaded onto a through stud, would be turned and clamped as close to the block as possible. Because of the pressure of the short time at New York, an oversight resulted in these feet being several inches below the sensor block. Thus, at least one resonance in a horizontal vibration mode could be from the elastic deflection of the legs of the sensor block.

The instrumentation setup for the measurement of carbody accelerations is block diagrammed in Figure 33. In this diagram, the signal flow is shown with solid lines and the power flow with dashed lines. The scaling amplifiers are included in the Endovco "g-monitor" assemblies, all of which are physically located in the interface box for this instrumentation set-up. For the New York City runs the scaling amplifiers were set so that full scale output, 2.5 volts dc, corresponded to 0.5g acceleration, yielding a linear accelerometer scale factor of 5 volts/g. The raw outputs of the angular accelerometer have a scale factor of 0.08325 volt/radian/sec^2. The six accelerometer outputs were FM recorded on six tracks of magnetic tape. A voice annotation was direct recorded on the seventh track. Somewhere on the return trip after the first run, the microswitch sending one pulse per car-sheel-revolution was damaged and ceased to function. Thus, the pulse generation mechanism is not indicated in Figure 33. The tape recording was monitored by playing back the recorded signal to a chart recorder. A 28 volt Ni-Cd battery pack supplied raw power to the accelerometers and the tape recorder. A 24 volt Edison cell battery pack supplied power for the chart recorder and rms voltmeter.

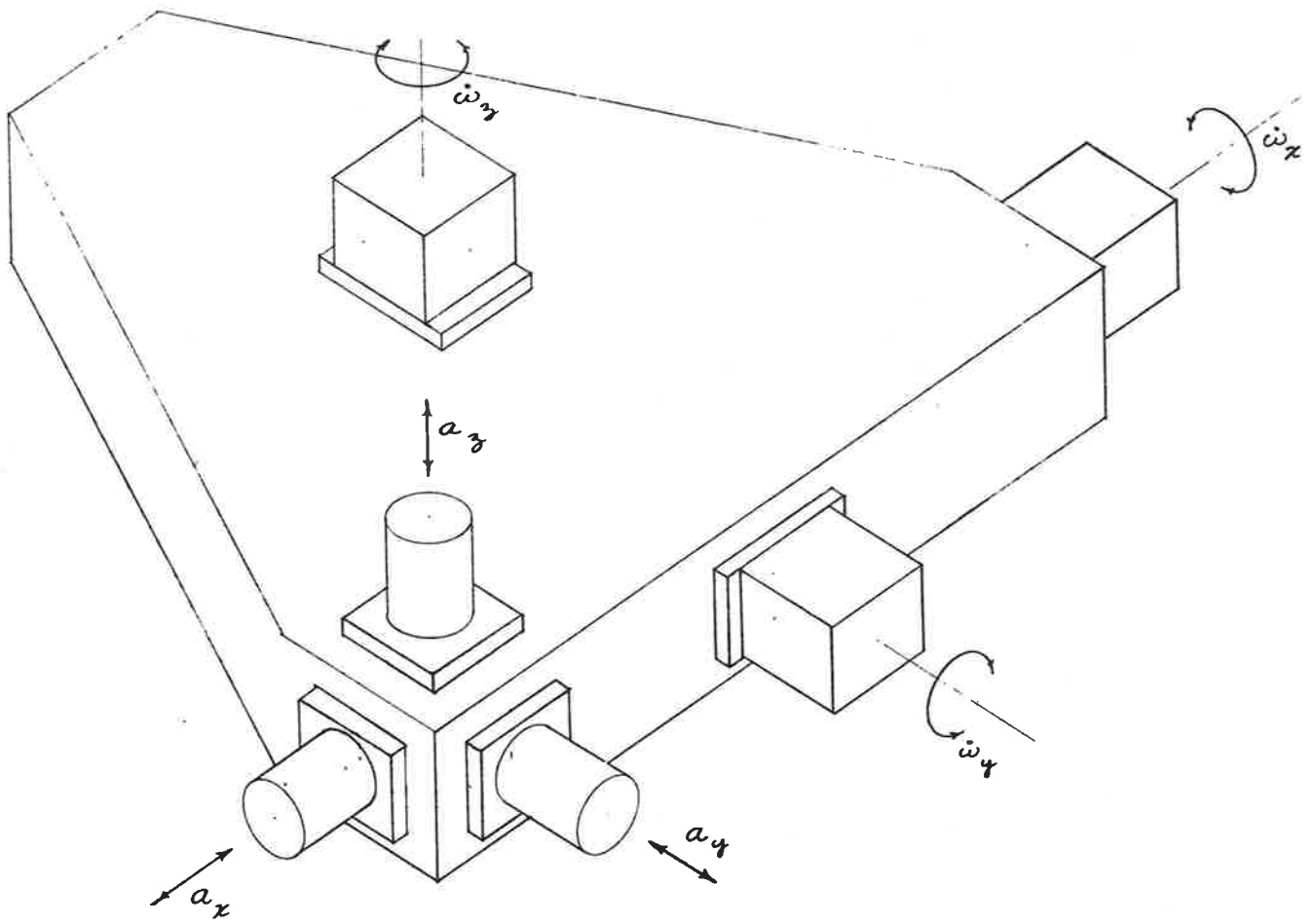

Figure 32. Car-Body Acceleration Sensor Assembly

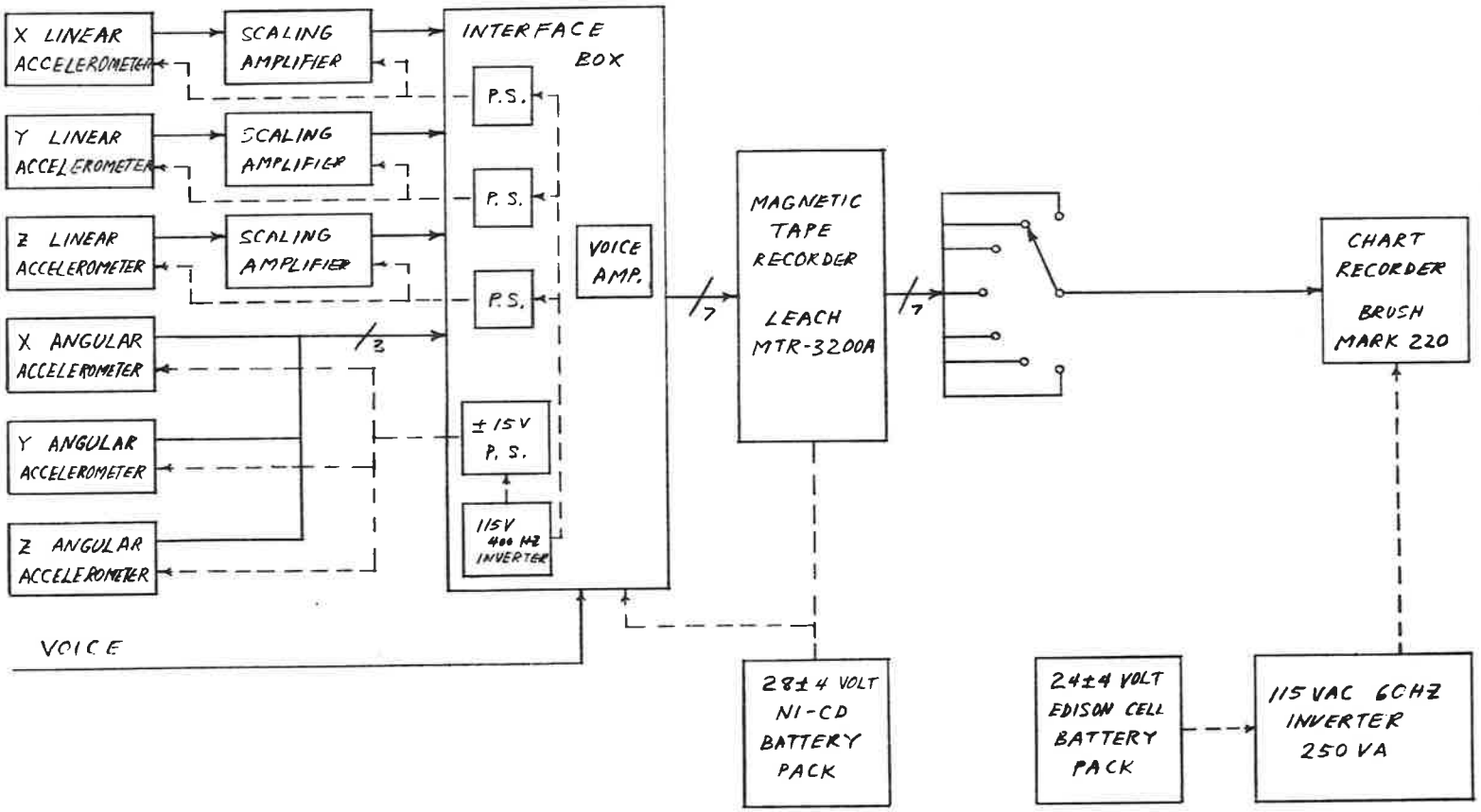

Figure 33. Instrumentation Block Diagram for Car-Body Acceleration Measurement

Copies of the specifications for the equipment used in this test are given in Appendix B. A List of equipment make and model number follows:

Linear accelerometer, Endevco QA-116-15
g-Monitor, Endevco SC-116-2
Angular accelerometer, Schaevitz ASM
115 volt 400 Hz inverter, Arnold Magnetics SKB-28-115-400-50
Magnetic tape recorder, Leach MTR-3200A
Chart recorder, Brush Mark 220.

DESCRIPTION OF TESTS

TEST ROUTE

The tests were conducted on the "Sea Beach" (N) line from 86th Street in Brooklyn to 57th Street in Manhattan. Our two R-42 cars were the lead cars of a special (no passenger) eight car train. From 86th Street Brooklyn to 59th Street Brooklyn (about two miles) the track consisted of conventional wood ties on stone ballast in an open cut and fill roadway.

At 59th Street the track enters the subway tunnel and continues with the same type of track construction until 36th Street Brooklyn. From 36th Street to Pacific Street there is a newer section of track using the split wood tie fastened directly to the concrete floor of the tunnel. From Pacific Street on, the track remains with the stone ballast wood tie type of construction in the tunnel. In crossing the Manhattan Bridge the track is an open wood tie on steel grider type of construction. The use of this route permitted us to obtain data on several different types of typical construction in a single set of test runs.

SEQUENCE OF EVENTS

Run No. 1

On the first run, the journal box accelerations were measured. The train operator was instructed to follow a speed profile typical for passenger operation on that line. The objective here being to map the test route in terms of speed, distance, and track induced accelerations. It was particularly appropriate to do this first since it was not known how long the hastely rigged speed and distance pulse markers (the micro-switch mounted near the axle) would last. They survived to the end of the first run only. A detail account of events that occurred during the first run is given in Appendix C. From this account the limited use that can be made of the pulse from the micro-switches for speed and distance information is evident. The operator slowed the train down for what would normally be stops but did not stop unless requested to or for traffic conditions. The run ended at 57th Street Manhattan. On the return trip, instrumentation was turned off and reconnected for the next test run.

Run No. 2

On the second and third runs, the accelerations of the floor of the car were measured. During run No. 2, the sensor assembly was placed on the floor of the car at a point on the car center-line approximately 20 feet aft of the pivot point of the front truck. Thus, the linear and angular accelerations experienced by that piece of the car-body floor for one test run are recorded. The detailed account of events during run No. 2 is given in Appendix C.

Run No. 3

On the third run, the acceleration sensor assembly was placed on the car floor directly over the front truck pivot point. The detail description of events on the third run is given in Appendix C.

By counting pulses recorded on the strip chart during each second of the run and pulses played back from the magnetic tape, an estimate of the train speed profile was obtained. This was done manually for each second of run 1 and the resulting speed profile is shown in Figures 5 and 6. Since no speed information is available for runs 2 and 3, the best policy would seem to be to assume that the train speed profile was similar to that of run 1 unless additional information is available to change that assumption. For example, during run 2, the train stopped on Manhattan Bridge to pick up construction workers. During runs 1 and 3, the train did not stop on the bridge. Because the subway crew was in a hurry to get us off their tracks before rush hour, run 3 seemed to be run at a higher average speed than either runs 1 or 2.

Taking these factors into consideration, the following speed ranges were observed during run 1 over the three data segments used:

On stone ballast road bed starting at signal 106, speed varies between 20 mph and 40 mph;

On concrete roadbed from signal 451 to signal 382, speed varies between 16 mph and 40 mph;

On the Manhattan Bridge from signal 268 to signal 215, speed varies between 15 mph and 24 mph.

TEST DATA PROCESSING

SUMMARY

Power spectral density analyses of the data were performed using a Saicor SAI-24/34 400 line, real time spectrum analyzer. This analyzer can resolve two sinusoidal signals of equal magnitude approximately 0.15 Hz apart in frequency on the 0-20 Hz analysis range. The position of a given spectral peak along the frequency axis is accurate to about ± 0.1 Hz on the 0-20 Hz analysis range. To provide reasonably good statistical accuracy, eight statistically independent samples of each type of data were averaged. Each sample was of 20 seconds duration. Three segments of data were analyzed, one for each type of road bed traversed, stone ballast, concrete and bridge. Strip chart recordings of rms values and low frequency components of the data were inspected to select the three data segments for spectral analysis.

TEST DATA PROCESSING, DESCRIPTION

One of the objectives of the New York City test was to obtain an initial or baseline set of data on the vibration environment both in the car and at the transducer location proposed for future track geometry measurements (the journal boxes). This baseline data set can then be compared with that obtained in future experiments and will permit comparisons with the results of other experimenters. To define the environment at the journal boxes, peak and rms values of acceleration are desired. Furthermore, a complete spectrum of vibration accelerations is desirable to define acceleration inputs to the car suspension systems. The spectrum of vibration accelerations in the car is required to permit comparison with published ride quality standards and for verification of models of the vehicle suspension system.

To permit identification of vibration frequencies to an accuracy sufficient to allow comparison with a theoretical model, a narrow band, constant bandwidth spectrum analysis was performed on each data segment to calculate power spectral density from each data segment. This was done using a Saicor SAI-24/34 400 line, real time spectrum analyzer/averager. With this analyzer, nominal line width on the lowest frequency analysis range, 0-20 Hz, would be 1/400 of 20 Hz or 0.05 Hz. However, to perform real time spectrum analysis, many operations are performed on the raw analog data by the analyzer. First, the data is passed through a low pass filter to prevent aliasing. Then the data is sampled at three times highest frequency of the

analysis range, coverted to digital format, and loaded into a recirculating memory which speeds up the signal presentation, thus compressing the time required to analyze the data. The sped-up memory output is converted to analog form, heterodyned with a weighting function and a stepped voltage-controlled-oscillator output to permit its analysis by a narrow-band crystal filter. The filter output is linearly detected and, in the PSD analysis used here, squared in a squaring circuit prior to digital averaging. The digital averager again converts the analog spectrum output to digital format and stores the magnitude of each line of each spectrum as it is measured. Division by the number of samples is done digitally. The contents of the averager memory are converted to analog form to permit viewing on an oscilloscope or plotting on a chart recorder or an X-Y plotter. A set of specifications for the SAI-24/34 is given in Appendix D.

All this processing does something to a single frequency "line" of a sinusoidal input. It broadens it. If 1/400 of the analysis range is considered the nominal resolution element of bandwidth B Hz, and, if a single frequency, sinusoidal signal is the input to a SAI-24/34, the displayed output spectrum plotted will be 3B wide at 3db down from the spectrum peak, 6.3B wide at -10db from the peak, and 9.8B wide at -20db from the peak. This analyzer spectrum was measured while using the Hamming window or weighting function in the analyzer. This spectral response showed that we can indeed, identify a single frequency input to a resolution of B Hz. However, if a second sinusoid of the same magnitude as the first is also present in the input, its frequency must be at least 3B Hz removed from that of the first sinusoid before a 3db valley can be seen between peaks. As the amplitude of the sinusoidal signals differ by an increasing amount, their frequency separation must increase to permit identification of the separate frequencies.

The frequency axis of the spectrum display is driven by the output of the VCO. The observed frequency of the displayed spectrum depends upon the calibration of the VCO sweep voltage. The VCO was calibrated according to the manufacturers instructions and then a frequency calibration run was made by adding the spectrum from calibrated (Beckman EPUT counter) sinusoidal inputs consecutively, in the averager memory. The results of this are shown in Figure 34. For example, the inputs to the 0-20 Hz range were at 1, 2, 4, 8, 12, 16, 18, and 19 Hz. Incidentally, care was taken to make each input exactly 0.5 V rms so that this frequency calibration also provides a rough indication of the frequency response of the analyzer. Figure 34 shows that at the low frequency end of the range, the frequency indicated for the 1 Hz input is 1.1 Hz, and at the high frequency end of the range, the frequency indicated for the 19 Hz input is slightly

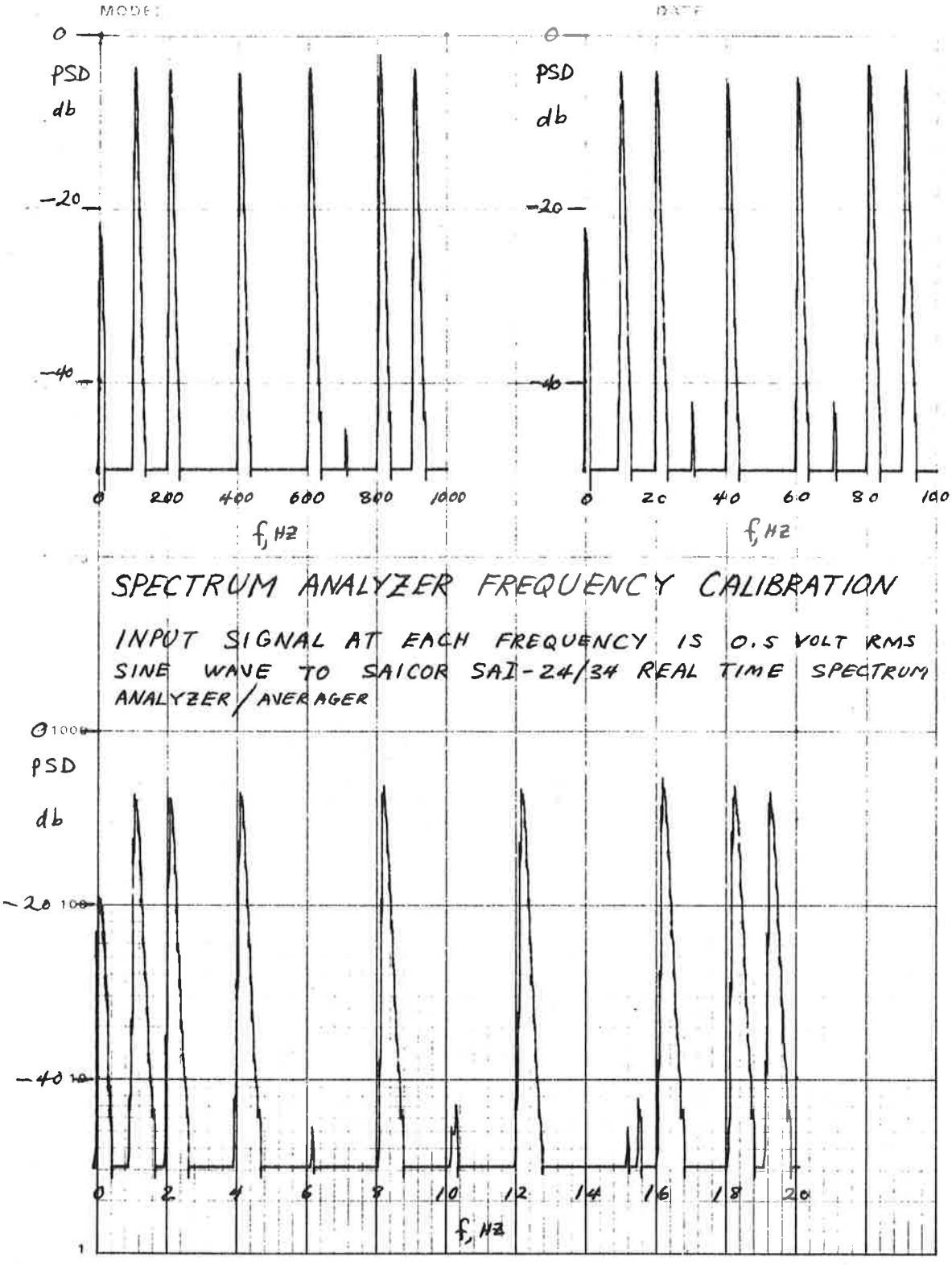

Figure 34. Spectrum Analyzer Frequency Calibration

more than 19.2 Hz. This type of analyzer is specified to be capable of frequency accuracies of ± B. Therefore, it is assumed that additional calibration adjustments should be made to this particular unit to bring it up to its performance capability.

The test route contained many switches, curves, and different types of roadbed. Thus, the suspension system experiences a wide variety of inputs, somewhat randomly applied. Furthermore, for the test, the train operator was instructed to operate at speeds typical of revenue service. As a consequence the operator slowed to very low speeds going through stations (or stopped) and accelerated to normal operating speed upon leaving the station. The result of this was that most of the time during the test, the train was either accelerating or decelerating. The primary processing intended for this data was the estimation of the power spectral density (PSD). To obtain a meaningful estimate of the PSD, the input data must form a stationary process. Considering the nature of train operation and the track it was operated on, the data would be expected to form a nonstationary process. Thus, the first step in data reduction is to select segments of data that appear to be quasi-stationary or almost stationary. To do this, the raw data was played back into a (true) rms voltmeter (HP 3400A). The dc output of the 3400A (corresponding to the rms value of the input) was recorded on a strip chart by a Brush Mark 200 recorder. The time segments of data for future analysis were selected so that the rms value of the data during the time segment selected had characteristics that remained much the same during the time segment. Ideally, the rms value of the data should be a constant over the time segment. However, "constant" statistical parameters have to be considered in terms of the averaging time used. The HP 3400A provide the rms value of a step function input in less than five seconds. In fact, examination of the rms output of the 3400A shows that it responds to changes in the rms value of a signal, where the frequency of change of rms value is up to 2 Hz. The range of frequencies for which the HP 3400A determines the rms value to within specified accuracy is 10 Hz to 10 MHz. Additional specifications for the HP 3400A are given in Appendix D. Since frequencies less than one Hz are of interest in this study, the averaging time of the HP 3400A is not sufficiently long to require that its output remain constant. Three time segments of data were selected, one for each type of road bed.

Because the 3400A has a specified low frequency cut-off of 10 Hz (actually it provides a credible rms output for signal frequencies down to 5 Hz), and because the low frequency vibration components were of great interest, the data was then played back through a 5 Hz (nominal) single pole low pass filter and recorded by the Brush Mark 200 recorder. This permitted verifi-

cation that the data segments selected contained as much or more interesting information than other parts of the data tape. Table 3 shows the measured frequency response of each low pass filter and the data that was recorded on that track of the magnetic tape.

TABLE 3. LOW PASS FILTER FREQUENCY RESPONSE AND DATA RECORDED ON EACH TRACK OF TAPE (BY RUN)

Tape Track	2	3	4	5	6	7
LPF 3 db Cut-off, Hz	4.6	5.0	5.0	5.0	5.2	4.9
Acceleration Data from Run 1	right front lateral	right rear vertical	left-rear longitu-dinal	left-rear lateral	left-rear verti-cal	left-front vertical
Acceleration Data from Runs 2 & 3	angular X, roll	linear X, longitudi-nal	linear Y, lat-eral	linear Z, ver-tical	angular Y, pitch	angular Z, yaw

The measurement of peak values of journal box acceleration still leaves something to be desired. The preliminary results mentioned earlier were obtained by observing the raw data on an oscilloscope as the entire data tape was played. Subsequently, another approach was tried. The data was transcribed from the tape at 7.5 ips to a tape at 37.5 ips. Then the latter tape was played back at 3:75 ips (1/10 real time) and the output recorded by the Brush recorder. The recorded output showed spikes in excess of the full scale output of the accelerometer. Many of these could be considered noise. However, there were several spikes of acceleration recorded by the left-rear vertical (triax) accelerometer that evidence decayed oscillation of an underdamped transient. These are most likely genuine data. The biggest of these spikes indicates a peak vertical acceleration of approximately 120g. A better means of measuring peak values will be to play the raw data into a probability analyzer which provides an amplitude histogram of the data. Such an analyzer is presently being purchased.

The length of each time segment of data is determined by the time required to collect and average a sufficient number of statistically independent samples of data to provide an acceptably good statistical estimate of the PSD. The time required to get one statistically independent sample is the reciprocal of the nominal filter bandwidth or 1/B. The greatest interest in this study is in the low end of the frequency spectrum. The lowest frequency analyzer range available on the SAI-24/34 is

0-20 Hz. Since B on this range is 0.05 Hz, it requires 20 seconds to obtain one statistically independent sample. On the SAI-34 averager, the smallest number of samples that can be averaged and scaled automatically is 8. If each data sample averaged is just 1/B long, then the number of statistical degrees of freedom is 2N, where N is the number of independent samples. Thus, eight samples provide 16 degrees of freedom. This implies that there is a 99% probability that the estimate of the PSD will be within +6db to -3db of the true PSD. Eight samples at 20 seconds each require 160 seconds of data. In one instance, Run #2 on Manhattan Bridge, only 105 seconds of quasi-stationary data were obtained because the train stopped on the bridge to pick up construction workers. In this case, five independent samples were averaged, with the fifth sample being entered into the average four times. (The analyzer was switched into "hold" at the end of the data segment.) In the case of some data segments, the processes represented by the data do not appear to be as stationary as might be desired. This represents another limitation on the validity of the PSD estimate.

To provide results that could be compared with other test results and standards, a spectrum analysis of each data segment on the 0-100 Hz frequency range was performed. To analyze as much of the same data as was analyzed at 0-20 Hz, a larger number of samples was averaged. In most cases, 32 samples of data were averaged, requiring 128 seconds of data.

To gain information on where significant energy was evidenced above 100 Hz and to observe the actual frequency cutoff of our instrumentation, a spectrum analysis of each data segment on the 0-1000 Hz frequency range was performed. Again, to analyze the same data as was used in the lower frequency analyses, 256 samples of data were averaged, requiring 102.4 seconds of data.

The data used from stone ballast road bed were taken between Union Square Station (14th Street) and Times Square Station, (42nd Street) in Manhattan. Wherever possible, the data analysis started at the same point, signal 115. Since there was only one section of concrete roadbed on the N line long enough to take significant data on, our concrete road bed data was taken on this section. This section of track is between 36th Street Station and Pacific Street Station in Brooklyn. Data analysis started at signal 451. Data analysis for the bridge type track construction started as soon as the train started to cross the Manhattan Bridge except for Run #2, where analysis started at signal 240. A complete set of the PSD analyses and the strip chart recordings of the rms and low frequency values of the data are shown in Appendix E.

To determine how the recorded acceleration data is influenced by instrumentation and other background noise, data was recorded while the train was stopped. At some point during each run, the train had to stop for an extended period of time for various reasons. During these stops, the tape recorder was left on so that background and instrumentation noise were recorded without requiring a special data gathering sequence. Since the data of primary interest are the results of vehicle suspension dynamics and track irregularities, background noise includes any accelerations sensed which are not primary data. Typical sources of background noise are rotating machinery on the rail cars, activity of passengers in the cars (walking, etc.), vibration of the roadbed itself from other vehicle traffic, etc. The predominant source of instrumentation noise is tape recorder flutter. For each run, the rms value and low frequency values of instrumentation and background noise (labeled instrumentation noise) are recorded on strip charts (Appendix E). For each PSD analysis, the appropriate noise spectra (labeled noise) is plotted under the data curve so that peaks in the data PSD that are primarily caused by peaks in the noise PSD can be clearly identified. From the PSD curves from Run #1, a low signal-to-noise ratio situation, the predominant effect of the 80 Hz tape recorder flutter can be observed.

REFERENCES

1. Rickley, E. J. et al, Noise Level Measurement on the UMTA Mark I Diagnostic Car, October 1971, Report No. DOT-TSC-UMTA-72-3.

2. Davis, E. W. et al, Comparison of Noise and Vibration Levels in Rapid Transit Vehicle Systems, Operations Research Inc., Silver Spring, Md., for National Capital Transportation Agency, Contract NTA-36, Report No. PB 184973, April 1964.

3. International Organization for Standardization, Guide for the Evaluation of Human Exposure to Whole-Body Vibration, ISO/TC 108/WG 7 (Secretariat-17) 23, December 1968, and ISO/TC 108 (Secretariat-31) 100E, June 1969.

4. Hanes, R. M., Human Sensitivity to Whole-Body Vibration in Urban Transportation Systems: A Literature Review, APL/JHU TPR004, Applied Physics Laboratory, Johns Hopkins University, Silver Spring, Md. for DOT/Urban Mass Transportation Administration, May 1970.

APPENDIX A

ESTIMATES OF DYNAMIC RESPONSE OF R-42 TRANSIT CARS

APPENDIX A
ESTIMATES OF DYNAMIC RESPONSE OF R-42 TRANSIT CARS

NATURAL FREQUENCIES

As a first approximation, some of the dynamic characteristics of a transit vehicle can be estimated from the behavior of simple, linear rigid body and beam models. A summary of the natural frequencies based on these models is presented in Table A-1.

TABLE A-1. ESTIMATED NATURAL FREQUENCIES OF R-42 CARS

Vertical Natural Frequencies	
First Body Bounce	1.63 Hz
Second Body Bounce	5.52 Hz
Lateral National Frequency	0.74 Hz
Angular Pitch Natural Frequencies	
First Body Pitch	2.13 Hz
Truck Pitch	5.17 Hz
Second Body Pitch	5.62 Hz
Angular Roll Natural Frequencies	
First Body Roll	1.16 Hz
Second Body Roll	7.05 Hz
Angular Yaw Natural Frequency	1.98 Hz
First Bending Mode	18.9 Hz simple support 27.1 Free beam
Kinematic truck hunting at 60 m.p.h.	0.56 Hz

MOTION IN A VERTICAL PLANE

Since the structure of a transit vehicle is essentially symmetric about vertical planes parallel to and perpendicular to the track, it can be assumed that vertical motion is effectively decoupled from the lateral and longitudinal motions of

the vehicle. Therefore, the three mass model in Figure A-1 provides a description of pitch and bounce motions of rigid car supported on linear, elastic, primary and secondary suspensions. m_1 and m_2 are the masses of each truck and an unloaded car respectively. k_1 is the spring constant for a set of four equalizer springs connecting the axle assembly to the truck. k_2 is the constant for a pair of bolster springs which connect the truck frame to the car body.

For an unloaded R-42 transit car, the values of these parameters, as well as the dimensions indicated in Figure A-1, are

$$k_2 = 14,193 \ \frac{lb}{in}$$

$$k_1 = 39,856 \ \frac{lb}{in}$$

$$m_1 = \frac{17,900 \ lb}{386 \ in/sec^2}$$

$$m_2 = \frac{74,400 \ lb}{386 \ in/sec^2}$$

L_1 = Truck length = 10'8"

L_2 = Car length = 60'6"

L = Wheel Base = 6'10"

$2a$ = Distance between truck centers = 44'7"

Using this data, the mass moment of inertia of a truck can be estimated as

$$\frac{m_1 L_1^2}{12},$$

(i.e., as a thin rod). Similarly the car moment of inertia is estimated as

$$\frac{m_2 L_2^2}{12}.$$

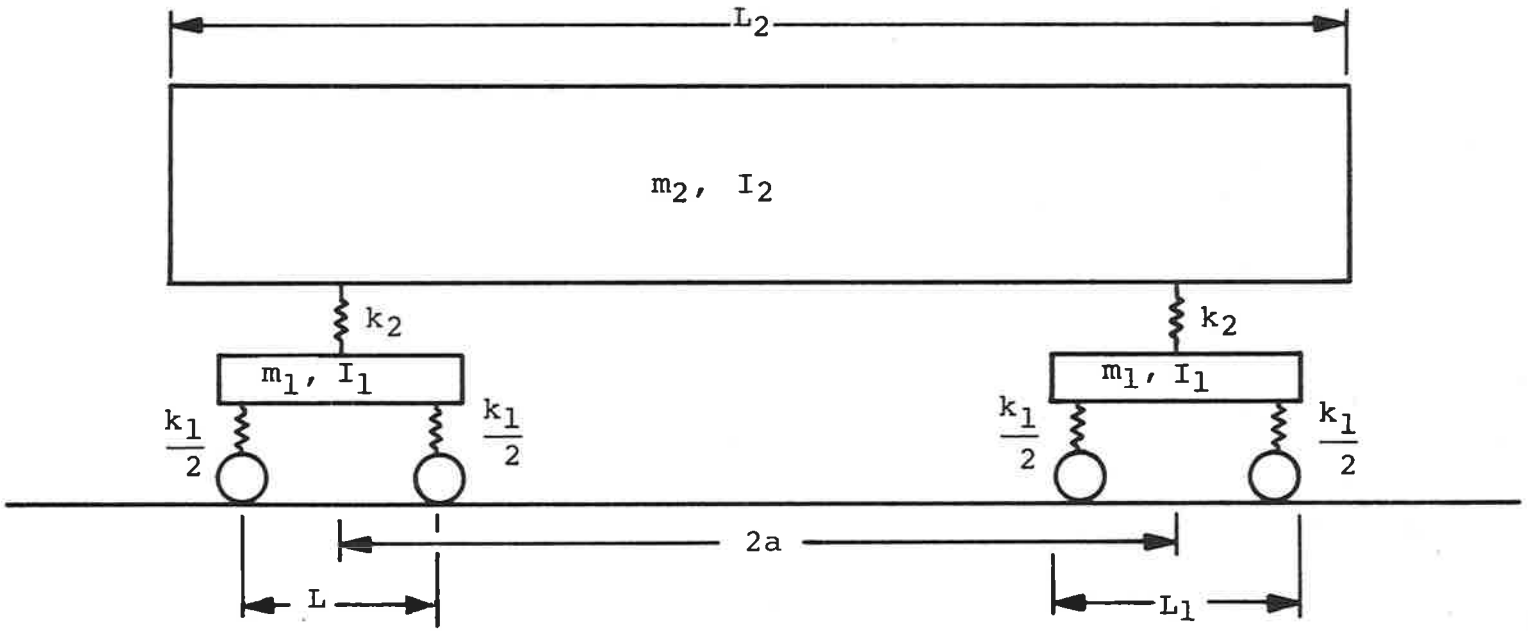

Figure A-1. Model for Derivation of Pitch and Bounce Motions

Since this model has six degrees of freedom, it can be described dynamically in terms of six modes of free vibration and their associated natural frequencies.

a. Two modes of truck pitching at a frequency,

$$f_1 = \frac{L}{4\pi}\sqrt{\frac{k_1}{I_1}} \quad .$$

These modes correspond to angular motions of the trucks independent of motion of the car body. Each truck oscillates about its connection to the bolster springs. (Figure A-2a)

b. Two modes of car body bouncing at frequencies,

$$f_{3,4} = \frac{1}{2\pi}\sqrt{\frac{k_1+k_2}{2m_1} + \frac{k_2}{m_2} \pm \sqrt{\left(\frac{k_1+k_2}{2m_1} + \frac{k_2}{m_2}\right)^2 - \frac{2k_1k_2}{m_1m_2}}} \quad .$$

In the mode corresponding to the lower frequency, the body and trucks translate in the same direction (Figure A-2b), while the higher frequency corresponds to a translational mode with the body moving in a direction opposite to that of the trucks (Figure A-2c).

c. Two modes of car body pitching at frequencies,

$$f_{5,6} = \frac{1}{2\pi}\sqrt{\frac{k_1+k_2}{2m_1} + \frac{a^2k_2}{I_2} \pm \sqrt{\left(\frac{k_1+k_2}{2m_1} + \frac{a^2k_2}{I_2}\right)^2 - \frac{2a^2k_1k_2}{m_1I_2}}}$$

In each of these modes the body oscillates angularly while the trucks translate in opposite directions. For one mode both the body and a line connecting the truck centers rotate in the same direction (Figure A-2d), while the line and the body rotate in opposite directions in the other mode (Figure A-2e).

ROLL MOTION

A similar estimate for roll frequencies can be made using an analogous lumped mass model in a plane perpendicular to the

(2a) Truck Pitching Modes

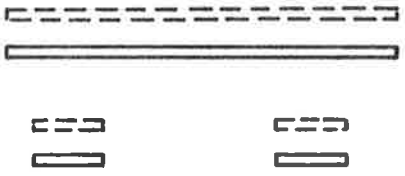

(2b)

(2c)

Body Bouncing Modes

(2d)

(2e)

Body Pitching Modes

Figure A-2. Pitch and Bounce Mode Descriptions

direction of the track (Figure A-3a). While it is reasonable to assume that angular motion of this model is decoupled from vertical motion, such vibrations would be related to lateral motions of the car and trucks. However, an initial estimate of roll frequencies can be made considering only rotation of the trucks and car and including the rotational stiffness provided by only the bolster and equalizer springs. In Figure A-3a the trucks are lumped as a single rotational mass with inertia

$$I_3 = \frac{2m_1 l_3^2}{12}$$

and the car body as a rotational mass with inertia

$$I_4 = \frac{2m_2 l_4^2}{12} .$$

m_1, m_2, k_1, and k_2 have the same values as listed above

For R-42 cars, the length parameters corresponding to Figure A-3a are:

l_3 = truck width = 6'10"

l_4 = car width and height = 10'

$2d_1$ = 4'6"

$2d_2$ = 6'4"

The frequencies of angular motion are:

$$f_{7,8} = \frac{1}{2\pi}\sqrt{\frac{k_1 d_1^2 + k_2 d_2^2}{I_3} + \frac{k_2 d_2^2}{I_4} \pm \sqrt{\left(\frac{k_1 d_1^2 + k_2 d_2^2}{I_3} + \frac{k_2 d_2^2}{I_4}\right)^2 - \frac{4k_1 k_2 d_1^2 d_2^2}{I_3 I_4}}}$$

One frequency corresponds to a roll mode with the trucks and body rotating in opposite directions (Figure A-3b), while the other frequency corresponds to a swing mode with both bodies rotating in the same direction (Figure A-3c).

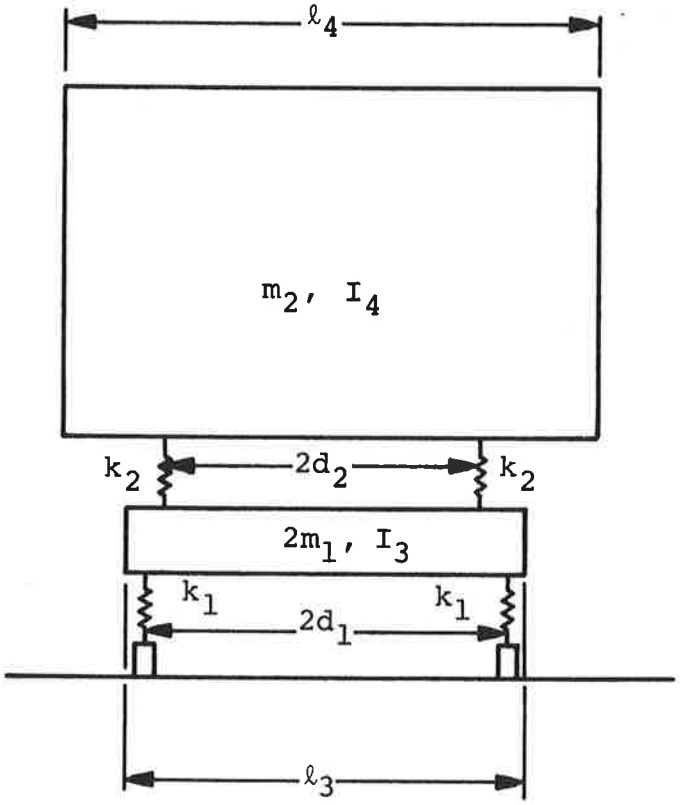

(3a)

(3b)

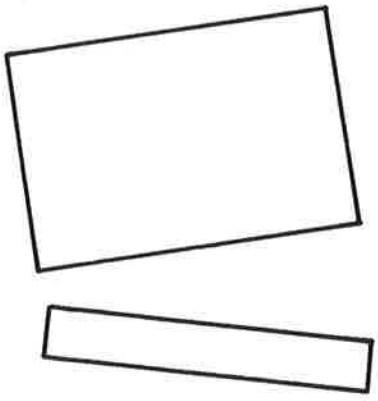

(3c)

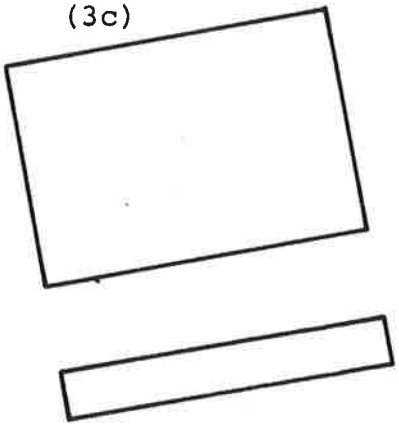

Figure A-3. Roll Model

LATERAL AND YAW FREQUENCIES

A rough approximation of the lateral and yaw frequencies for small vibrations can be made by assuming that all of lateral restraint is provided by the truck swing links. Figure A-4 illustrates the simplified action of the swing link suspension. For small horizontal deflections, horizontal forces, F, are linearly related to displacements, x, so that an equivalent spring constant $k_e = mg/l$, can be defined. The frequency of lateral vibrations of the car,

$$f_L = \frac{1}{2\pi} \sqrt{\frac{k_e}{m}} = \frac{1}{2\pi} \sqrt{\frac{g}{l}} ,$$

is equivalent to the frequency of a pendulum of length, l, equal to length of the swing links. For an R-42 truck the swing links are 18 inches long so that the lateral body frequency is 0.74 Hz.

The body yaw frequency can be estimated by assuming the swing links to act as parallel springs located at the truck centers (Figure A-5). Taking the yaw mass moment of inertia equal to the pitch inertia I_2, the yaw frequency is given by

$$f_y = \frac{1}{2\pi} \sqrt{\frac{a^2 k_e}{I_2}} = \frac{a}{e} f_L$$

where a and L_2 are the parameters defined in Figure A-1.

KINEMATIC HUNTING

A rigid wheelset or truck with coned or profiled wheels has a characteristic periodic lateral motion when moving very slowly along a track (Figure A-6). Since the wavelength of this motion is a function of only the geometry of the wheelset or truck and the gauge of the track, it is termed a kinematic hunting mode.[A3]

For a single wheelset this wavelength is,

$$\lambda_W = 2\pi \sqrt{\frac{r_o l}{\delta}}$$

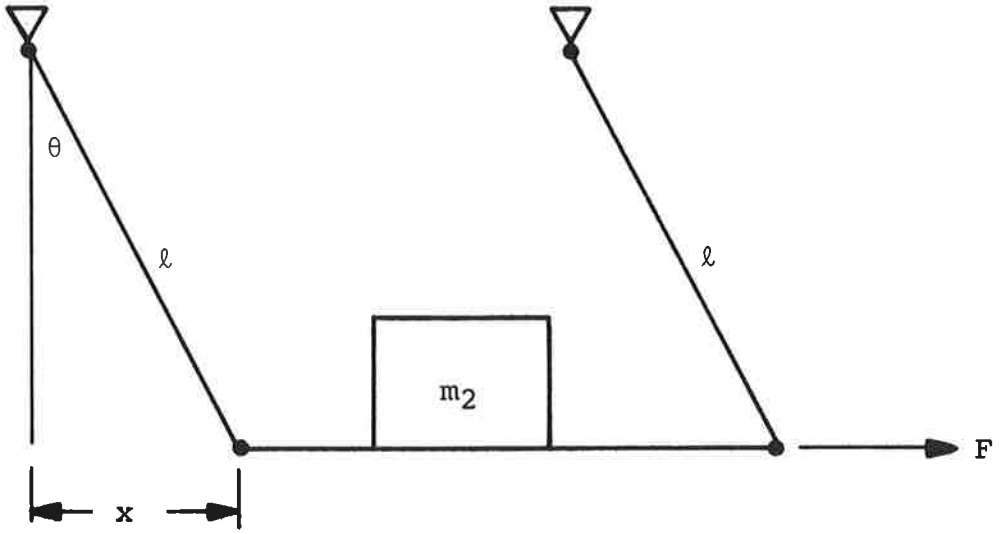

$$F = mg \tan\theta \approx \frac{mg}{\ell} x$$

$$= k_e x$$

Figure A-4. Swing Link Suspension Kinematic Model

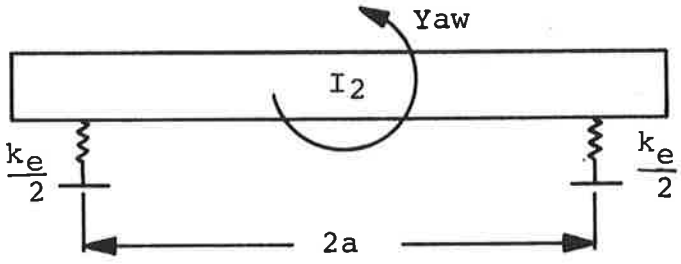

Figure A-5. Yaw Model

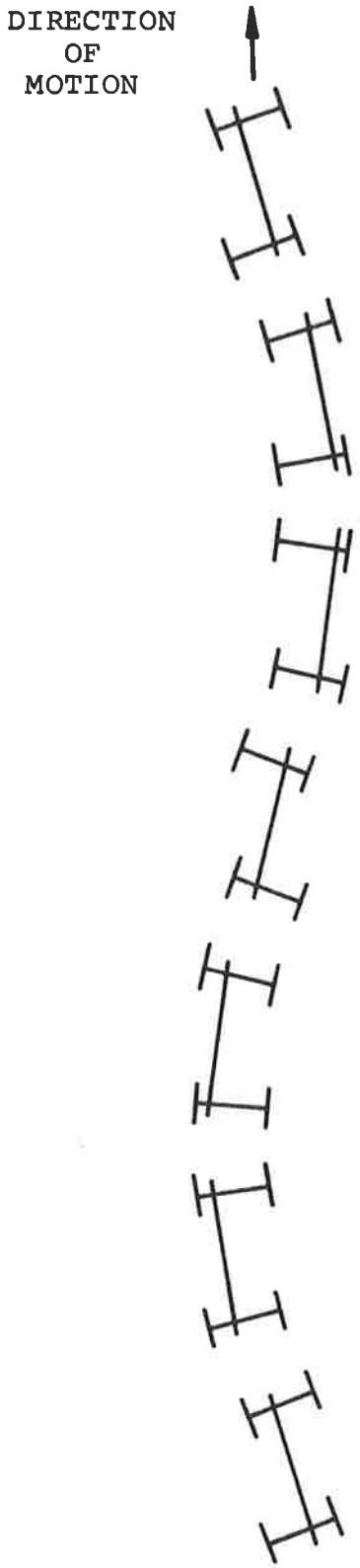

Figure A-6. Truck Lateral Motion

where

2ℓ = contact gauge

r_o = 17" = wheel radius

δ = 0.05 = cone angle or conicity

so that the wavelength is

λ_W = 51.3 ft.

For a pair of wheelsets rigidly attached to a truck the expression is modified such that,

$$\lambda_T = \lambda \sqrt{1 + \beta^2} = 90.4 \text{ ft}$$

where $\beta = \frac{\text{Truck wheel base}}{2l}$

The corresponding frequencies $f_W = V/\lambda_W$ and $f_t = V/\lambda_T$ are shown in Figure A-7 as a function of the speed, V, of the vehicles.

As indicated in References A3, A4, A5, and A6, this relationship of frequency and velocity also applies to wheelset or truck oscillations for high speed motions of a complete vehicle, i.e., car body and trucks.

For example, the dynamic instability of large oscillations of the car body, body or primary hunting, is excited at the speed for which the frequency of kinematic hunting concides with any of the natural frequencies of the body in roll, yaw, or lateral translation on its suspension.

Secondary hunting which is a high speed instability resulting in violent oscillation of wheelsets or trucks, occurs at a high speed critical velocity of the vehicle. The frequency of this hunting is essentially the kinematic hunting frequency corresponding to this speed.

BEAM BENDING

The effect of flexibility on the dynamics of the body can be estimated by considering some simple beam models. While the flexible supports provided by the suspension represent complicated boundary conditions for a mathematically exact frequency

equation, an estimate can be bounded by models of a beam on simple supports at the bolster springs (Figure A-8a) and a free beam of the full car length (Figure A-8b).

The lowest frequencies of these models are

$$\frac{\pi}{2}\sqrt{\frac{EIg}{W\ell_1^3}}\ , \text{ and } \frac{(4.73)^2}{2\pi}\sqrt{\frac{EIg}{W\ell_2^3}}$$

respectively. They correspond to the first bending mode of each model.

W = weight of the car body

E = modules of elasticity of the structural material

I = Area moment of inertia of the effective structural cross section.

As a first approximation, the effective structure of an R-42 car is assumed to be a hollow, 1/4 in. thick steel tube, 90 in. in diameter, so that the parameters in the frequency equations:

$W = 74{,}400$ lb

$E = 3 \times 10^7$ psi

$l_1 = 535$ in.

$l_2 = 736$ in.

$I = 143{,}000$ in^4.

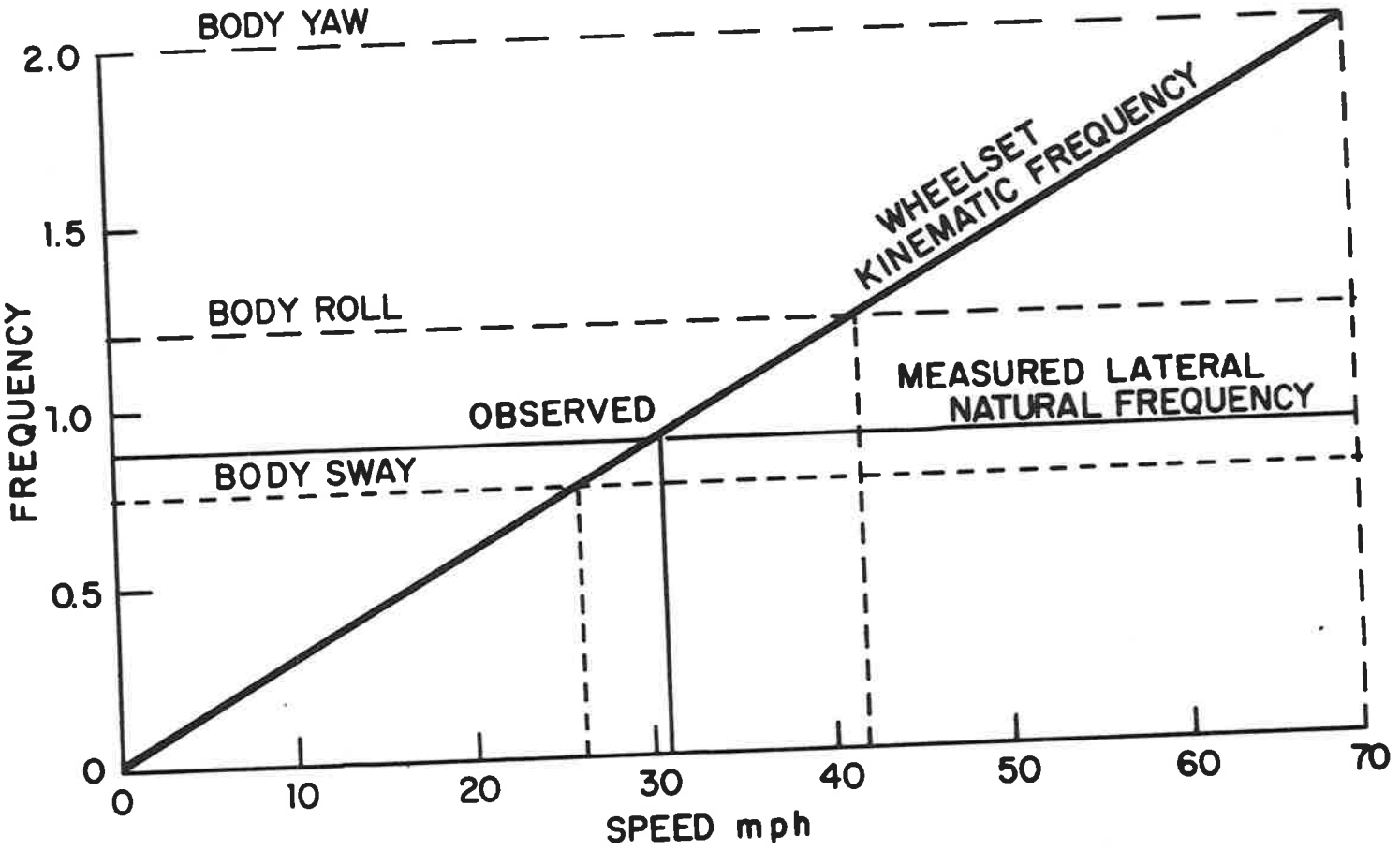

Figure A-7. Kinematic Hunting

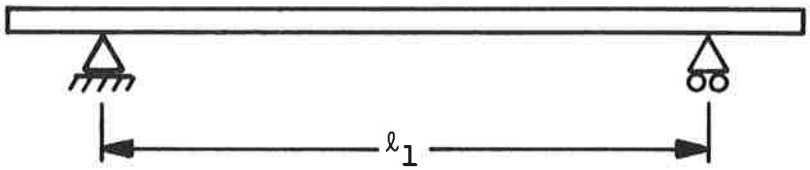

(8a)

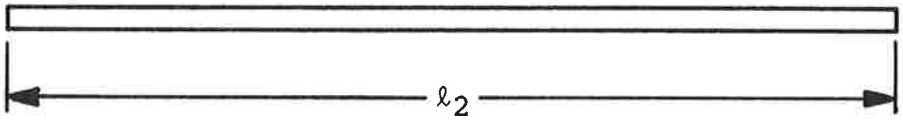

(8b)

Figure A-8. Beam Bending Models

VEHICLE RESPONSE TO TRACK IRREGULARITIES

EQUATIONS OF MOTION FOR VERTICAL DYNAMICS

For an evaluation of the vertical response to track profile irregularities, a modification of the model in Figure A-1 which includes damping in the secondary suspension can be used to describe the vehicle (Figure A-9). Since the parameters of interest are the motion of the car body and displacements of the wheels, a convenient set of coordinates to describe the system is y_2 and θ_2, the vertical and angular displacements of the car body, and v_1, v_2, v_3, v_4. the displacements of the trucks at their connections to the equalizer springs. Since the motion described by this model is not coupled to roll or lateral response of the vehicle, the wheel inputs, v_{10}, v_{20}, v_{30}, v_{40} represent the average of the two rail profiles.

$$m_2\ddot{y}_2 + 2c_2\left[\dot{y}_2 - \frac{1}{4}\left(\dot{v}_1+\dot{v}_2+\dot{v}_3+\dot{v}_4\right)\right] + 2k_2\left[y_2 - \frac{1}{4}\left(v_1+v_2+v_3+v_4\right)\right] = 0 \quad (1)$$

$$I_2\ddot{\theta}_2 + 2ac_2\left[a\dot{\theta}_2 + \frac{1}{4}\left(\dot{v}_1+\dot{v}_2-\dot{v}_3-\dot{v}_4\right)\right] + 2ak_2\left[a\theta_2 + \frac{1}{4}\left(v_1+v_2-v_3-v_4\right)\right] = 0 \quad (2)$$

$$\frac{m_1}{4}\left(\ddot{v}_1+\ddot{v}_2\right) + \frac{I_1}{L^2}\left(\ddot{v}_1-\ddot{v}_2\right) + \frac{c_2}{2}\left[a\dot{\theta}_2-\dot{y}_2 + \frac{1}{2}\left(\dot{v}_1+\dot{v}_2\right)\right] + \frac{k_1}{2}v_1 + \frac{k_2}{2}\left[a\theta_2-y_2 + \frac{1}{2}\left(v_1+v_2\right)\right] = 0 \quad (3)$$

$$\frac{m_1}{4}\left(\ddot{v}_1+\ddot{v}_2\right) - \frac{I_1}{L^2}\left(\ddot{v}_1-\ddot{v}_2\right) + \frac{c_2}{2}\left[a\dot{\theta}_2-\dot{y}_2 + \frac{1}{2}\left(\dot{v}_1+\dot{v}_2\right)\right] + \frac{k_1}{2}v_2 + \frac{k_2}{2}\left[a\theta_2-y_2 + \frac{1}{2}\left(v_1+v_2\right)\right] = 0 \quad (4)$$

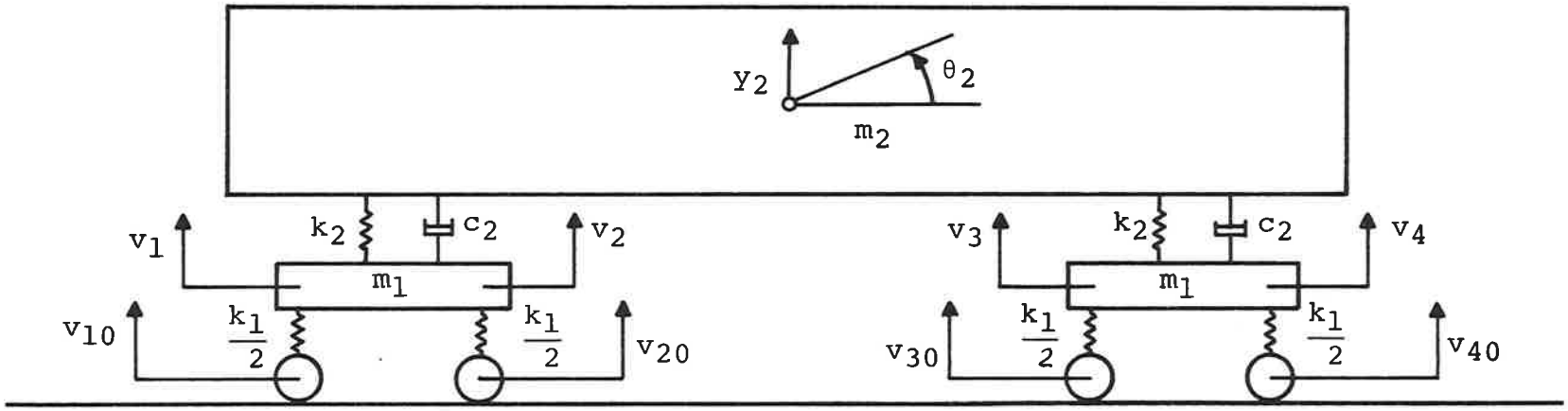

Figure A-9. Damped Vertical Dynamic Model

$$\frac{m_1}{4}\left(\ddot{v}_3+\ddot{v}_4\right) + \frac{I_1}{L^2}\left(\ddot{v}_3-\ddot{v}_4\right) + \frac{c_2}{2}\left[\frac{1}{2}\left(\dot{v}_3+\dot{v}_4\right) - a\dot{\theta}_2 - \dot{y}_2\right] + \frac{k_1}{2} v_3$$

$$+ \frac{k_2}{2}\left[\frac{1}{2}\left(v_3+v_4\right) - a\theta_2 - y_2\right] = 0 \qquad (5)$$

$$\frac{m_1}{4}\left(\ddot{v}_3+\ddot{v}_4\right) - \frac{I_1}{L^2}\left(\ddot{v}_3-\ddot{v}_4\right) + \frac{c_2}{2}\left[\frac{1}{2}\left(\dot{v}_3+\dot{v}_4\right) - a\dot{\theta}_2 - \dot{y}_2\right] + \frac{k_1}{2} v_4$$

$$+ \frac{k_2}{2}\left[\frac{1}{2}\left(v_3+v_4\right) - a\theta_2 - y_2\right] = 0 \qquad (6)$$

As discussed previously, the normal modes containing pitch and bounce motions of the car body can be decoupled from the pitch motion of the trucks. In addition, the bounce can be uncoupled from unsymmetric translation of the trucks (Figures A-2d and A-2e) and the pitch from symmetric translation (Figures A-2b and A-2c) so that the dynamics of the car can be interpreted in terms of two simpler equivalent two degrees of freedom systems.

Symmetric translation of the trucks can be represented by $v_1=v_2=v_3=v_4=y_1$. Substitution in the equations of motion reduces the six equations to,

$$m_1\ddot{y}_1 + c_2\left(\dot{y}_1-\dot{y}_2\right) + k_1y_1 + k_2\left(y_1-y_2\right) = 0 \qquad (7)$$

$$m_2\ddot{y}_2 + 2c_2\left(\dot{y}_2-\dot{y}_1\right) + 2k_2\left(y_2-y_1\right) = 0 \qquad (8)$$

Thus the vertical motion of the car body can be interpreted in terms of the equivalent system of Figure A-10a which also is described by Equations 7 and 8. Similarly, the unsymmetric translation of the trucks can be represented by $v_1=v_2=Y_3= -v_3= -v_4$. In this case, the six equations of motion reduce to,

$$m_1\ddot{y}_3 + c_2\left(\dot{y}_3+a\dot{\theta}_2\right) + k_1y_3 + k_2\left(y_3+a\theta_2\right) = 0 \qquad (9)$$

$$I_2\ddot{\theta}_2 + 2a\, c_2\left(\dot{y}_3+a\dot{\theta}_2\right) + 2a\, k_2\left(y_3+a\theta_2\right) = 0 \qquad (10)$$

which describe the equivalent system of Figure A-10b.

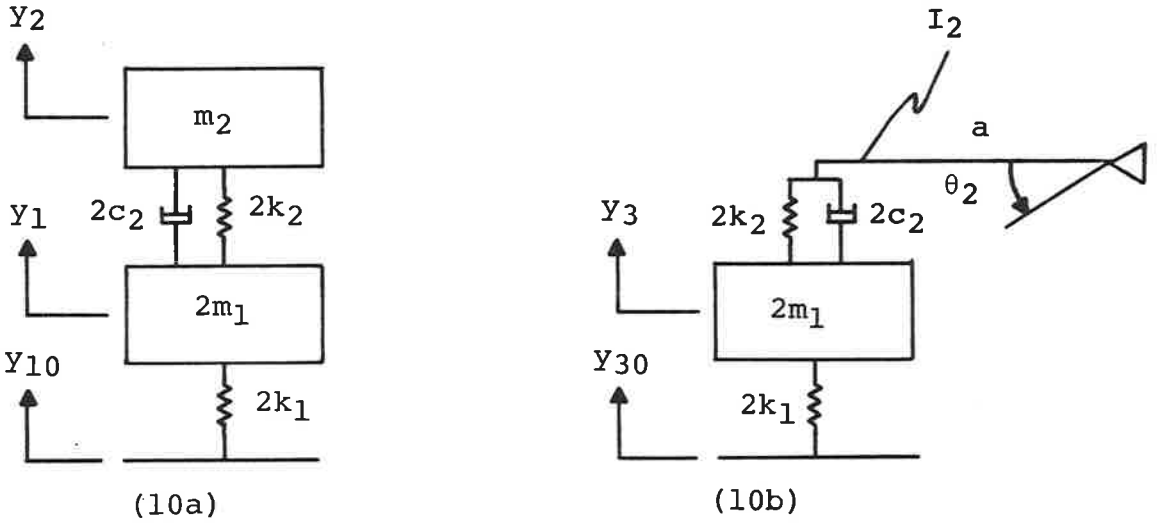

Figure A-10. Simplified Models for Vertical Dynamics

These equivalent descriptions provide a description of inputs at the vehicle wheels in terms of simple base motions of the equivalent systems. For example, a unit movement of each of the wheel displacements, v_{10}, v_{20}, v_{30}, v_{40}, is equivalent to a unit base displacement y_{10}, where, $y_{10} = 1/4\ (v_{10}+v_{20}+v_{30}+v_{40})$. Similarly, angular body motion is excited by an equivalent base motion,

$$y_{30} = \frac{1}{4}\ v_{10}+v_{20}-v_{30}-v_{40}\ .$$

Figures 10a and 10b indicate that these base motions are inputs to the system represented by forcing functions $k(y_{10})$ and $k(y_{30})$ on the right hand sides of Equations 7 and 9, respectively.

The transfer functions for these inputs are,

$$\frac{\bar{y}_2}{\bar{y}_{10}} = H_1(s) = \frac{\left(1 + \frac{2\xi s}{\omega_2}\right)}{\left[1 + \frac{2\xi s}{\omega_2} + \frac{\omega_1^2 + (2+\mu)\omega_2^2}{2\omega_1^2\omega_2^2}\, s^2 + \frac{(2+\mu)\xi}{\omega_2\omega_1^2}\, s^3 + \frac{s^4}{2\omega_1^2\omega_2^2}\right]}$$

$$\frac{\bar{\theta}_2}{\bar{y}_{30}} = H_2(s) = \frac{-\left(1 + \frac{2G\xi s}{\omega_2}\right)}{a\left[1 + \frac{2G\xi s}{\omega_2} + \frac{\omega_1^2 + (2G+\mu)\omega_2^2}{2G\omega_1^2\omega_2^2}\, s^2 + \frac{(2G^2+\mu)\xi}{G\omega_2\omega_1^2}\, s^3 + \frac{s^4}{2G\omega_1^2\omega_2^2}\right]}$$

where,

$$\omega_1^2 = \frac{k_1}{m_1},\ \omega_2^2 = \frac{k_2}{m_2},\ \mu = \frac{m_2}{m_1},\ G = \frac{a^2}{\rho^2},\ \xi = \frac{c_2}{2m_2\omega_2}$$

The vertical response of any point in the car is a linear combination of the y_2 and θ_2 responses.

REFERENCES

A1. Koffman, J. L. and Batchelor, G. H., "Effect of Suspension Characteristics on Adhesion," Proc. Instn. Mech. Engrs., Vol. 178, Pt. 3, 1963-64.

A2. Rapid Transit Passenger Car Data 1947-70, New York City Transit Authority, Sept. 1970.

A3. Wickens, A. H., "The Dynamic Stability of Railway Vehicle Wheelsets and Bogies having Profiles Wheels," Int. J. Solids and Str., 1965, Vol. 1.

A4. Cooperrider, N. K., "High Speed Dynamics of Conventional Railway Trucks," Ph.D. Dissertation, Stanford U., 1968.

A5. Supporting Studies for HSGT System Reports, High-Speed Ground Transportation Systems Engineering Study, TRW Systems, Redondo Beach, Calif., OHSGT Contract C-353-66, June 1970.

A6. Wickens, A. H., "The Dynamics of Railway Vehicles on Straight Track: Fundamental Considerations of Lateral Stability," Conf. on Wheel-Rail Interaction, Proc. Instn. Mech. Engrs. 1965-66.

APPENDIX B

INSTRUMENTATION SPECIFICATIONS

PIEZO ACCELEROMETER COLUMBIA MODEL 704 SPECIFICATIONS

VOLTAGE SENSITIVITY: Nominal	10 pk mv/pk g, (with an external capacitance of 300 mmfd)
CHARGE SENSITIVITY: Nominal	10 pk-pcmb/pk g
FREQUENCY RESPONSE: Flat within ±5% 1000 megohm load	1 cps to 6 kc
RESONANT FREQUENCY: (First Minor Mode)	30 kc
MAXIMUM ACCELERATION: Vibration	1000 peak g sinusoidal
Shock	2000 g, 50 microsec. half-sine wave pulse
MINIMUM ACCELERATION:	Determined by signal to noise ratio of associated electronics
MAXIMUM CROSS AXIS SENSITIVITY	3% (1% special order)
AMPLITUDE LINEARITY:	±1%
NOMINAL CAPACITY: (Including cable capacity)	900 mmfd
OUTPUT RESISTANCE:	5×10^{11} ohms
TEMPERATURE RANGE: Standard Units	-100°F to +350°F with less than ±10% variation in sensitivity
MOUNTING TORQUE SENSITIVITY:	None
ACOUSTIC NOISE SENSITIVITY:	Less than 0.1 g equivalent to 150 db S.P.L. (Re 2×10^{-4} Microbar)
HUMIDITY:	Epoxy seal
ALTITUDE:	Not affected

SALT SPRAY:	Meets MIL-E-5272B. Para 4.6.1 when connector is sealed
MATERIAL:	Stainless steel
WEIGHT:	10 grams excluding mounting bolt
DIMENSIONS:	0.680" dia. x 0.42" high
MOUNTING:	Clearance hole for #6-32 bolt on 704-1, #10-32 on 704-2
GROUNDING:	Insulated when used with insulated mounting bolt (supplied)
CABLE: Low Noise Assembly	Model LN-HT-10 supplied. Approx. 10 ft., 300 mmfd cap., -100°F to +500°F
OUTPUT CONNECTOR:	Coaxial, #10-32 thread mates with cable assembly supplied

SPECIFICATIONS
ENDEVCO MODEL 2642M26
CHARGE AMPLIFIER

Description: This specification describes the fully transistorized Charge Amplifier Endevco Model 2642M26. This Amplifier has two outputs with a gain difference of 5. It also has a 2 kc low pass filter to limit the upper frequency range of the amplifier.

Electrical

Input Characteristics

Input Connection: The input is single ended with one side connected to circuit ground.

Input Source Impedance: The input of the amplifier is restricted to capacitive type devices and should not be loaded with less than 50 megohms resistance.

Source Capacitance: The maximum allowable source capacitance is 4000 pf. Gain will vary less than ± 1% for a ± 1500 pf change.

Vibration noise plus residual noise, as measured with an oscilloscope, will not exceed 2.5 pk pcmbs referred to the input or 25 mv pk-pk referred to the output, whichever is greater, for sinusoidal vibration of .120 DA from 5 to 55 cps and 20 pk g's from 55 to 2000 cps.

Continuous sinusoidal overload without damage: 20,000 pcmb (10 volts pk-pk with 4000 pf source capacitance).

Output Characteristics: Both outputs meet the following specifications:

Output Connection: The output is single ended with one side connected to circuit ground.

Output Impedance: 50 ohms, nominal, DC connected.

DC Output Bias Voltage: +2.5 ± 5% volts DC with load resistance of 100 K ohms or higher.

Linear Output Range (referred to bias level): ± 2.5 volts, nominal Output limited at zero volts _0.05 v/-0.00v and 5.50v ± 0.15v.

Load Impedance: 100 K ohms or more.

Residual Noise: 1.8 pcmbs pk-pk referred to the input or 10mV pk-pk referred to the output, whichever is greater.

Transfer Characteristics:

Low Charge Gain Channel: Adjustable over the range of at least 1 to 10 mV output/picocoulomb input. Meets specifications over the range of at least 2 to 10 mV output/picocoulombs input.

High Charge Gain Channel: Adjustable over the range of at least 5 to 50 mV output/picocoulomb input.

Frequency Response (referenced to 100 cps, R.T. response):

± 5%	5 cps to 1 K cps
±5/-10%	3 cps to 1400 cps
-3 db	at 2000 cps ± 200 cps
Cutoff slope:	20 db per octave or greater

Linearity: Within ± 2% of reading from best straight line approximation to the curve of output amplitude versus input amplitude for sinusoidal signals up to a level such that either peak approaches within 100 mV of a limiting level.

Warm-up Time: 30 seconds, maximum, to meet all other specifications.

Total Harmonic Distortion: 2% maximum to 2 K cps; for output signals up to a level such that either peak approaches within 100 mV of a limiting level.

Power

Power Requirements: 28 +4/-8 V DC at 20 mA maximum.

Power Transient and Ripple Characteristics: The amplifier meets specifications over a supply voltage range from 15 to 42 volts, including power supply ripple, pulse transients or step changes in voltages.

The maximum transient or ripple output over the frequency range from 0 to 20 Kcps is no more than 10 mV referred to the output or .5 picocoulombs referred to the input, whichever is greater, for 1 volt change on the power supply within the range of 15 to 42 V DC.

Isolation: Circuit ground is isolated from case by 1 megohm minimum at 50 volts DC. Note: For minimum noise circuit ground must be returned to case ground some place in the system.

Overload Recovery: A half sine input of 1 millisecond duration and an amplitude corresponding to 1300 pcmb will result in no effect other than clipping.

Environmental

Temperature Range: -40°F to +185°F

Humidity: 100% per MIL-E-5272C, paragraph 4.4.1 when gain adjust screw is solder sealed.

RF Fields: Meets the requirements of MIL-L-26600, Class 1b.

Vibration: .120 DA 5-55 cps; 20 g pk 55-2000 cps.

Shock: The spurious output from the amplifier will not exceed 2 pcmb pk-pk referred to the input or 35 mV pk-pk, whichever is greater, for a 100 g 6 ms half sine shock.

Altitude: 300,000 ft. or more.

Steady State Acceleration: 50 g's in any direction.

SPECIFICATIONS
LEACH MTR 3200 A
MAGNETIC TAPE RECORDER

Item	Specification
Size	8.625" x 9.5" x 20"
Volume	1,639 cubic inches
Weight	44 pounds maximum (including electronics)
Mounting	Hard mount to 20" x 9.5" flat surface with 1/4-20 bolts
Reel Size	8 inch modified IBM or 8 inch standard NARTB reels.
Tape Capacity 1 mil tape	1,800 feet
Record/Reproduce Modes	Analog (direct), FM
Tape Speeds	(7-1/2 - 15) electrically selectable. Fast forward and rewind is 60 ips or 120 ips
Tape Widths	1/2"
Number of Tracks	7
Speed Regulation	Within 0.25% over full tape length
Start or Stop Time	Less than 1 second at 60 ips (better at lower speeds)
Power Requirements	80 watts - 28 vdc (maximum)
Direction of Operation	Equal accuracy with record or reproduce in both directions
Function Controls	Record and/or reproduce, fast forward, fast reverse, stop
Mode Controls	High/Low speed selection, forward/reverse/power on/off

Item	Specification
Rewind Time	2,400 feet in 4 minutes
Head Geometry	Multi-track dual-interlaced. Record/Reproduce head stacks per IRIG standards
Tape Sensors	Electrically conductive for automatic stops at either end of tape*
Control	Via local switches or pulse control from external source.
Shock	10_g-11ms 1/2sine -3% p/p flutter maximum at 60 ips 25_g-8ms 1/2sine -5% p/p flutter maximum at 60 ips
Vibration	10_g rms random operating - 6% p/p flutter 10_g peak - 5 cps to 2,000 cps at reasonat points, 6% p/p flutter
Flutter	Less than 0.5% peak-to-peak. DC to 10 kcs at 60 ips. 0.1% rms cumulative. 0.1 cps to 300 cps.
Acceleration	25_g operating, 100_g non-operating
Temperature	-10°C to +71°C operating (range entended to -40° with use of 50 watt heater)
Humidity	95% operating. 100% with condensation non-operating
Altitude	Up to 150,000 feet - all speeds operating. (Unlimited for 20 hr.)

*Optical end of tape sensors optional.

SPECIFICATIONS
FM RECORD/REPRODUCE

Frequency Response and Signal to Noise Ratio:

Tape Speed	Carrier	Bandwidth	S/N
7 1/2 ips	13.5 kc	DC-2.5 kc	40 db

Input Sensitivity	0.5 v p/p to 5.0 v p/p
Input Impendance	100 KΩ minimum
Output Level	5.0 v p/p
Output Impedance	600Ω maximum
Linearity	1.0% of best straight line
Center Frequency Stability	0.5% long term under nevironment

SPECIFICATIONS
ANALOG RECORD/REPRODUCE

Frequency Response and Signal to Noise Ratio:

Tape Speed	Bandwidth #3db	S/N
7 1/2	300 cps 31.25 kcs	30 db

Input Sensitivity	0.5 v rms to 5.0 v rms
Input Impedance	100 KΩ minimum
Distortion	1% third harmonic at normal record level
Output Impedance	600Ω maximum
Output Level	5.0 volts p/p

SPECIFICATIONS
GOULD BRUSH 220 RECORDER

Number of Channels	2 analog, 2 event located on left and right margins
Channel Span	40mm (50 divisions)
Frequency Response	At 50-div: Flat within ± 2% of full scale from d-c to 40 Hz At 10-div: Flat within ± 2% of full scale from d-c to 100 Hz 3 dB down @ 125 Hz
Non-linearity	Less than ± 0.5% full scale d-c
Trace Presentation	Rectilinear
Trace Width	0.01" nominal
Marking Method	Pressurized Fluid
Marking Fluid Capacity	1 oz. (sufficient for one year of normal recording); replaceable throwaway cartridge
Measurement Range	1 millivolt per chart division to 500 V d-c fullscale (50 chart divisions)
Attenuator Steps	1, 2, 5, 10, 20, 50, 100, 200, mV/div., 0.5, 1, 2, 5, 10, V/div., "OFF"
Input Circuit	Differential, balanced-to-ground
Input Impedance	10 megohms balanced, 5 megohms each terminal to ground
In-phase Rejection	60 dB @ 60 Hz with 1 kilohm unbalance at most sensitive range
Signal Limiter	Built-in, adjustable, instant-acting electronic limiters prevent damage to analog pens on off scale signals
Zero-line Instability (drift) after 15-min. warm-up	± 0.1 div/8 hours; ± 0.1 div/°C from 15-35°C; ± 0.05 div/volt for ± 10% line voltage change

Gain Instability (maximum)	± 0.1%/8 hours; ± 0.05%/°C from 15-35°C; ± 0.05%/volt for ± 10% line voltage change
Chart Speeds	1, 5, 25, and 125 mm/sec. push-button (electrically) selected Optional models include 1, 5, 25, and 125mm/min. for total of 8 speeds
Chart Speed Accuracy	± 0.25%
Chart Description	Two 40mm grids graduated in 50 divisions. Graduated increments on time axis. Event marker channels on both channels and interchannel
Power Input	115 volts a-c ± 10% 60 Hz, 120 watts 175 VA
Weight	25 lbs.

SPECIFICATIONS
TOPAZ INVERTER 250GW-12-24-60

Frequency Stability	± 1% as listed
Temperature	Operating -20°C to +50°C · Storage -40°C to +80°C
Protection (Circuits included)	Input reverse polarity · Low or high input voltage · Overload and short circuit
Total Harmonic Distortion	<5% at full load
Output Voltage	115 VAC normally spplied · 230 VAC abailable where listed
Voltage Regulation	Line: ± 2% · Load: ± 3%

60 Hz Sine Wave Output

Dual Input 12 or 24 volts dc (Selectable input range for operation from 11-15 VDC or 22-30 VDC)

OUTPUT (SINEWAVE)		INPUT Amperage (No load to full load)		Full Load Eff.	HEIGHT Inches Overall	Net Wt. (Lbs.)	Ship Wt. (Lbs.)
Power VA	Volts AC	@ 12 VDC	@ 24 VDC		All units 19"w x 13 1/2" d		
250	115	8 - 32	4 - 16	60%	5-1/4	39	55

SPECIFICATIONS
ENDEVCO MODEL QA-116-15 ACCELEROMETER
(TERMINOLOGY PER ISA RP37.1)

Range (Full Scale)		± 15g
Sensitivity (Nominal)		250 mV/g
Output Resistance (Nominal)		250 ohms
Frequency Response (5%)		DC to 500 Hz
Natural Frequency (Nominal)		1000 Hz
Noise (Nominal):	0 - 10 Hz	100 microvolts rms
	0 - 500 Hz	300 microvolts rms
	500 - 10K Hz	600 microvolts rms
	Broadband	1 mV rms
Excitation Voltage		± 15 VDC ± 10%, or + 28 VDC ± 5%
Excitation Current		17 ma quiescent, 35 ma full scale
Sensitivity Shift with Excitation Voltage		0.005%/V
Zero Shift with Excitation Voltage		50 micro g/V
Resolution (DC)		0.000001g
Threshold (DC)		0.000001g
Linearity (DC)		0.03% of reading
Hysteresis (Less Than)		0.001% of full scale
Repeatability		0.003% of full scale
Zero Unbalance (Less Than)		± 0.02g
Damping (Approximate)		0.6
Thermal Zero Shift (Max.)		0.002g/°F
Thermal Sensitivity Shift (Max.)		0.01%°/F
Transverse Sensitivity		0.002 g/g

SPECIFICATIONS
MODEL SC-116-2 "g" MONITOR
(WHEN USED WITH QA-116-15 ACCELEROMETERS)

Ranges (full scale)	0.1g	0.2g	0.5g	1.0g	2.0g	5.0g	10.0g	20.0g
Accuracy (complete system)	1%	0.5%	0.2%	0.1%				

Linearity (of reading)	0.1%
Frequency Response (5%)	DC to 500 Hz
Output Voltage (full scale)	± 2.5 volts
Output Impedance (less than)	2 ohms
Output Current (max.)	10 ma
Output Noise (max. all ranges)	1 mv rms
Power	115V, 50-60 Hz
Enclosure	Portable cabinet
Weight	6.25 lbs.

SPECIFICATIONS
SCHAEVITZ MODEL ASM ANGULAR ACCELEROMETER

Range Rad/Sec^2	Cross Axis Sensitivity Rad/Sec^2/g	Nominal Natural Frequency Hz	Output Impedance K ohms
$\pm$ 50	0.2	30	20

Linearity	$\pm$ 0.1%
Hysteresis	0.02% full scale
Resolution	0.0005% full scale
Shock Survival	50g - 11 ms
Acceleration Survival Sinusoidal	10g (20 to 2.000 Hz)
Constant	50g

SPECIFICATIONS
ARNOLD MAGNETIC SKB-28-115-400-50 INVERTER

Input Voltage	24 to 30 VDC
Output Voltage (isolated)	115 VRMS
Frequency	400 ± 0.5% C.P.S
Power	50VA at 50°C
	30 VA at 71°C
Wave Shape	Sinusoidal with 4% harmonic distortion (at specified load)
Power Factor	Any
Operating Temperature	-55°C to +71°C
Environment	per MIL-E-5272C
Size, Weight	2 1/2" x 4" x 2 1/2" high - 28oz.
Regulation (typical)	As the below variable changes; it has these effects:

VARIABLE	FROM	TO	FREQUENCY	VOLTAGE
Input Voltage	24 VDC	30	+ 0.3%	+0.5%
Load Current	0.25 AMP	0.5	± 0.3%	±2.0%
Temperature	-55°C	+71°	+ 2.0%	+3.5%
Power Factor	0.8	1.0	+ 0.5%	+1%

APPENDIX C

ACCOUNT OF EVENTS DURING TESTING

APPENDIX C
ACCOUNT OF EVENTS DURING TESTING

RUN NO. 1

The test train left the Coney Island shop at 10:00 a.m. in the rain. the test run began at 10:24 a.m., entering the N-line at the 86th Street Station, Brooklyn. Although the operator slowed the train for most stations, we did not stop unless he had to for traffic reasons or unless requested. The record of speed pulses and thus, stops, is not too well recorded on the magnetic tape because the pulse train drops out at low speeds and makes it appear that the train has stopped when, in fact, it only has slowed down. Fortunately, two micro-switches were mounted near the same axle. The circuits were hooked up so that one switch provided pulses to the tape recorder. The other switch provided pulses to one channel of the Brush 220 chart recorder. The strip chart of this test run gives an accurate pulse event record for the first part of this run. The first time the train was stopped was near the Ft. Hamilton Parkway Station. Purpose of the stop was to clean the front window of the train to permit better observation of the signal markers. The train made a normal stop at the 36th Street (Brooklyn) Station. For the four and one-half minutes following this stop the train was to run at full speed over the concrete road bed. However, the test train caught up to a passenger carrying train and "full multiple" was not realized for more than a few seconds. The next stop was a "regular" stop at Pacific Street Station. Just after the test train began to cross the Manhattan Bridge, the voltage supplied by the Edison cell battery to the 60 Hz inverter dropped to a level such that the inverter cut out, causing a power loss to the chart recorder. Additional cells were hooked up in series with the battery to bring the voltage up to the required value and thus continue operation of the chart recorder. The repairs were completed and chart recording continued shortly after entering the subway tunnel on the Manhattan side of the river (at signal 199). Just after passing through the Canal Street Station (no stops), the tape on which was being recorded the acoustic data and on which had been prerecorded the time reference signal (used as a carrier frequency on the voice channel) ended. While this tape was being changed, voice and pulse train were lost to the magnetic tape that was recording accelerations. The test train made a normal stop at Times Square Station. The next stop was a signal stop for a train ahead on the track. This lasted four minutes. The final stop was at 57th Street Station, the end of Run #1 at 11:15 a.m.

RUN NO. 2

Run No. 2 started at the Kings Highway Station in Brooklyn at 12:45 p.m. The test train followed a passenger carrying train leaving Kings Highway Station, so the first part of the run was done at relatively low speed, approximately 15 mph. As the test train entered the 59th Street Station in Brooklyn, one of the New York Transit Authority people tripped over the microphone cable breaking it loose from its connection to the interface box. The test train was stopped at 59th Street while repairs were made to the microphone cable. During this stop, both the tape recorder and chart recorder were turned off. The microphone cable was reconnected in three minutes and 20 seconds and the testing continued. The next stop was required by traffic conditions at signal 472, approximately one minute before entering 36th Street Station, Brooklyn. The next stop was on the Manhattan Bridge to pick up some construction workers on the road crew. Testing then continued until the train stopped to discharge the construction workers at the Canal Street Station, Manhattan. The test train then continued to the end of the test run at 57th Street Station, Manhattan at 1:03 p.m.

RUN NO. 3

The New York subway personnel wanted us off of the east-west portion of the "N line" track in Brooklyn and the east end remainder of this track that connects to the Coney Island yard after about 2 p.m. so that our test train would not interfere with the heavy traffic preparing for the evening rush hour. Thus, on the return trip after Run No. 2, the test train was switched to the 4th Avenue (Brooklyn) line. Although data was recorded from the 95th Street Station on, Run No. 3 was considered to start at the 59th Street Station (Brooklyn) because from thereon, we were running over the same track as on previous runs. The first stop was a signal stop at signal 472 for 60 seconds. The test train made a "regular" stop at the 36th Street (Brooklyn) Station and at the Pacific Street Station. The test train stopped once more after leaving Times Square Station before stopping at the end of the run at 57th Street (Manhattan) Station at 2:23 p.m.

APPENDIX D

SPECIFICATIONS FOR DATA PROCESSING EQUIPMENT

APPENDIX D
SPECIFICATIONS FOR
DATA PROCESSING EQUIPMENT

SPECIFICATIONS
400 LINE SPECTRUM ANALYZER,
SAICOR SAI-24/34

Input

Impedance	50 KΩ
Attenuation	Coarse attenuation in 6 db steps from 0-48 db. Accuracy of ±.2 db. Fine attenuation 0.6 db (continuous). Accuracy of ±.5 db. Overload light indicates when the range of the input A/D converter is exceeded
Ten Frequency Scales	0-20 Hz, 0-100 Hz, 0-1 KHz, 0-2 KHz, 0-5 KHz, 0-10 Khz, 0-20 KHz
3 db Resolution:	
Flat Weighting	400 lines
Cosine Weighting	Number of lines reduced to two-thirds of the above
Input A/D Converter (Sampling Rate)	Nine Bit Resolution. Conversion rate in internal sampling is set at 3 times maximum frequency of frequency range switch. On external sampling the rate is controlled by applying an external pulse train (T^2L compatible pulse) at the desired sampling rate.
Dynamic Range	The full scale to minimum detectable signal is 50 db
Noise Level	With no signal applied the noise level is 54 db below full scale

Sensitivity	The minimum full scale input signal level is 707 mv rms (sine wave referred). The maximum full scale input is 50 v rms
Coupling	AC or DC coupling, AC 3 db corner at 1 Hz
Display Modes	
Fast (oscilloscope)	160 msec
Slow (recorders)	16 sec
Single (Plot)	192 sec
Manual	The analysis filter is controlled by a 10 turn potentiometer. (i.e., wave analyzer)
Memory	
Capture	Self and manual transient capture modes are available. The self mode allows the automatic capture of a transient when this signal exceeds a preset adjustable threshold. Manual capture is accomplished by depressing the "hold" pushbutton or inserting a TTL logic pulse into the appropriate rear panel BNC
Erase	Memory contents are cleared by depressing the erase pushbutton or inserting TTL logic pulse into the rear panel BNC provided
Read Out	Memory contents are available for viewing and read-out (peak voltage level is 1 volt). The readout time for the entire memory is 400 μsec
Weighting	Data in storage is unmodified (rectangular window) in flat mode. In cosine mode data is modified by a trigonometric function consisting of a cosine curve on a pedestal (Hanning window)

Output

Frequency Response (Flatness)	± 1 db for all analysis ranges
Linearity of Spectrum Output	± 1/2% of full scale or ± 1 db whichever is greater
Frequency Linearity	±.5% of the full analysis range
Weighting	
Analyzer	Linear, logarithmic and square law spectrum outputs. All modes scaled to a +5 volt maximum output
Integrator	Linear, logarithmic and square logarithmic weighting
Gain	
Vernier	A Vernier gain control provides 20 db of gain at the analyzer output
Calibrate	A six position rotary switch provides calibration markers (D.C. levels) at 10 db increments at the integrator output 0 db corresponds to +5 volts

Integration

Sums per Bin	8, 16, 32, 64, 128, 256, 512 or continuous averaging. Normalization to 5 V full scale Ensemble averaging is providing for non-redundant spectra
Start-Stop-Resume	Depressing the resume pushbutton causes a repeat of the processing cycle by adding to the existing memory contents. Depressing the start pushbutton erases the memory and begins a new processing cycle. May also be controlled remotely
Power	115 volts ± 10%, 220 volts ± 10% switch selectable, 50 to 400 Hz, 100 watts

Size	Two units, 17" wide, 22 1/4" deep. 10 1/2" high and 5 1/4" high
Weight	All units approximately 34 lbs

SPECIFICATIONS
HEWLETT-PACKARD TRUE RMS VOLTMETER
MODEL 3400A

Voltage Range	1 mV to 300 V full scale, 12 ranges
DB Range	-72 to +52 dBm (0 dBm = 1 mW in 600Ω)
Frequency Range	10 Hz to 10 MHz
Response	Responds to rms value (heating value) of input signal
Meter Accuracy	% of Full Scale (20° to 30°C)

10 Hz	50 Hz	1 MHz	2 MHz	3MHz	10 MHz
±5%	±1%	±2%	±3%	±5%	

AC-toDC Converter Accuracy — % of Full Scale (20°C to 30°C)

10 Hz	50 Hz	1 MHz	2MHz	3 MHz	10 MHz
±5%	±0.75%	±2%	±3%	±5%	

Output	Negative 1 V dc into open circuit for full-scale deflection, proportional to meter deflection; 1 mA maximum; nominal source impedance 1000Ω
Output Noise	< 1 mV rms
Crest Factor	(ratio of peak-to-rms amplitude of input signal): 10:1 at full scale (except where limited by maximum input), inversely proportional to meter deflection (e.g., 20:1 at half-scale, 100:1 at tenth-scale)
Input Impedance	0.001 V to 0.3 V range: 10 MΩ shunted by <50 pF: 1.0 V to 300V range; 10 MΩ shunted by <20 pF